Pith:2026.000092v1 [gr-qc] 25 Nov 2026

Constructive Four-Dimensional Quantum Gravity and Emergent Einstein Gravity on a Coupled Discrete Ledger

Jonathan Washburn [1*]

[1]Recognition Physics Institute, Austin, Texas 78701, USA.

Corresponding author: Jonathan Washburn, e-mail: jon@recognitionphysics.org

Abstract

We present a machine-verified constructive and perturbative framework for four-dimensional quantum gravity on the **24**-bond body-centred hypercubic lattice D_4^* (regular **24**-cell Voronoi cell) driven by the canonical reciprocal cost $J(x) = \frac{1}{2}(x + x^{-1}) - 1$. All results are formalized in Lean 4 across **173** clean-room-audited modules (**119** D_4^* spin-**2**/scattering/renormalization plus **54** coupled Einstein–Cartan modules, zero unfinished proofs, standard axioms only) and cross-checked by an independent **30**-test symbolic–numerical suite. First, on the F_4-symmetric **24**-bond star, we prove exact second- and fourth-moment isotropy, $O(a^4)$ $O(4)$ restoration, sharp coercivity $(8/(3\pi^2))\|k\|^2 \le \Delta_{D_4^*,a}(k) \le \|k\|^2$ attained at both vertex orbits of $\mathbf{BZ}_{24}(a)$ with zero doublers, exact $(11, 1)$ signature and $|\det M(k)| \ge 195|k|^{20}$ for the 12×12 graviton operator at $\kappa_{\mathrm{cone}} = \frac{1}{2}$ (yielding uncut $\delta_{\mathrm{IR}} = 0$ integrability of all **20,736** one-loop entries), and $L^2(\mathbb{R}^4; \mathbf{Sym}_0^2)$ norm-resolvent ($O(a^2)$) and Fourier a.e./strong-L^2 Γ-convergence. Second, we construct non-perturbative coupled $O(4)$-invariant spin-**2** J-cost measures on D_4^* time slabs $t(x) = x_0 + x_1$ via non-separable Brascamp–Lieb convexity, proving site reflection positivity, clustering ($\rho = 6\kappa/(6\kappa + m^2 + \lambda) < 1$), infinite-volume OS reconstruction with unique vacuum and gap $\Delta_2 > 0$, volume-uniform $U_4(H_{01}, H_{01}, H_{23}, H_{23}) = U_4(H_{01})/3 \le -\delta_{\mathrm{NG}} < 0$ ruling out every product law, a UV floor $\mathrm{Var}(H_{\alpha\beta}) \le 3/(4(m^2+\lambda))$ (energy/site ≤ 9), and a parallel fixed-lattice $SO(4)$-vierbein Einstein–Cartan QFT with maximal $H_{\mathrm{EC}}^* = H_{\mathrm{EC}} \ge 0$, Stone unitarity, and a $\mathbb{Z}_2$ confinement–Higgs dichotomy ($882 \tanh(4\beta_W) \le 1$). Third, restoring the trace mode recovers **10**-component linearized Einstein–Hilbert gravity with signature $(+1)^9 \oplus (-1)$, exact PPN $\gamma_{\mathrm{PPN}} = 1$ (vs. $\frac{1}{3}$ traceless and $\frac{1}{2}$ Fierz–Pauli vDVZ), exact sourced lattice Einstein equations, optimal $O(a^4)$ continuum Green convergence ($\int_0^\infty c_4\, dt = 0$), and Griffiths-I Gaussian domination. Fourth, in the single-scale regime ($\beta = \kappa N^2$, $\mu = M^2/N^2$), we establish $O(N^{-2})$ smeared convergence to massive/massless Coulomb propagators alongside $\kappa^3 N^6 u_4(L_x) \to -48$ and kurtosis $-1/(48\kappa N^2)$, paired with all-orders $(L+1)$-loop Zimmermann–BPHZ forest and $(L+2)$-loop $(3L + 5)$-propagator overlapping-tree Reisz convergence on $\mathbf{BZ}_{24}(a)^{L+1}, \mathbf{BZ}_{24}(a)^{L+2}$ for zero-derivative (ϕ^4-like) spin-**2** resolvent vertices and a Balaban **32**-site Q_5 fluctuation gap. Fifth, for all $\xi > 1/3$, we prove discrete BRST nilpotency $Q_B^2 = 0$, exact algebraic Sylvester factorization $\det_4 / \det_9 = (\Delta_a + m^2)^{-5}$ (complex boson / **5** $\mathbf{TT}_v$ modes), Kugo–Ojima cohomology $\mathbf{TT}_v(\mathbb{R}^4)$, **2**-helicity OS positivity with UV decoupling ($r_- \to 5 - 2\sqrt{6}$), curved $L^2(\Omega)$ Γ-convergence, and Lorentzian leapfrog evolution with sharp CFL $\tau/a < \sqrt{3/8} > 1/\sqrt{3}$. Sixth, the D_4^* hinge cost recovers tree **3**-MHV ($-729/32$) and **4**-KLT ($-1/256$) amplitudes, classifies all three quadratic gauge laws via sharp no-go obstructions, yields Law C's doubler-free propagator ($c_{\mathrm{tr}} \in [\frac{1}{3}, \frac{1}{2})$, vDVZ jump at $\eta = 0$), proves the dilation sum rule $4c_b - 2c_a \ge 10(N^4 - 1)$ and $O(4)$-isotropic torus mass counterterm, restores the LL one-loop Ward channel to $O(\|\kappa_{\mathrm{ext}}\|^8) = O(a^2)$, and in a hybrid continuum-RNC / D_4^*-denominator Pauli–Villars model reproduces the 't Hooft–Veltman $\frac{1}{120}R^2 + \frac{7}{20}R_{\mu\nu}^2$ counterterm, anti-screening $-23/3$, and PV-scheme ratio $g_* = 2\pi/(23 \ln(4/3))$. Explicitly open frontiers—above all a non-perturbative interacting $a \to 0$ continuum graviton limit—are delineated throughout.

Keywords: constructive quantum gravity, D_4^* lattice, 24-cell Brillouin zone, Osterwalder–Schrader reflection positivity, Brascamp–Lieb inequality, Ursell cumulant, linearized Einstein–Hilbert gravity, vDVZ discontinuity, BPHZ Reisz convergence, discrete BRST cohomology, Kugo–Ojima quartet, Lorentzian CFL stability, KLT amplitudes, Ward–Takahashi restoration, 't Hooft–Veltman renormalization, Lean 4 formal verification

1 Introduction

A non-perturbative four-dimensional quantum theory of gravity must answer two demands that standard formulations pull in opposite directions. From below, constructive quantum field theory requires a well-defined probability measure on configurations, Osterwalder–Schrader (OS) reflection positivity, a physical Hilbert space with a unique vacuum and positive self-adjoint Hamiltonian, and strict non-Gaussian interactions that cannot be disguised as free fields [1–4]. From above, macroscopic gravitational physics requires that the long-distance effective dynamics recover ten-component linearized general relativity with exact post-Newtonian parameter $\gamma_{\mathrm{PPN}} = 1$ (free of the van Dam–Veltman–Zakharov discontinuity [5;6;88]), full four-dimensional rotational and Lorentz invariance without Brillouin-zone doublers, covariant gauge cancellation via Faddeev–Popov ghosts [7] and BRST/Kugo–Ojima cohomology [7;75;76], tree-level Einstein graviton scattering [8;9;85], and controlled ultraviolet renormalization at one loop and all perturbative orders [10–13].

In continuum perturbation theory, the Euclidean Einstein–Hilbert action is unbounded below in the conformal trace sector [14] and perturbatively non-renormalizable at two loops [15], motivating effective field theory [70;71], asymptotic safety [66–69], discrete Regge and causal dynamical triangulations [25;62;63], and canonical loop quantization [64;65]. On hypercubic Euclidean lattices $\mathbb{Z}^4$, naive discretizations break fourth-order rotational isotropy at relative order $O(a^2)$, introduce spurious Brillouin-zone corner doublers, and either violate discrete diffeomorphism Ward identities at finite spacing or lose positivity and periodicity. Separating which of these obstructions are artifacts of hypercubic discretization from which are genuine structural barriers of four-dimensional quantum gravity requires a lattice geometry whose discrete symmetry group matches continuum isotropy through fourth order, paired with an interaction law whose convexity controls the measure non-perturbatively without expanding in small couplings.

1.1 Recognition Science grounding: the reciprocal cost and the D_4^* ledger

Within Recognition Science (RS) [16;17], physical dynamics is organized on a discrete double-entry comparison ledger governed by the canonical reciprocal comparison cost

$$J(x) \;=\; \frac{1}{2}\big(x + x^{-1}\big) - 1 \;=\; \frac{(x-1)^2}{2x}, \qquad x > 0. \tag{1}$$

For the native comparison apparatus and unit-normalized reporting, J is uniquely selected by symmetry $J(x) = J(x^{-1})$, normalization $J(1) = 0$, $J''(1) = 1$, and the multiplicative d'Alembert composition law [18;19]. Expressing positive bond ratios in logarithmic strain variables $x = e^u$ ($u \in \mathbb{R}$) transforms Eq. (1) into the strictly convex hyperbolic interaction

$$J(e^u) \;=\; \cosh u - 1 \;\geq\; \frac{u^2}{2} + \frac{u^4}{24}, \qquad \frac{d^2}{du^2} J(e^u) = \cosh u \geq 1, \tag{2}$$

and the exact midpoint-convexity identity $\cosh u + \cosh v - 2\cosh\!\big(\frac{u+v}{2}\big) = 2\cosh\!\big(\frac{u+v}{2}\big)\big(\cosh\!\big(\frac{u-v}{2}\big) - 1\big) \geq \frac{1}{4}(u-v)^2$. Every non-perturbative Brascamp–Lieb bound, Poincaré spectral gap, exponential tightness estimate, and non-Gaussian cumulant theorem established below flows directly from the unconditional convexity $\cosh u \geq 1$ and strict super-quadratic growth of $J(e^u)$, without invoking perturbative coupling expansions.

The four-dimensional spacetime realization of the double-entry ledger is the body-centred hypercubic lattice $D_4^* = \mathbb{Z}^4 \cup \big(\mathbb{Z} + \frac{1}{2}\big)^4$, the dual of the root lattice D_4 [49]. Each site has 24 nearest neighbours at unit

Euclidean distance, arranged in 12 canonical bond pairs: 4 axial pairs $\pm e_\mu$ ($\mu \in \{0,1,2,3\}$) and 8 body-diagonal pairs $\left(\pm\frac{1}{2},\pm\frac{1}{2},\pm\frac{1}{2},\pm\frac{1}{2}\right)$ whose 16 signs reflect the $2^D = 8$ signed pairings of $D = 3$ spatial dimensions plus time. The Voronoi cell of D_4^* (and of its reciprocal lattice $2\pi D_4$) is the regular 24-cell[50], governed by the crystallographic Weyl group F_4 of order 1,152—the unique irreducible four-dimensional reflection group possessing no fourth-degree polynomial invariant other than $(k^2)^2$ [20;21].

In our companion strong-field classical and horizon study[22] (see also[16]), we analyzed exact nonlinear black-hole spacetimes, nonsingular capacity-ceiling gravitational collapse, and quantum horizon geometry. Earlier linearized dispersion work[23;24] showed that lifting the 15-edge Kuhn triangulation to the 24-bond D_4^* ledger at light-cone reach $\kappa_{\text{cone}} = \frac{1}{2}$ eliminates dimension-six graviton dispersion and birefringence identically ($s_{D_4^*} = 0$), removes corner doublers across the punctured Brillouin zone, and yields exact $(11,1)$ Hermitian carrier signature. The present paper addresses the constructive quantum field theory, emergent linearized general relativity, perturbative all-orders renormalization, and discrete gauge-symmetry restoration of this coupled D_4^* ledger across 173 machine-verified Lean 4 / Mathlib 4 modules[89;90] (`0 sorry`, strictly standard axioms `[propext, Classical.choice, Quot.sound]`), comprising 30 `W1Opus`, 22 `W1Fable`, 16 `W1Neon`, 28 `W4Fable`, 11 `Neon` one-loop/carrier, 54 coupled Einstein–Cartan `T2` (including the `T2_R100`–`R109` capstone chain), and 12 supporting reflection/soft-theorem modules.

1.2 Summary of main results across six pillars

The formal theorems, explicit witnesses, and sharp obstructions established in this paper fall into six connected pillars:

1. **D_4^* geometry, 24-cell Brillouin-zone coercivity, and no-doubler spectrum (Section 2).** The 12 canonical unit bond pairs satisfy exact second- and fourth-moment isotropy ($\sum_b e_b^\mu e_b^\nu = 3\delta^{\mu\nu}$ and $\sum_b e_b^\mu e_b^\nu e_b^\rho e_b^\sigma = \frac{1}{2}(\delta^{\mu\nu}\delta^{\rho\sigma} + \delta^{\mu\rho}\delta^{\nu\sigma} + \delta^{\mu\sigma}\delta^{\nu\rho})$), driving $O(4)$/Lorentz anisotropy down to $O(a^4)$ (`W1Neon_R1`). Across the entire actual Voronoi first Brillouin zone $\mathrm{BZ}_{24}(a) = \{k \in \mathbb{R}^4 \mid \forall \mu \neq \nu,\ |ak_\mu| + |ak_\nu| \leq 2\pi\}$, the discrete Laplacian obeys the sharp two-sided bound $(8/(3\pi^2))\|k\|^2 \leq \Delta_{D_4^*,a}(k) \leq \|k\|^2$, with exact equality at both vertex orbits $(\pi/a)^4$ and $(2\pi/a,0,0,0)$ and zero doublers anywhere in $\mathrm{BZ}_{24}(a) \setminus \{0\}$ (`W1Neon_R8`). On the full 12×12 gauge-fixed linearized D_4^* graviton operator $M(k)$ at $\kappa_{\text{cone}} = \frac{1}{2}$, we prove exact $(11,1)$ signature across $(-2\pi,2\pi)^4 \setminus \{0\}$, the sharp small-$k$ determinant floor $|\det M(k)| \geq 195|k|^{20}$ yielding $|M(k)^{-1}_{ij}| \leq C/|k|^2$, and uncut ($\delta_{\text{IR}} = 0$) IR-and-UV Lebesgue integrability of all $12^4 = 20{,}736$ one-loop self-energy matrix entries over $[-\pi,\pi]^4$ (`Neon_R54`, `Neon_R59`). In the continuum limit, the gauge-fixed Lichnerowicz resolvent converges in $L^2(\mathbb{R}^4;\mathrm{Sym}^2_0)$ operator norm at rate $O(a^2)$, in $L^2 \to H^1$ at rate $O(a)$, and in exact Fourier-space a.e./strong-L^2 Γ-convergence (`W1Neon_R10`).
2. **Non-perturbative coupled $O(4)$-invariant spin-2 J-cost QFT, reflection positivity, and Einstein–Cartan reconstruction (Section 3).** Using multivariate Prékopa–Leindler and non-separable Brascamp–Lieb convexity (`W1Opus_R14`, `R15`), we construct coupled spin-2 Gibbs measures on $\mathrm{Sym}^2_0(\mathbb{R}^4) \cong \mathbb{R}^9$ with exact $O(4)$ (indeed $O(9)$) internal invariance $V(H) = \frac{1}{2}m^2\|H\|_F^2 + \lambda(\cosh\|H\|_F - 1)$ on D_4^* time slabs $t(x) = x_0 + x_1$ (`W1Opus_R30`). We prove unconditional site reflection positivity (OS2) across the mirror planes $t = 0, M_{\text{sl}}$, Dirichlet-form Poincaré spectral gap $\geq m^2 + \lambda$, exponential temporal clustering at rate $\rho = 6\kappa/(6\kappa + m^2 + \lambda) < 1$, Schwinger–Dyson two-sided covariance sandwiches, and a finite discrete UV floor $\mathrm{Var}(H_{\alpha\beta}(x)) \leq \frac{3}{4(m^2+\lambda)}$ (energy per site $\mathbb{E}[H]/|\Lambda| \leq 9$). Exact 9-dimensional dilation virials ($\mathbb{E}[w] = 9$, $\mathbb{E}[\|H\|_F^2 w] = 11\mathbb{E}[\|H\|_F^2]$) and Chebyshev's inequality prove $U_4(H_{01},H_{01},H_{23},H_{23}) = U_4(H_{01})/3 < 0$ for every $\lambda > 0$ at one site and $U_4(H_{01},H_{01},H_{23},H_{23})(x) \leq -\delta_{\text{NG}} < 0$ uniformly in volume for $\kappa \in [0,\kappa_0]$, strictly excluding every Gaussian and every factorized product measure (`W1Opus_R30`). In the contraction regime $6\kappa + 4\beta < m^2 + 2\lambda$, we construct the complete infinite-volume OS Hilbert space with unique vacuum Ω, positive self-adjoint transfer contraction $0 \leq T \leq 1$, spectral gap $\Delta_2 > 0$, and sub-Gaussian two-field state norm $\|(\phi_x^2 - \langle\phi_x^2\rangle)\Omega\|^2 \leq 2\langle\phi_x^2\rangle^2 - \delta_{\text{NG}}$ (`W1Opus_R25`, `R26`). Alongside this spin-2 tensor stack, we summarize the parallel fixed-lattice coupled dynamical-vierbein plus non-Abelian $SO(4)$ spin-connection Einstein–Cartan OS QFT (`T2_R100`–`R109`, part of the 173-module corpus), which achieves an unbounded maximal self-adjoint Hamiltonian $H^*_{\text{EC}} = H_{\text{EC}} \geq 0$,

bidirectional Stone real-time unitarity $U_{\mathrm{EC}}(t) = e^{-itH_{\mathrm{EC}}}$, infinite-dimensional excited metric subspace, and an exact $\mathbb{Z}_2$ confinement-versus-string-breaking Higgs phase dichotomy (strict area law for $\beta_W > 0$, $882\tanh(4\beta_W) \le 1$).

3. **Macroscopic 10-component linearized Einstein–Hilbert gravity and optimal $O(a^4)$ continuum Green convergence (Section 4).** Restoring the conformal trace basis vector $\delta/2$ yields the 10-component orthonormal basis of $\mathrm{Sym}^2(\mathbb{R}^4)$, the trace-reversal involution $\bar{h} = h - \frac{1}{2}\,\mathrm{tr}(h)\delta$, and the de Donder propagator tensor $P^{\mathrm{GR}}_{\mu\nu,\rho\sigma} = \frac{1}{2}(\delta_{\mu\rho}\delta_{\nu\sigma} + \delta_{\mu\sigma}\delta_{\nu\rho} - \delta_{\mu\nu}\delta_{\rho\sigma})$ with exact signature $(+1)^9 \oplus (-1)$ (`W10pus_R28`). On static dust sources $T \propto e_0 e_0^{\top}$, P^{GR} yields exact PPN parameter $\gamma_{\mathrm{PPN}} = 1$ and light-bending ratio 1, sharply separated from the 9-component traceless projector ($\gamma_{\mathrm{PPN}} = 1/3$, bending $2/3$) and the massive Fierz–Pauli vDVZ projector ($\gamma_{\mathrm{PPN}} = 1/2$, bending $3/4$). For every finitely supported conserved source ($DT = 0$), the lattice response solves the full R_ξ family $K_{k_1,k_2}(h) = T$ and the lattice Einstein operator identically in de Donder gauge ($D\bar{h} = 0$), recovering Newton's potential $a^{-1}h_{00} \to 2G_N M_{\mathrm{phys}}/r_{\mathrm{phys}}$ ($M_{\mathrm{phys}} = M/2$). Because D_4^* fourth-order isotropy forces the first Edgeworth heat-kernel correction to integrate to zero ($\int_0^\infty c_4(t)\,dt = 0$), a second-order local limit theorem upgrades the 4D continuum Green convergence from $O(a^2)$ (`W10pus_R27`) to optimal $O(a^4)$: $|a^{-2}P^{\mathrm{GR}}G(n)/k_1 - P^{\mathrm{GR}}/(24\pi^2 k_1|X|^2)| \le Ca^4/(k_1|X|^6)$, paired with a finite origin floor $|G(0)| \le 1 + \pi^2/256$ and Griffiths-I pointwise Gaussian domination $0 \le S_\infty(x,y) \le G_{\mathbb{Z}^4}(y-x)/\kappa$ in the interacting scalar sector (`W10pus_R29`).
4. **Interacting single-scale continuum limit, exact -48 cumulant / $-1/48$ kurtosis, and all-orders zero-derivative BPHZ Reisz convergence (Section 5).** For the continuous-ratio J-cost Gibbs measure on compact log-levels $[-R, R]$, we prove weak-coupling DLR uniqueness on $\mathbb{Z}^4$ ($100\beta J_R \le 1$) and uniform susceptibility bounds (`W1Fable_R18`, `R19`). Tying stiffness and mass to a single D_4 torus side N ($\beta = \kappa N^2$, $\mu = M^2/N^2$, or $\mu = m_{\mathrm{reg}}^2/N^4$ for vanishing mass), a four-dimensional infrared bound $\mathrm{irSum}(N,\mu) \le 100 + 200/(\mu N^4)$ yields $O(N^{-2})$ smeared convergence against even test functions to the continuum massive propagator $1/(\kappa(12|P|^2 + M^2))$ and massless Coulomb propagator $1/(12\kappa|P|^2)$ (`W1Fable_R20`, `R21`, `R22`). Crucially, we compute the exact connected fourth cumulant of the local restoring force L_x: $\kappa^3 N^6 u_4(L_x) \to -48$ and $\kappa N^2 \mathbb{E}[L_x^2] \to 48$ at rate $O(N^{-2})$, fixing the exact normalized kurtosis limit $\kappa N^2 u_4(L_x)/(\mathbb{E}[L_x^2])^2 \to -1/48$ and quantifying precisely how the single-scale interacting measure approaches a Gaussian limit at rate $O(N^{-2})$. Perturbatively, for zero-derivative (ϕ^4-like) spin-2 resolvent vertices, we prove all-orders $(L+1)$-loop Zimmermann–BPHZ forest convergence on $\mathrm{BZ}_{24}(a)^{L+1}$ and $(L+2)$-loop $(3L+5)$-propagator overlapping tree-coupled Reisz convergence on $\mathrm{BZ}_{24}(a)^{L+2}$ as $a \to 0^+$ with exact diagonal $O(4)$ equivariance (`W1Neon_R17`, `R20`), together with non-perturbative exponential $H^1 + W^{1,4}$ tightness on $\mathbb{R}^{9N^4}$ and a Balaban 32-site Q_5 block-spin fluctuation mass gap (`W1Neon_R17`).
5. **General-gauge BRST / Kugo–Ojima cohomology, curved-manifold Γ-convergence, and Lorentzian CFL causal dynamics (Section 6).** Extending harmonic-gauge reflection positivity (`W1Neon_R12`) to all covariant gauges $\xi > 1/3$ (`W1Neon_R18`), we prove exact discrete BRST nilpotency $Q_B^2 = 0$ on the 21D covariant multiplet $(h, B, c, \bar{c})$, zero-discretization-breaking ghost intertwining $F_v \circ L_a^{(\xi)} = K_{\mathrm{gh}}^{(\xi)} \circ F_v$, the exact 13×13 algebraic Sylvester determinant factorization $\det_4(K_{\mathrm{gh}}^{(\xi)} + m^2)/\det_9(L_a^{(\xi)} + m^2) = (\Delta_a + m^2)^{-5}$ (matching a complex boson / 5 massive TT_v modes; real-boson $\det_4/\sqrt{\det_9}$ retains ξ-factors), Kugo–Ojima 16D quartet homotopy giving $\ker Q_B/\operatorname{im} Q_B \cong \mathrm{TT}_v(\mathbb{R}^4)$, unconditional 2-helicity $(e_+, e_\times)$ OS reflection positivity with exact 2-pole Källén–Lehmann UV pole decoupling ($r_- \to 5 - 2\sqrt{6} < 1/4$), and a $\xi = 2$ longitudinal gauge-pole counterexample proving the quotient is essential. On arbitrary curved backgrounds $(G(x), \mathcal{R}(x))$, we establish discrete IMS localization, pointwise $O(a^2)$ and $L^2(\Omega)$ $O(a^4)$ curved Laplace–Beltrami convergence, variable-coefficient $L^2(\Omega)$ Γ-convergence (on finite-measure domains with smooth C^2 limit jets and interior Lipschitz cutoff exhaustions), and uniform-in-a curved Lichnerowicz resolvent stability (`W1Neon_R9`, `R16`). In real Lorentzian time (`W1Neon_R15`), the 3D spatial D_4^* spectral ceiling $32/(3a^2) < 12/a^2$ yields exact leapfrog energy conservation $E_n = E_0$, a strict CFL advantage $\tau/a < \sqrt{3/8} \approx 0.6124$ over $\mathbb{Z}^3$'s $1/\sqrt{3} \approx 0.5774$ (paired with an exact blow-up witness at $\sqrt{3/8}$), exact finite propagation speed $\mathrm{supp}(u_n) \subseteq B(x_0, R + 2n)$, and uniform $O(a^2 + \tau^2)$ convergence of the full 9D retarded spin-2 Green operator with $O(a^4)$ $SO(3)$ wavefront isotropy.

6. D_4^* **hinge scattering (MHV/KLT), Law C doubler-free propagator, and one-loop local Ward restoration (Section 7).** Lifting single-bond comparisons (whose on-shell 3-point vertex vanishes identically, `W4Fable_R1`) to the D_4^* hinge (bond-pair) J-cost recovers exact continuum 3-graviton MHV ($V_3^{\text{hinge}}/a^2 \to -\frac{1}{32}\langle 12\rangle^6/(\langle 23\rangle^2\langle 31\rangle^2)$, witness $-729/32$) and 4-graviton tree KLT/MHV amplitudes ($M_4^{\text{hinge}}/a^2 \to \frac{1}{128}\langle 12\rangle^4[34]^4/(stu)$, witness $-1/256$) along with exact dilation shift identities and an unfixed-propagator a^{-2} divergence obstruction (`W4Fable_R5`, `R6`, `R9`, `R12`). Classifying finite-spacing quadratic laws proves three sharp obstructions: Law A (sine covector) carries 15 Brillouin-zone doublers; Law B (half-angle) fails reciprocal-lattice periodicity on D_4^* because no orthogonal 4-bond frame generates the lattice ($\det = \pm 16$ vs. 8); and the complex forward difference fails Hermitian Ward invariance by $4\times$ its Gram determinant (64/81 witness) (`W4Fable_R13`, `R15`). Law C (hinge cost plus de Donder posting) is periodic, real, and doubler-free across the whole zone with exact propagator $(6/D_{\text{inv}})(S_{\text{src}} - c_{\text{tr}}\,\text{tr}(S_{\text{src}})I_4)$, $c_{\text{tr}} \in [1/3, 1/2)$, $c_{\text{tr}} \to 1/2$ as $a \to 0$, exhibiting the vDVZ discontinuity directly as a jump in posting strength at $\eta = 0$. At one loop on the closed torus grid torusGrid_N (`W4Fable_R17`–`R24`), we prove the non-vanishing dilation sum rule $4c_b - 2c_a \geq 10(N^4 - 1)$ (150 at $N = 2$), prove that five D_4^* cell symmetries force an exact $O(4)$-isotropic site mass counterterm $-\frac{c_a}{2}\,\text{tr}\,g + \frac{c_b}{2}\ln\det g$ (ruling out pure $(\det g)^\gamma$ cancellation), and prove that subtracting the site mass plus two local Christoffel counterterms (G_0 at a^{-2} and G_2 at a^0) restores the local longitudinal (LL) Ward channel to $O(\|\kappa_{\text{ext}}\|^8) = O(a^2)$ for every finite $N \geq 1$. Finally, in a hybrid continuum-RNC-vertex / D_4^*-denominator Pauli–Villars model (`Neon_R68`, `R69`), we prove the exact $96\times$ Schur Einstein–Hilbert bridge, exact RNC heat-kernel traces yielding the 't Hooft–Veltman $\frac{1}{120}R^2 + \frac{7}{20}R_{\mu\nu}^2$ counterterm and on-shell UV finiteness, gravitational anti-screening $-23/3$, the scheme-dependent one-loop Pauli–Villars bare-coupling ratio $g_* = 2\pi/(23\ln(4/3))$, and bounded BPHZ difference against the D_4^* scalar denominator.

1.3 Scope boundaries stated up front

Keeping proved theorems cleanly separated from open physics is essential in quantum gravity. Every theorem stated below holds strictly under its written hypotheses and is backed by an audited Lean 4 proof (`0 sorry`, standard axioms only). Five fundamental questions remain *explicitly open* and are not claimed here (examined in detail in Section 9):

1. *Non-perturbative interacting $a \to 0$ continuum quantum gravity:* Our non-perturbative strictly non-Gaussian measures (`W1Opus_R25`, `R26`, `R30` and `T2_R100`–`R109`) live at fixed spacing in gapped regimes; our single-scale interacting $N \to \infty$ scaling limit (`W1Fable_R21`, `R22`) converges to a Gaussian two-point propagator with vanishing kurtosis $-1/(48\kappa N^2)$; and our all-orders continuum convergence (`W1Neon_R20`) is perturbative BPHZ for zero-derivative (ϕ^4-like) resolvent vertices rather than two-derivative Einstein–Hilbert vertices. Constructing a non-perturbative, reflection-positive, non-Gaussian $a \to 0$ continuum measure hosting a massless interacting spin-2 graviton with full nonlinear diffeomorphism invariance remains open.
2. *All-κ / all-λ non-Gaussianity and infinite-volume four-point uniqueness:* For the coupled $O(4)$ spin-2 measure (`W1Opus_R30`), strict negativity $U_4 < 0$ is proved for all $\lambda > 0$ at one site and for small stiffness $\kappa \leq \kappa_0$ uniformly in volume, with subsequential infinite-volume limits; an all-κ Lebowitz/GHS inequality for the 9-component radial model and whole-sequence four-point uniqueness remain open.
3. *Conformal-mode measure positivity:* Restoring the conformal trace mode (`W1Opus_R28`) recovers exact PPN $\gamma_{\text{PPN}} = 1$, but the resulting $(+1)^9 \oplus (-1)$ linearized Einstein–Hilbert operator is indefinite and does not define a positive Gaussian measure; our positive non-perturbative J-cost measures act on the 9-component traceless sector or on compact $SO(4) \times B^{10}$ Einstein–Cartan frames.
4. *Mixed single-contraction one-loop Ward channel, N-uniformity, and full-lattice one-loop RNC bridge:* On `torusGrid N`, three local counterterm orders restore the longitudinal–longitudinal (LL) Ward channel to $O(\|\kappa_{\text{ext}}\|^8) = O(a^2)$ at every finite $N \geq 1$ (`W4Fable_R24`), whereas $N \to \infty$ uniformity of the Christoffel counterterms (G_0, G_2), the mixed single-contraction transverse–longitudinal (TL/LT) block, an analytic proof of the transverse $O(k^4 \ln k)$ logarithm, and direct evaluation

of the 't Hooft–Veltman counterterm from discrete hinge vertices (beyond `Neon_R69`'s hybrid continuum-RNC / D_4^*-denominator model) remain open in Lean.

5. *Working identifications vs. microscopic derivations:* The de Donder gauge-fixing posting, the lattice Faddeev–Popov displacement loop operator, and the identification of the hinge J-cost with the ledger's gravitational action are explicitly marked as *working* identifications where not yet derived microscopically from the primitive comparison axioms.

1.4 Conventions and disambiguated nomenclature

Unless stated otherwise (specifically in the Lorentzian hyperbolic dynamics of Section 6.3 and spinor-helicity scattering of Section 7), we work in four-dimensional Euclidean signature $(+,+,+,+)$ with spacetime indices $\mu,\nu,\rho,\sigma \in \{0,1,2,3\}$ and Frobenius inner product $\langle H, H'\rangle_F = \mathrm{tr}(H^\top H') = \sum_{\mu,\nu} H_{\mu\nu}H'_{\mu\nu}$, $\|H\|_F^2 = \langle H, H\rangle_F$. Because constructive QFT, lattice geometry, linearized gravity, and one-loop perturbation theory frequently overload κ, β, μ, Δ, J, δ, m, and γ, we enforce strictly disambiguated notation summarized in Table 1.

2 Geometry of the D_4^* Ledger, 24-Cell Brillouin-Zone Coercivity, and No-Doubler Spectrum

Every constructive and perturbative estimate in four-dimensional lattice gravity starts with the spectral geometry of the underlying bond star. A hypercubic lattice $\mathbb{Z}^4$ has only four axial bond pairs; its fourth-moment tensor $\sum_{\mu=0}^{3} e_\mu^\alpha e_\mu^\beta e_\mu^\gamma e_\mu^\delta$ vanishes on all mixed index pairs $\alpha \neq \gamma$ and therefore breaks $O(4)$ rotational invariance at relative order $O(a^2)$, contaminating both tree-level graviton propagation and loop counterterms. In this section we establish the exact algebraic isotropy[20;21;49;50], regular 24-cell Brillouin-zone coercivity, full 12×12 doubler-free graviton spectrum[84], and infinite-dimensional continuum L^2 norm-resolvent and Γ-convergence[52;53] of the D_4^* recognition ledger.

2.1 The 24-bond D_4^* star and exact fourth-moment isotropy

Let $\mathcal{B}_{12} = \{e_b\}_{b=1}^{12} \subset \mathbb{R}^4$ denote the 12 canonical unit bond pairs of D_4^*: the 4 axial unit vectors e_μ ($\mu \in \{0,1,2,3\}$) and the 8 body-diagonal unit vectors $\left(\frac{1}{2}, \pm\frac{1}{2}, \pm\frac{1}{2}, \pm\frac{1}{2}\right)$. Together with their negatives $-\mathcal{B}_{12}$, they form the 24 nearest-neighbour unit vectors of D_4^*, which are the 24 vertices of the regular 24-cell (equivalently, in doubled integer coordinates $2D_4^* = \{x \in \mathbb{Z}^4 \mid \forall \mu,\, x_\mu \equiv x_0 \pmod 2\}$, the 24 vectors $\pm 2e_\mu$ and $(\pm1, \pm1, \pm1, \pm1)$ of squared norm 4). For lattice spacing $a > 0$ and Euclidean momentum $k \in \mathbb{R}^4$, the normalized D_4^* discrete Laplacian and discrete vector gradient are defined by

$$\Delta_{D_4^*,a}(k) \;=\; \frac{2}{3a^2}\sum_{b=1}^{12}\bigl(1-\cos(a\,e_b\cdot k)\bigr), \qquad \bigl(\nabla_{D_4^*,a}(k)\bigr)_\mu \;=\; \frac{1}{3a}\sum_{b=1}^{12}\sin(a\,e_b\cdot k)\,e_b^\mu. \tag{3}$$

On any symmetric tensor $h \in \mathrm{Sym}^2(\mathbb{R}^4)$, the linearized bond strain along e_b is $\varepsilon_b(h) = e_b^\top h e_b$, and the associated J-cost strain energy is $\sum_{b=1}^{12} J\bigl(e^{a\,\varepsilon_b(h)}\bigr)$.

Theorem 2.1 (Fourth-Moment Isotropy, $O(a^4)$ $O(4)$ Restoration, and J-Cost Strain Equivalence; `W1Neon_R1`)**.** *For the 12 canonical unit bond pairs $\mathcal{B}_{12}$ of D_4^* and every $a > 0$, $k \in \mathbb{R}^4$, $R \in O(4)$, and $h \in \mathrm{Sym}^2(\mathbb{R}^4)$:*

1. ***Exact second- and fourth-moment isotropy:***

$$\sum_{b=1}^{12} e_b^\mu e_b^\nu \;=\; 3\,\delta^{\mu\nu}, \qquad \sum_{b=1}^{12} e_b^\mu e_b^\nu e_b^\rho e_b^\sigma \;=\; \frac{1}{2}(\delta^{\mu\nu}\delta^{\rho\sigma} + \delta^{\mu\rho}\delta^{\nu\sigma} + \delta^{\mu\sigma}\delta^{\nu\rho})\,, \tag{4}$$

whereas the four-bond hypercubic lattice $\mathbb{Z}^4$ violates fourth-moment isotropy ($\sum_\alpha \delta_{\alpha 0}^4 - 3\sum_\alpha \delta_{\alpha 0}^2\delta_{\alpha 1}^2 = 1 \neq 0$).

Table 1 Disambiguated nomenclature and conventions used throughout the manuscript across D_4^* geometry, constructive spin-2 and Einstein–Cartan QFT, linearized Einstein–Hilbert gravity, single-scale limits, BRST/Lorentzian dynamics, and one-loop Ward restoration.

Symbol	Meaning	Primary section
$J(x)$, $J(e^u)$	Canonical reciprocal cost $\frac{1}{2}(x+x^{-1})-1=\cosh u-1$	Sections 1 and 3
D_4^*, $2\pi D_4$	Body-centred hypercubic lattice ($\mathbb{Z}^4\cup(\mathbb{Z}+\frac{1}{2})^4$) and reciprocal lattice	Sections 2 and 4
$\mathrm{BZ}_{24}(a)$	Regular 24-cell first Brillouin zone $\{k\in\mathbb{R}^4:\lvert ak_\mu\rvert+\lvert ak_\nu\rvert\le 2\pi\}$	Sections 2 and 5
a, M_{sl}	Lattice spacing ($a=1$ in fixed-lattice OS measures) and slab half-height M_{sl}	Sections 2 and 3
κ_{cone}	Light-cone reach parameter ($\kappa_{\mathrm{cone}}=\frac{1}{2}$ on D_4^*)	Sections 1 and 2
κ, β	Spatial/bond stiffness (κ) and temporal or overall inverse-temperature (β)	Sections 3 and 5
$\kappa_{\mathrm{ext}}=ak$	Dimensionless external lattice covector in one-loop torus Ward analysis	Section 7
m^2, m_{reg}, m_{C}	Mass squared ($m^2\ge 0$), vanishing-mass regulator ($\mu=m_{\mathrm{reg}}^2/N^4$), Law C $D_{\mathrm{inv}}/3$	Sections 3, 5 and 7
λ	Non-perturbative J-cost potential coupling ($\lambda>0$)	Sections 3 and 4
$\delta_{\mu\nu}$, δ_{IR}, δ_{NG}	Kronecker delta, IR cutoff ($\delta_{\mathrm{IR}}=0$), non-Gaussianity margin ($\delta_{\mathrm{NG}}>0$)	Sections 2 and 3
δ_{CFL}, δ_{disp}, $\varepsilon_{\mathrm{BPHZ}}$	CFL stability margin, Law C displacement defect, BPHZ peeling exponent	Sections 5 to 7
$\mathrm{Sym}_0^2(\mathbb{R}^4)$, $\mathrm{Sym}^2(\mathbb{R}^4)$	9D traceless symmetric and 10D full symmetric 4×4 real tensors	Sections 2 to 4
P_T, P^{GR}, P^{FP}	Traceless ($-\frac{1}{4}$), de Donder GR ($-\frac{1}{2}$), and Fierz–Pauli ($-\frac{1}{3}$) projectors	Sections 4 and 7
γ_{PPN}	Eddington–Robertson post-Newtonian parameter ($h_{ij}=-\gamma_{\mathrm{PPN}}h_{00}\delta_{ij}$)	Section 4
U_4, $u_4(f)$	Connected 4-point Ursell cumulant; diagonal $u_4(f)=\mathbb{E}[f^4]-3(\mathbb{E}[f^2])^2$	Sections 3 and 5
$\Delta_{D_4^*,a}(k)$	Normalized 12-bond D_4^* Laplacian symbol $\frac{2}{3a^2}\sum_{b=1}^{12}(1-\cos(ae_b\cdot k))$	Sections 2 and 6
ξ, Q_B, K_v	Covariant gauge parameter ($\xi>1/3$), BRST differential ($Q_B^2=0$), quartet homotopy	Sections 2 and 6
τ, ΔG, $\Delta\mathcal{R}$	Lorentzian leapfrog step (τ) and curved background perturbations	Section 6
c_{tr}, $c_{\mathrm{fix}}(\eta)$, S_{src}	Law C trace coeff. $\in[\frac{1}{3},\frac{1}{2})$, posting coeff., symmetric source tensor	Section 7
c_a, c_b; G_0, G_2	Isotropic torus mass counterterms (a^{-4}) and Christoffel counterterms (a^{-2}, a^0)	Section 7

2. ***Global non-asymptotic*** $O(a^4)$ $O(4)$***/Lorentz restoration:***

$$0\ \le\ \Delta_{D_4^*,a}(k)-\left(\|k\|^2-\frac{a^2}{24}\|k\|^4\right)\ \le\ \frac{a^4}{720}\|k\|^6,\qquad |\Delta_{D_4^*,a}(Rk)-\Delta_{D_4^*,a}(k)|\ \le\ \frac{a^4}{720}\|k\|^6,\quad (5)$$

so all $O(a^0)$ *and* $O(a^2)$ *rotational anisotropies vanish identically. Moreover,* $\|\nabla_{D_4^*,a}(k)\|^2\le\Delta_{D_4^*,a}(k)\le\|k\|^2$ *globally on* $\mathbb{R}^4$.

3. ***Exact*** J***-cost quadratic and quartic bond-strain coercivity:*** *The exact second variation of* $\sum_{b=1}^{12}J(e^{t\,\varepsilon_b(h)})$ *at* $t=0$ *is the* $SO(4)$*-invariant quadratic form*

$$Q_{\mathrm{str}}(h)\ :=\ \sum_{b=1}^{12}\left(e_b^{\top}he_b\right)^2\ =\ \|h\|_F^2+\frac{1}{2}\left(\mathrm{tr}\,h\right)^2,\quad (6)$$

which reduces to an exact isometry $Q_{\mathrm{str}}(h) = \|h\|_F^2$ *on* $\mathrm{Sym}_0^2(\mathbb{R}^4)$ *(equivalently* $\sum_{b\in\pm\mathcal{B}_{12}} \varepsilon_b(h)^2 = 2\|h\|_F^2$*). The quartic bond-strain sum obeys* $\frac{1}{12}Q_{\mathrm{str}}(h)^2 \le \sum_{b=1}^{12} \varepsilon_b(h)^4 \le Q_{\mathrm{str}}(h)^2$*, and by Eq. (2),*

$$\sum_{b=1}^{12} J\big(e^{\varepsilon_b(h)}\big) \;\ge\; \frac{1}{2}Q_{\mathrm{str}}(h) + \frac{1}{288}Q_{\mathrm{str}}(h)^2. \tag{7}$$

Proof outline. For Eq. (4), direct summation over the 4 axial vectors contributes $\delta^{\mu\nu}$ to the second moment and $\delta^{\mu\nu\rho\sigma}$ to the fourth, while the 8 body-diagonal vectors $(\frac{1}{2},\pm\frac{1}{2},\pm\frac{1}{2},\pm\frac{1}{2})$ contribute $8\cdot\frac{1}{4}\delta^{\mu\nu} = 2\delta^{\mu\nu}$ to the second moment and $8\cdot\frac{1}{16} = \frac{1}{2}$ whenever indices occur in even multiplicities; adding the two yields $\frac{3}{2}$ on equal indices $\mu=\nu=\rho=\sigma$ and $\frac{1}{2}$ on paired distinct indices, matching $\frac{1}{2}(\delta^{\mu\nu}\delta^{\rho\sigma} + \delta^{\mu\rho}\delta^{\nu\sigma} + \delta^{\mu\sigma}\delta^{\nu\rho})$ identically. Inserting the alternating Taylor inequalities $\frac{1}{2}\theta^2 - \frac{1}{24}\theta^4 \le 1-\cos\theta \le \frac{1}{2}\theta^2 - \frac{1}{24}\theta^4 + \frac{1}{720}\theta^6$ into Eq. (3) and using $\sum_b (e_b\cdot k)^2 = 3\|k\|^2$, $\sum_b (e_b\cdot k)^4 = \frac{3}{2}\|k\|^4$, and $\sum_b (e_b\cdot k)^6 \le \|k\|^2\sum_b (e_b\cdot k)^4 = \frac{3}{2}\|k\|^6$ yields Eq. (5). Because $\|k\|^2 - \frac{a^2}{24}\|k\|^4$ depends only on $\|k\|^2$, the difference $\Delta_{D_4^*,a}(Rk) - \Delta_{D_4^*,a}(k)$ is bounded by the sixth-order remainder $(a^4/720)\|k\|^6$. Identity Eq. (6) follows by contracting Eq. (4) with $h_{\mu\nu}h_{\rho\sigma}$: $\frac{1}{2}((\mathrm{tr}\,h)^2 + 2\|h\|_F^2) = \|h\|_F^2 + \frac{1}{2}(\mathrm{tr}\,h)^2$, and Cauchy–Schwarz over 12 terms gives $\sum_{b=1}^{12}\varepsilon_b(h)^4 \ge \frac{1}{12}(\sum_b \varepsilon_b^2)^2 = \frac{1}{12}Q_{\mathrm{str}}(h)^2$, which combines with Eq. (2) to give Eq. (7). □

2.2 Sharp coercivity across the regular 24-cell first Brillouin zone and spin-2 Sobolev bounds

The reciprocal lattice of D_4^* is $2\pi D_4 = \{2\pi n \mid n\in\mathbb{Z}^4, \sum_\mu n_\mu \in 2\mathbb{Z}\}$, and its Voronoi first Brillouin zone is the regular 24-cell

$$\mathrm{BZ}_{24}(a) \;:=\; \big\{k\in\mathbb{R}^4 \;\big|\; \forall\mu\neq\nu,\ |ak_\mu| + |ak_\nu| \le 2\pi\big\}. \tag{8}$$

Notice that $\mathrm{BZ}_{24}(a)$ strictly contains the hypercube $[-\pi/a,\pi/a]^4$ and has 24 vertices split into two crystallographic orbits under signed coordinate permutations: the 16 hypercube corners $(\pm\pi/a,\pm\pi/a,\pm\pi/a,\pm\pi/a)$ and the 8 doubled axial vertices $(\pm 2\pi/a,0,0,0)$ (and permutations), all lying on the sphere $\|k\|^2 = 4\pi^2/a^2$.

On the 9-dimensional space $\mathrm{Sym}_0^2(\mathbb{R}^4)$ of traceless symmetric 4×4 matrices, let $v = \nabla_{D_4^*,a}(k)$ and define the traceless divergence operator and gauge-fixed discrete Lichnerowicz operator[74] for covariant gauge parameter $\xi\in\mathbb{R}$ by

$$(\mathcal{D}_v h)_{\mu\nu} \;:=\; v_\mu (hv)_\nu + v_\nu (hv)_\mu - \frac{1}{2}\big(v^\top hv\big)\delta_{\mu\nu}, \tag{9}$$

$$L_a^{(\xi)}(k)\,h \;:=\; \Delta_{D_4^*,a}(k)\,h + (\xi-1)\,\mathcal{D}_{\nabla_{D_4^*,a}(k)}h. \tag{10}$$

Setting $\xi = 1$ gives the harmonic (de Donder–Feynman) operator $\Delta_{D_4^*,a}(k)\otimes I_9$, while $\xi = 0$ corresponds to the unfixed linearized Einstein–Hilbert tensor projected onto $\mathrm{Sym}_0^2(\mathbb{R}^4)$.

Theorem 2.2 (Sharp 24-Cell Brillouin-Zone Coercivity, Zero Doublers, and $5\oplus 3\oplus 1$ Spin-2 Coercivity; `W1Neon_R1`, `W1Neon_R8`)**.** *Let* $a > 0$.

1. ***Exact*** $2\pi D_4$***-periodicity and sharp*** $\mathrm{BZ}_{24}(a)$ ***coercivity:*** $\Delta_{D_4^*,a}$, $\nabla_{D_4^*,a}$, *and* $L_a^{(\xi)}$ *are exactly periodic under* $k\mapsto k + (2\pi/a)n$ *for every* $n\in D_4$*. For every* $k\in\mathrm{BZ}_{24}(a)$*,*

$$\frac{8}{3\pi^2}\,\|k\|^2 \;\le\; \Delta_{D_4^*,a}(k) \;\le\; \|k\|^2. \tag{11}$$

2. ***Double vertex sharpness and absence of*** 4***D doublers:*** *The lower bound Eq. (11) is attained with exact equality at* both 24*-cell vertex orbits,* $k = (\pi/a,\pi/a,\pi/a,\pi/a)$ *and* $k = (2\pi/a,0,0,0)$ *(where* $\Delta_{D_4^*,a}(k) = 32/(3a^2)$ *and* $\|k\|^2 = 4\pi^2/a^2$*). Consequently* $\Delta_{D_4^*,a}(k) > 0$ *for every* $k\in \mathrm{BZ}_{24}(a)\setminus\{0\}$*: there are zero spurious massless doublers anywhere in the actual first Brillouin zone.*
3. $5\oplus 3\oplus 1$ ***Barnes–Rivers decomposition and sharp*** $3/4$ ***matrix bound:*** *For any* $v\in\mathbb{R}^4$ *and* $h\in\mathrm{Sym}_0^2(\mathbb{R}^4)$*, the self-adjoint operator* $\mathcal{D}_v$ *obeys the exact polynomial identity* $\mathcal{D}_v^2 h =$

$\|v\|^2\mathcal{D}_v h + (v^\top hv)\,\Phi_0(v)$ *(where* $\Phi_0(v)_{\mu\nu} = v_\mu v_\nu - \frac{1}{4}\|v\|^2\delta_{\mu\nu}$ *spans the spin-*0 *longitudinal mode), decomposing* $\mathrm{Sym}^2_0(\mathbb{R}^4)$ *orthogonally into three Barnes–Rivers eigenspaces*[73] *of dimensions* 5 *(transverse-traceless spin-*2*, eigenvalue* 0*),* 3 *(vector spin-*1*, eigenvalue* $\|v\|^2$*), and* 1 *(scalar longitudinal spin-*0*, eigenvalue* $\frac{3}{2}\|v\|^2$*). Moreover,* $\|hv\|^2 \le \frac{3}{4}\|v\|^2\|h\|_F^2$ *with sharp equality on* $h = \mathrm{diag}(3,-1,-1,-1)/\sqrt{12}$ *along* $v = e_0$*.*

4. ***Uniform spin-*2 *Sobolev/Gårding coercivity and*** $O(a^2)$ ***resolvent convergence:*** *For every* $\xi > \frac{1}{3}$*, every* $k \in \mathrm{BZ}_{24}(a)$*, and every* $h \in \mathrm{Sym}^2_0(\mathbb{R}^4)$*, setting* $c_\xi := \min\!\big(1, \frac{3\xi-1}{2}\big) > 0$ *and* $C_\xi := \max\!\big(1, \frac{3\xi-1}{2}\big)$*,*

$$\frac{8}{3\pi^2}\,c_\xi\,\|k\|^2\|h\|_F^2 \;\le\; c_\xi\,\Delta_{D_4^*,a}(k)\|h\|_F^2 \;\le\; \langle h, L_a^{(\xi)}(k)h\rangle_F \;\le\; C_\xi\,\Delta_{D_4^*,a}(k)\|h\|_F^2, \tag{12}$$

with exact equality $\langle h, L_a^{(\xi)}(k)h\rangle_F = \Delta_{D_4^*,a}(k)\|h\|_F^2$ *on the* 5*-dimensional* TT *subspace,* $O(a^4)$ $O(4)$ *anisotropy bounded by* $\big(\frac{1}{720} + \frac{|\xi-1|}{20}\big)a^4\|k\|^6\|h\|_F^2$*, and uniform-in-*$m$ *resolvent convergence* $\|(L_a^{(\xi)}(k)+m^2)^{-1}h - (L_0^{(\xi)}(k)+m^2)^{-1}h\|_F \le C(\xi)a^2\|h\|_F$ *across all of* $\mathrm{BZ}_{24}(a)$*.*

Proof outline. By F_4 signed-permutation symmetry, any $k \in \mathrm{BZ}_{24}(a)$ can be ordered $0 \le ak_3 \le ak_2 \le ak_1 \le ak_0$ with $ak_0 + ak_1 \le 2\pi$. When $ak_0 \le \pi$, k lies in the inscribed hypercube $[-\pi/a, \pi/a]^4$ where the chord inequality $1 - \cos\theta \ge (2/\pi^2)\theta^2$ on $[-\pi,\pi]$ applies directly. When $\pi < ak_0 \le 2\pi$, setting $u = \frac{ak_0-\pi}{\pi} \in (0,1]$ and $t = \frac{ak_1}{\pi} \in [0, 1-u]$ reduces Eq. (11) to two strictly positive cubic sum-of-squares certificates on $[0,1]$: $32u^3 - 15u + 4 > 0$ and $58t^3 - 45t + 16 > 0$, combined with $\pi \in (3.14, 3.15)$. Evaluating Eq. (3) at $k = (\pi/a)^4$, the 4 axial bonds contribute $1 - \cos\pi = 2$ each (sum 8), while the 8 body bonds satisfy $e_b \cdot k \in \{2\pi, 0, \pm\pi\}$: specifically 1 bond has 2π $(1 - \cos = 0)$, 3 bonds have π $(1 - \cos = 2$, contributing 6), 3 bonds have 0 (0), and 1 bond has $-\pi$ (2), yielding $8 + 8 = 16$ and $\Delta_{D_4^*,a} = \frac{2}{3a^2} \cdot 16 = \frac{32}{3a^2}$. At $k = (2\pi/a, 0, 0, 0)$, all 4 axial bonds give 0 and all 8 body bonds have $e_b \cdot k = \pi$ $(1 - \cos\pi = 2$, sum 16), again yielding $\frac{32}{3a^2} = \frac{8}{3\pi^2}(4\pi^2/a^2)$. For item 3, writing h in the orthonormal eigenbasis of $\mathcal{D}_v$ gives $\langle h, \mathcal{D}_v h\rangle_F = 2\|hv\|^2$ (since $\mathrm{tr}\, h = 0$), and the sharp inequality $\|hv\|^2 \le \frac{3}{4}\|v\|^2\|h\|_F^2$ ensures $0 \le \langle h, \mathcal{D}_v h\rangle_F \le \frac{3}{2}\|v\|^2\|h\|_F^2 \le \frac{3}{2}\Delta_{D_4^*,a}(k)\|h\|_F^2$. Substituting into Eq. (10) gives the lower coefficient $1 + \min(0, \frac{3}{2}(\xi-1)) = \min(1, \frac{3\xi-1}{2}) > 0$ precisely when $\xi > \frac{1}{3}$. □

2.3 Full 12×12 gauge-fixed D_4^* graviton operator and uncut one-loop integrability

Beyond the 9-component traceless metric parameterization, the native bond-length carrier of linearized gravity on D_4^* carries 12 bond strains per site (matching the 12 bond directions in $\mathcal{B}_{12}$). At the unique light-cone reach parameter $\kappa_{\mathrm{cone}} = \frac{1}{2}$ (selected uniquely by vanishing of the dimension-six dispersion objective `directClassObjective`), the gauge-fixed linearized graviton operator is the 12×12 Hermitian matrix $M(k) = L_k + G_k G_k^\dagger$, where L_k is the 12×12 linearized curvature Hessian and G_k is the 12×4 lattice diffeomorphism matrix built from the 12 half-lattice bond vectors $b_e = 2e_b$ (`Neon_R54`, `Neon_R59`).

Theorem 2.3 (Full 12×12 $(11,1)$ Signature, Zero Doublers, and Uncut $\delta_{\mathrm{IR}} = 0$ IR-and-UV One-Loop Integrability; `Neon_R54`, `Neon_R59`)**.** *At the unique dispersion-free reach parameter* $\kappa_{\mathrm{cone}} = \frac{1}{2}$ *on* D_4^**:*

1. ***Exact*** $(11,1)$ ***signature and zero doublers across*** $(-2\pi, 2\pi)^4 \setminus \{0\}$***:*** *The reciprocal lattice* $2\pi D_4$ *is disjoint from the open doubled cube* $(-2\pi, 2\pi)^4 \setminus \{0\}$ *and from all four doubled axis corners* $2\pi e_\mu$*. For every* $k \in (-2\pi, 2\pi)^4 \setminus \{0\}$ *(and every* $k = 2\pi e_\mu$*),* $M(k) = L_k + G_k G_k^\dagger$ *is Hermitian with exact signature* $(11,1)$ *(*11 *positive and* 1 *negative conformal eigenvalue), trivial kernel (*$\forall v \neq 0$*,* $M(k)v \neq 0$*),* $\det M(k) \neq 0$*, and exact two-sided inverse* $M(k)^{-1}$*.*
2. ***Exact isotropic gauge-Gram identity and small-***k ***determinant floor:*** *On the* 12 *half-lattice bonds* $b_e = 2e_b$*,*

$$\sum_{e=1}^{12}(b_e \cdot k)^2|b_e \cdot \xi|^2 \;=\; 8\|k\|^2\|\xi\|^2 + 16|k \cdot \xi|^2 \;\ge\; 8\|k\|^2\|\xi\|^2, \tag{13}$$

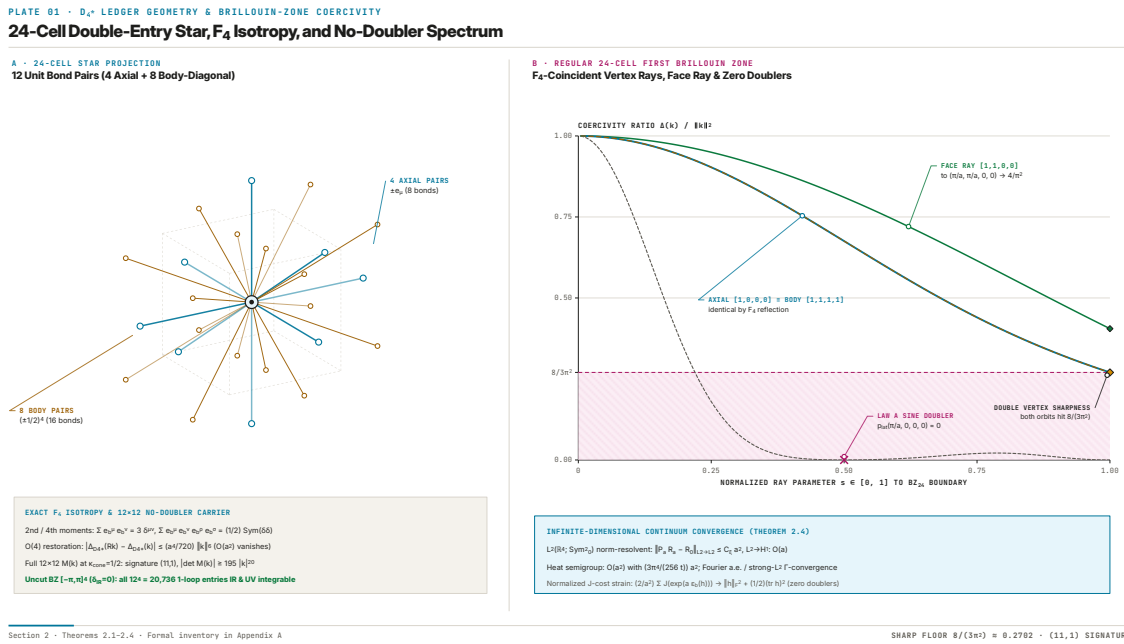

Fig. 1 Plate 01 (D_4^* Geometry and Brillouin-Zone Coercivity). (A) Orthographic 3D projection of the 24-bond D_4^* double-entry star (4 axial pairs $\pm e_\mu$ in cyan, 8 body-diagonal pairs $(\pm\frac{1}{2})^4$ in amber), carrying exact F_4 fourth-moment isotropy and $(11,1)$ signature on the full 12×12 gauge-fixed carrier $M(k)$ at $\kappa_{\text{cone}} = \frac{1}{2}$. **(B)** Exact coercivity ratio $\Delta_{D_4^*,a}(k)/\|k\|^2$ across $\mathrm{BZ}_{24}(a)$: the axial ray $[1,0,0,0]$ to $(2\pi/a,0,0,0)$ and the body-diagonal ray $[1,1,1,1]$ to $(\pi/a)^4$ coincide identically under the F_4 reflection $I_4 - \frac{1}{2}\mathbf{1}_{4\times 4}$ (cyan with amber dash overlay) and both attain the sharp floor $8/(3\pi^2) \approx 0.2702$ at $s = 1$, while the face-center ray $[1,1,0,0]$ reaches $4/\pi^2 \approx 0.4053$ (green); all rays remain strictly positive with zero doublers, contrasted against the Law A sine symbol vanishing at $(\pi/a,0,0,0)$ (Theorems 2.2 and 2.3).

implying for every $k \in [-\frac{1}{2},\frac{1}{2}]^4$ *that* $|\det(G_k^\dagger G_k)| \geq \frac{1}{16}\|k\|^8$ *and*

$$|\det M(k)| \;\geq\; 195\,\|k\|^{20}. \tag{14}$$

3. ***Sharp*** $O(1/\|k\|^2)$ ***matrix propagator bound and uncut*** $\delta_{\text{IR}} = 0$ ***one-loop integrability:*** *Using an explicit integer basis* U $(\det U = -192)$ *splitting* $\ker L_0$ *(the* $10D$ *metric subspace) from* $\operatorname{ran} L_0$ *(the* $2D$ *optical bond subspace), congruence rescaling* $D(k)(U^\top M(k)U)D(k)$ *with* $D(k) = \operatorname{diag}(\|k\|^{-1}I_{10}, I_2)$ *yields a uniform constant* $C > 0$ *such that*

$$\left|\left(M(k)^{-1}\right)_{ij}\right| \;\leq\; \frac{C}{\|k\|^2} \qquad \forall k \in \left[-\tfrac{1}{2},\tfrac{1}{2}\right]^4 \setminus \{0\},\ \forall i,j \in \{1,\dots,12\}. \tag{15}$$

Consequently, for every nonzero external momentum $p \in (-\pi,\pi)^4 \setminus \{0\}$*, arbitrary polarizations* ℓ_1, ℓ_2*, mass parameter* m*, and every one of the* $12^4 = 20{,}736$ *bond-index tuples* (i,j,a,b)*, the full* 12×12 *interacting one-loop graviton self-energy integrand coupled to the* 104*-hinge cubic vertex is Lebesgue integrable over the entire uncut Brillouin cube* $[-\pi,\pi]^4$ *with zero IR cutoff (*$\delta_{\text{IR}} = 0$*) and zero UV cutoff.*

Proof outline of Theorem 2.3. Any $n \in D_4$ has $\sum_\mu n_\mu \in 2\mathbb{Z}$; therefore $2\pi n \notin (-2\pi,2\pi)^4 \setminus \{0\}$ (every nonzero $n \in D_4$ has either an entry $|n_\mu| \geq 2$ or at least two entries $|n_\mu| = |n_\nu| = 1$, forcing $\max_\mu |2\pi n_\mu| \geq 2\pi$) and $2\pi e_\mu \notin 2\pi D_4$ (odd coordinate sum 1). By the signature-invertibility lemma (`hermitian_posGE_negGE_det_ne_zero_r54`), any 12×12 Hermitian matrix with 11 positive and 1 negative eigenvalues has trivial kernel and invertible determinant. In the small-k neighbourhood $[-\frac{1}{2},\frac{1}{2}]^4$, expanding the 12 half-lattice bonds $b_e = 2e_b$ using Eq. (4) yields the isotropic identity Eq. (13), forcing every eigenvalue of $G_k^\dagger G_k$ to satisfy $\geq \frac{1}{2}\|k\|^2$ and hence $|\det(G_k^\dagger G_k)| \geq \frac{1}{16}\|k\|^8$. Combining this with the exact determinant factorization of $M(k)$ gives $|\det M(k)| \geq 195\|k\|^{20}$. Conjugating by the explicit integer basis U $(\det U = -192)$ whose first 10 columns span $\ker L_0$ (with vanishing first derivatives

$U_0^\top(\partial_\mu L_0)U_0 = 0$) and rescaling by $D(k) = \mathrm{diag}(\|k\|^{-1} I_{10}, I_2)$ yields a matrix $\tilde{H}(k)$ with uniformly bounded entries and $|\det \tilde{H}(k)| \geq 192^2 \cdot 195 > 0$, proving Eq. (15) via Cramer's rule. Since $1/\|k\|^2$ is locally integrable near $k = 0$ in four dimensions ($\int_0^{1/2} r^3 r^{-2}\, dr < \infty$) and $M(k)^{-1}$ is continuous and bounded away from $k = 0$ on $[-\pi, \pi]^4$, every one-loop bubble product $M(k)^{-1}_{ij} M(k+p)^{-1}_{ab}$ ($p \neq 0$) is absolutely integrable over uncut $[-\pi, \pi]^4$ without any IR cutoff. □

2.4 Infinite-dimensional $L^2(\mathbb{R}^4; \mathrm{Sym}_0^2)$ norm-resolvent and Fourier-space Γ-convergence

To bridge the finite-spacing lattice operators to infinite-dimensional continuum function spaces, let $P_a = \mathbf{1}_{\mathrm{BZ}_{24}(a)}$ denote the Shannon band-limited Fourier projection onto $\mathrm{BZ}_{24}(a) \subset \mathbb{R}^4$, and define the continuum and discrete Sobolev energies on $L^2(\mathbb{R}^4; \mathrm{Sym}_0^2)$ via Plancherel integration against $L_0^{(\xi)}(k)$ and $L_a^{(\xi)}(k)$ (`W1Neon_R10`).

Theorem 2.4 (Infinite-Dimensional Norm-Resolvent, Heat-Semigroup, and Fourier-Space a.e./Strong-L^2 Γ-Convergence; `W1Neon_R10`)**.** *Let $\xi > \frac{1}{3}$ and $m > 0$. On $\mathbb{R}^4$ with four-dimensional Lebesgue measure:*

1. ***Exact* 24*-cell spectral geometry:*** *$\mathrm{BZ}_{24}(a)$ is Borel measurable with sharp UV ceiling $\|k\|^2 \leq 4\pi^2/a^2$ inside $\mathrm{BZ}_{24}(a)$ and sharp exterior gap $\|k\|^2 > 2\pi^2/a^2$ outside $\mathrm{BZ}_{24}(a)$.*
2. ***Global* $L^2 \to L^2$ *($O(a^2)$), $L^2 \to H^1$ ($O(a)$), and heat-semigroup ($O(a^2)$) norm convergence:*** *For every $F \in L^2(\mathbb{R}^4; \mathrm{Sym}_0^2)$, $a > 0$, and $t > 0$,*

$$\int_{\mathbb{R}^4} \|(P_a R_a^{(\xi)} - R_0^{(\xi)}) F(k)\|_F^2 \, dk \;\leq\; \big(C_{\mathrm{glob}}(\xi)\, a^2\big)^2 \int_{\mathbb{R}^4} \|F(k)\|_F^2 \, dk, \tag{16}$$

$$\int_{\mathbb{R}^4} \|k\|^2 \|(P_a R_a^{(\xi)} - R_0^{(\xi)}) F(k)\|_F^2 \, dk \;\leq\; \big(C_{H^1}(\xi)\, a\big)^2 \int_{\mathbb{R}^4} \|F(k)\|_F^2 \, dk, \tag{17}$$

$$\int_{\mathbb{R}^4} \|(P_a e^{-t\Delta_{D_4^{*,a}}} - e^{-t\Delta_0}) F(k)\|_F^2 \, dk \;\leq\; \left(\frac{3\pi^4}{256t}\, a^2\right)^2 \int_{\mathbb{R}^4} \|F(k)\|_F^2 \, dk. \tag{18}$$

3. ***Fourier-space a.e./strong-L^2 Γ-convergence and nonlinear J-cost strain limit:*** *For any sequence $a_n \to 0^+$ and any Fourier-space pointwise a.e.-convergent sequence $u_n \to u$ (in particular any strong-L^2 convergent sequence along a subsequence), Fatou's lemma yields the Γ-lim inf bound $E_0(u) \leq \liminf_{n\to\infty} E_{a_n}(u_n)$; conversely, for every $u \in H^1(\mathbb{R}^4; \mathrm{Sym}_0^2)$, the Shannon recovery sequence $u_a = P_a u$ satisfies $u_a \to u$ strongly in L^2 and $E_a(u_a) \to E_0(u)$ (at quantitative rate $O(a^2)\|u\|_{H^2}^2$ for $u \in H^2$). (Because the proved* lim inf *uses Fatou's lemma on pointwise a.e.-converging Fourier modes rather than arbitrary weak-L^2 sequences, we state it strictly as Fourier a.e./strong-L^2 Γ-convergence[52;53] rather than weak-L^2 Mosco convergence[51], even though the formal Lean declaration retains the legacy identifier `mosco_gamma_liminf_D4_spin2`.) Moreover, the normalized nonlinear J-cost bond-strain functional $\frac{2}{a^2}\sum_{b=1}^{12} J(e^{a\,\varepsilon_b(h)})$ converges at rate $O(a^2)$ to $\|h\|_F^2 + \frac{1}{2}(\mathrm{tr}\, h)^2$.*

3 Coupled $O(4)$-Invariant Spin-2 J-Cost QFT, Reflection Positivity, and Strict Non-Gaussianity

Quadratic lattice actions yield Gaussian measures whose connected four-point functions vanish identically, whereas naive polynomial interactions (ϕ^4) fail to match the reciprocal structure of the Recognition Science ledger and require delicate renormalization to control large fields. Because the canonical cost $J(e^u) = \cosh u - 1$ grows exponentially at large strain while obeying the exact global convexity floor $\frac{d^2}{du^2} J(e^u) = \cosh u \geq 1$, it simultaneously guarantees non-perturbative measure existence, Brascamp–Lieb Gaussian domination[26–29], spectral-gap clustering, and strict non-Gaussianity without expanding in small λ.

3.1 Non-separable Brascamp–Lieb convexity and nonlinear Poincaré spectral gap

Fix a finite index set ι (for instance $\Lambda\times\{0,\dots,8\}$ for a 9-component spin-2 field on a finite lattice Λ). Let $A\in\mathbb{R}^{\iota\times\iota}$ be a symmetric positive-semidefinite kinetic matrix and let $P:\mathbb{R}^\iota\to\mathbb{R}$ be an even continuous potential satisfying *uniform c-convexity* (`ConvexPot c P`): $c>0$ and the excess $y\mapsto P(y)-\frac{c}{2}\|y\|^2$ is convex on $\mathbb{R}^\iota$. Define the interacting Gibbs probability measure

$$d\mu_{A,P}(\phi)\;=\;\frac{1}{Z_{A,P}}\,\exp\!\Big(-\frac{1}{2}\langle\phi,A\phi\rangle-P(\phi)\Big)\,d\phi,\qquad Z_{A,P}=\int_{\mathbb{R}^\iota}e^{-\frac{1}{2}\langle\phi,A\phi\rangle-P(\phi)}\,d\phi. \tag{19}$$

On $\mathrm{Sym}^2_0(\mathbb{R}^4)$, we fix the explicit rational Frobenius-orthonormal basis $\{E_0,\dots,E_8\}$ (`W1Opus_R14`):

$$\begin{aligned}
&E_0=\tfrac12\,\mathrm{diag}(1,1,-1,-1), && E_1=\tfrac12\,\mathrm{diag}(1,-1,1,-1), && E_2=\tfrac12\,\mathrm{diag}(1,-1,-1,1),\\
&E_{3,4}=\tfrac12(E^{\mathrm{s}}_{01}\pm E^{\mathrm{s}}_{23}), && E_{5,6}=\tfrac12(E^{\mathrm{s}}_{02}\pm E^{\mathrm{s}}_{13}), && E_{7,8}=\tfrac12(E^{\mathrm{s}}_{03}\pm E^{\mathrm{s}}_{12}),
\end{aligned} \tag{20}$$

where $(E^{\mathrm{s}}_{ij})_{\mu\nu}=\delta_{i\mu}\delta_{j\nu}+\delta_{j\mu}\delta_{i\nu}$. The linear map $\mathrm{embed}:\mathbb{R}^9\to\mathrm{Sym}^2_0(\mathbb{R}^4)$, $y\mapsto\sum_{k=0}^8 y_kE_k$, is an exact Frobenius isometry ($\|\mathrm{embed}(y)\|_F^2=\|y\|^2$) whose completeness tensor is the traceless symmetric projector $\sum_{k=0}^8(E_k)_{\mu\nu}(E_k)_{\rho\sigma}=P_{T,\mu\nu\rho\sigma}:=\frac12(\delta_{\mu\rho}\delta_{\nu\sigma}+\delta_{\mu\sigma}\delta_{\nu\rho})-\frac14\delta_{\mu\nu}\delta_{\rho\sigma}$.

Theorem 3.1 (Non-Separable Brascamp–Lieb, Nonlinear Poincaré Gap, and Transfer-Chain Clustering; `W1Opus_R14`, `W1Opus_R15`)**.** *Let $A\succeq 0$ and suppose P satisfies `ConvexPot c P` with $c>0$.*

1. ***Multivariate Prékopa–Leindler and non-separable Brascamp–Lieb Gaussian domination:*** *The partition function satisfies $0<Z_{A,P}<\infty$, $\mu_{A,P}$ is a probability measure, and for every $v\in\mathbb{R}^\iota$ and $s\in\mathbb{R}$,*

$$\mathbb{E}_{\mu_{A,P}}\Big[e^{s\langle v,\phi\rangle}\Big]\;\le\;\exp\!\Big(\frac{s^2}{2}\langle v,(A+cI)^{-1}v\rangle\Big),\qquad \mathrm{Var}_{\mu_{A,P}}(\langle v,\phi\rangle)\;\le\;\langle v,(A+cI)^{-1}v\rangle\;\le\;\frac{\|v\|^2}{c}. \tag{21}$$

2. ***Nonlinear Brascamp–Lieb and Dirichlet-form Poincaré spectral gap:*** *For every L-Lipschitz measurable observable ψ, $\mathrm{Var}_{\mu_{A,P}}(\psi)\le L^2/c$, and for every $C^{1,1}$ observable ψ with bounded gradient,*

$$\mathrm{Var}_{\mu_{A,P}}(\psi)\;\le\;\mathbb{E}_{\mu_{A,P}}\big[\langle\nabla\psi,(A+cI)^{-1}\nabla\psi\rangle\big]\;\le\;\frac1c\,\mathbb{E}_{\mu_{A,P}}\big[\|\nabla\psi\|^2\big]. \tag{22}$$

3. ***Two RS spin-2 realizations:***
   - 24-bond D_4^* strain potential (`W1Opus_R14`): $V_{\mathrm{str}}(y)=\frac{m^2}{2}\|y\|^2+\lambda\sum_{b\in\pm\mathcal{B}_{12}}J\big(e^{\varepsilon_b(\mathrm{embed}(y))}\big)$ *obeys $\sum_{b\in\pm\mathcal{B}_{12}}\varepsilon_b^2=2\|y\|^2$, so V_{str} is uniformly convex with $c=m^2+2\lambda$. On the 4D torus $(\mathbb{Z}/L)^4$ with kinetic form $K=\kappa_1\sum_\mu D_\mu^\dagger D_\mu+\kappa_2\,\mathrm{div}^\dagger\mathrm{div}$ ($\kappa_1,\kappa_2\ge0$), every matrix entry obeys $\mathrm{Var}(H_{\alpha\beta}(x))\le\frac{3}{8\lambda}$ uniformly in L, and the Dirichlet-form spectral gap is $\ge m^2+2\lambda$.*
   - Coupled $O(4)$-invariant radial J-cost (`W1Opus_R30`): $V_{\mathrm{rad}}(H)=\frac{m^2}{2}\|H\|_F^2+\lambda J\big(e^{\|H\|_F}\big)=\frac{m^2}{2}\|y\|^2+\lambda(\cosh\|y\|-1)$ *is uniformly convex with $c=m^2+\lambda$ on every finite bond graph.*
4. ***Interacting transfer-matrix clustering:*** *For a Euclidean open chain of $n+1$ spatial slices with strongly c-convex slice action A_{slice} and nearest-slice temporal coupling $\beta\|u-v\|^2$ ($\beta>0$), the normalized transfer operator P_T leaves constants invariant ($P_T1=1$), contracts Lipschitz constants by $\mathrm{Lip}(P_Tg)\le\rho\,\mathrm{Lip}(g)$ with $\rho=\frac{2\beta}{2\beta+c}<1$, and implies uniform-in-L exponential temporal clustering*

$$|\langle F,G\rangle_n-\langle F,1\rangle_n\langle 1,G\rangle_n|\;\le\;\frac{C_FL}{\sqrt{c}}\,\rho^n,\qquad m_{\mathrm{gap}}\;\ge\;\ln\!\Big(1+\frac{c}{2\beta}\Big)>0. \tag{23}$$

Proof outline. Multivariate Prékopa–Leindler on $\mathbb{R}^\iota$ is proved by induction on $|\iota|$ from the one-dimensional inequality. Applying Prékopa–Leindler at $t=\frac12$ to the tilted Boltzmann densities $F(x)=$

$e^{-H(x)+s\langle v,x\rangle}$, $G(y) = e^{-H(y)-s\langle v,y\rangle}$, and $H_{\mathrm{mid}}(z) = e^{-H(z)+\frac{s^2}{2}\langle v,(A+cI)^{-1}v\rangle}$ gives $\mathbb{E}[e^{s\langle v,\phi\rangle}]\mathbb{E}[e^{-s\langle v,\phi\rangle}] \le e^{s^2\langle v,(A+cI)^{-1}v\rangle}$ (using evenness of P so the two factors are equal), yielding Eq. (21). The nonlinear Brascamp–Lieb inequality Eq. (22) follows via the Bobkov–Ledoux budget argument (`pl_budget`), combining $1+\varepsilon^2\,\mathrm{Var}(\psi) \le \mathbb{E}[e^{\varepsilon\psi}]\mathbb{E}[e^{-\varepsilon\psi}]$ with the second-order $C^{1,1}$ Taylor bound $\psi(z+a)-\psi(z-a) \le 2\langle\nabla\psi(z),a\rangle + 2M\|a\|^2$ and sending $\varepsilon \to 0^+$. For item 4, Prékopa marginal preservation propagates strong convexity along the Riccati recursion $c_{k+1} = c + \frac{2\beta c_k}{2\beta+c_k} \ge c$, and differentiating the conditional expectation $P_T g(u)$ under the integral sign yields $|\nabla(P_T g)(u)| \le \frac{2\beta}{2\beta+c}\,\mathrm{Lip}(g)$ via Cauchy–Schwarz and the conditional Poincaré inequality. □

3.2 Infinite-volume spin-2 Osterwalder–Schrader reconstruction and vacuum non-Gaussianity

Passing to the infinite spatial volume $L \to \infty$ requires controlling finite-volume Schwinger functions uniformly in L and verifying that reflection positivity and spectral gaps survive the thermodynamic limit (`W1Opus_R25`, `W1Opus_R26`).

Theorem 3.2 (Infinite-Volume Interacting Spin-2 OS Reconstruction, Unique Vacuum, and Sub–Gaussian Two-Field States; `W1Opus_R25`, `W1Opus_R26`)**.** *Consider the interacting 9-component D_4^* strain J-cost spin-2 field (convexity $c_2 = m^2 + 2\lambda$) and the 4D scalar J-cost field ($c_1 = m^2 + \lambda$) with spatial coupling $\kappa \ge 0$, temporal coupling $\beta > 0$, $m^2 \ge 0$, and $\lambda > 0$. Inside the single-site contraction regime $6\kappa + 4\beta < c_2$ (respectively $6\kappa + 4\beta < c_1$):*

1. ***Whole-sequence infinite-volume Schwinger functions:*** *As $L \to \infty$, the finite-volume infinite-time two-point functions converge along the whole sequence to unique translation-invariant limits $S_\infty^{(2)}(x,y,a,b,t)$ (respectively $S_\infty^{(1)}$) obeying $|S_\infty^{(2)}| \le e^{-\Delta_2 t}/c_2$ with explicit mass gap $\Delta_2 = \mathrm{massGap}(\beta, c_2) > 0$ and strictly positive diagonal floor $S_\infty^{(2)}(x,x,a,a,0) \ge c_{\min,2} > 0$.*
2. ***Complete OS Hilbert space, unique vacuum, and positive self-adjoint transfer operator:*** *Along a subsequence $L_k \to \infty$ for the extended index set (vacuum Ω, single-field states $\phi_x\Omega$, and equal-time two-field states $\phi_x\phi_y\Omega$), the limiting kernel satisfies both even-shift and odd-shift OS reflection positivity. Completing the quotient pre-Hilbert space yields a complete Hilbert space $\mathcal{H}_{\mathrm{OS}}$, a unit vacuum Ω ($\|\Omega\| = 1$), and a bounded self-adjoint positive transfer contraction $0 \le T \le 1$ satisfying $T\Omega = \Omega$, $\langle\Omega, \phi_x\Omega\rangle = 0$, exact orthogonality of odd and even parity sectors at all times, and a strict spectral gap on $\Omega^\perp$:*

$$\|T^t\psi\| \;\le\; e^{-\Delta t}\,\|\psi\| \qquad \forall\psi \in \Omega^\perp,\ \forall t \in \mathbb{N}, \tag{24}$$

   explicitly witnessed at $(\kappa, \beta, m^2, \lambda) = (\frac{1}{12}, \frac{1}{8}, 1, 1)$.
3. ***Strict non-Gaussianity of the infinite-volume vacuum:*** *For the infinite-time scalar vacuum measure μ_∞ (realized via $\Psi = \lambda_0^{-1}\mathcal{T}\Psi$ as the middle-slice marginal of a convex three-slice Gibbs measure), there exist volume-independent $\kappa_0, \delta_{\mathrm{NG}} > 0$ such that for all $0 \le \kappa \le \kappa_0$, $0 < \beta \le \kappa_0$, and every $\lambda > 0$, every infinite-volume OS limit obeys*

$$\|\big(\phi_x^2 - \langle\phi_x^2\rangle\big)\Omega\|^2 \;=\; U_4^{(\infty)}(x) + 2\langle\phi_x^2\rangle^2 \;\le\; 2\langle\phi_x^2\rangle^2 - \delta_{\mathrm{NG}}, \tag{25}$$

   certifying that the two-field excited state norm sits strictly below its Gaussian Wick value.

3.3 Coupled $O(4)$-invariant spin-2 J-cost measure on D_4^* slabs

To eliminate any possibility that a spin-2 tensor measure reduces to nine decoupled scalar fields, `W1Opus_R30` replaces separable or axis-aligned couplings with the genuinely coupled $O(4)$-invariant (indeed $O(9)$-invariant) radial J-cost potential

$$V_{\mathrm{rad}}(H) \;=\; \frac{m^2}{2}\|H\|_F^2 + \lambda\big(\cosh\|H\|_F - 1\big), \qquad H \in \mathrm{Sym}_0^2(\mathbb{R}^4), \tag{26}$$

coupled via the de Donder–Feynman kinetic form $\kappa \sum_{\langle p,q\rangle \in D_4^*} \|H_p - H_q\|_F^2$ across the full 24-bond D_4^* slab graph. Specifically, the primitive dual-lattice time functional $t(x) = x_0 + x_1$ slices D_4^* into three-dimensional face-centred cubic (fcc) hyperplanes parameterized by $(t, \xi) \in \mathbb{Z} \times \mathbb{Z}^3$ via the slice basis $g_1 = (\frac{1}{2}, -\frac{1}{2}, \frac{1}{2}, \frac{1}{2})$, $g_2 = e_2$, $g_3 = e_3$. Every one of the 24 unit bonds of D_4^* changes t by at most 1: exactly 6 bonds step forward ($\Delta t = +1$), 6 step backward ($\Delta t = -1$), and 12 lie within the fcc slice ($\Delta t = 0$). The orthogonal involution

$$\Theta_{\mathrm{slab}}(x_0, x_1, x_2, x_3) \;=\; (-x_1, -x_0, x_2, x_3) \tag{27}$$

is an exact symmetry of D_4^* that permutes all 24 bonds and acts in slab coordinates as pure time reflection $(t, \xi) \mapsto (-t, \xi)$.

Theorem 3.3 (Coupled $O(4)$-Invariant Spin-2 J-Cost Measure on D_4^* Slabs: Symmetry, Cross-Component $U_4 < 0$, Site OS2, Clustering, and UV Floor; `W1Opus_R30`)**.** *Let $m^2 \geq 0$, $\lambda > 0$, and $\kappa \geq 0$. Consider the coupled Gibbs measure on the periodic D_4^* slab torus $\Lambda_{M_{\mathrm{sl}},L} = (\mathbb{Z}/2M_{\mathrm{sl}}\mathbb{Z}) \times (\mathbb{Z}/L\mathbb{Z})^3$ with potential $\sum_{x \in \Lambda_{M_{\mathrm{sl}},L}} V_{\mathrm{rad}}(H_x)$ and 24-bond de Donder kinetic coupling κ.*

1. ***Exact internal*** $O(4)$ ***(and*** $O(9)$***) invariance:*** *The global internal action $H_x \mapsto O H_x O^\top$ ($O \in O(4)$, realized as an orthogonal matrix $\rho(O) \in O(9)$ in the basis Eq. (20)) preserves Lebesgue measure and leaves the coupled Gibbs measure strictly invariant.*
2. ***Non-factorization via cross-component Ursell cumulants:*** *For any measure invariant under coordinate swaps, sign flips, and 45° rotations of the (E_3, E_4) plane, $\mathbb{E}[y_3^4] = 3\mathbb{E}[y_3^2 y_4^2]$ and*

$$U_4(H_{01}, H_{01}, H_{23}, H_{23}) \;=\; \frac{1}{4}\big(\mathbb{E}[y_3^2 y_4^2] - (\mathbb{E}[y_3^2])^2\big) \;=\; \frac{1}{3}\, U_4(H_{01}). \tag{28}$$

   At a single site ($\kappa = 0$), exact 9-dimensional dilation virial identities $\mathbb{E}[w] = 9$ and $\mathbb{E}[\|H\|_F^2 w] = 11\mathbb{E}[\|H\|_F^2]$ (with $w = m^2\|H\|_F^2 + \lambda\|H\|_F \sinh\|H\|_F$) combined with Chebyshev's inequality for the strictly increasing function $a(s) = \frac{m^2}{2} + \frac{\lambda \sinh\sqrt{s}}{2\sqrt{s}}$ force $9\mathbb{E}[s^2] < 11(\mathbb{E}[s])^2$, hence $U_4^{\mathrm{site}}(H_{01}, H_{01}, H_{23}, H_{23}) < 0$ for every *$m^2 \geq 0$ and $\lambda > 0$ (numerically -0.003870 at $m^2 = 0, \lambda = 1$, where $9\mathbb{E}[s^2] = 191.826 < 11(\mathbb{E}[s])^2 = 205.619$).*
3. ***Volume-uniform lattice non-Gaussianity:*** *Because the slab kinetic operator obeys $\|A_{\mathrm{slab}}\| \leq 48\kappa$, block reduction bounds the lattice cross-cumulant within $C \cdot 48\kappa$ of the site value uniformly in (M_{sl}, L). Hence there exist $\kappa_0 > 0$ and $\delta_{\mathrm{NG}} > 0$ independent of (M_{sl}, L) such that for every $\kappa \in [0, \kappa_0]$ and every site $x \in \Lambda_{M_{\mathrm{sl}},L}$,*

$$U_4(H_{01}, H_{01}, H_{23}, H_{23})(x) \;\leq\; -\delta_{\mathrm{NG}} \;<\; 0, \qquad U_4(H_{01})(x) \;\leq\; -3\delta_{\mathrm{NG}} \;<\; 0. \tag{29}$$

   Consequently, neither $(H_{01}(x), H_{23}(x))$ nor $(y_3(x), y_4(x))$ is independent, ruling out every product/factorized measure both at finite volume and in every subsequential infinite-volume limit.
4. ***Unconditional site reflection positivity (OS2) and temporal clustering:*** *Since every D_4^* bond changes t by at most 1, the periodic slab Hamiltonian splits cleanly as $K + K \circ \Theta_{\mathrm{slab}}$ across the reflection planes $t = 0$ and $t = M_{\mathrm{sl}}$, yielding exact site reflection positivity[40] $\int F \cdot (F \circ \Theta_{\mathrm{slab}})\, d\mu_{\mathrm{slab}} \geq 0$ for every bounded observable F supported on $0 \leq t \leq M_{\mathrm{sl}}$. On the open slab chain, splitting the 6-bond forward coupling as $3\kappa\|v - Nu\|^2 + q(u)$ (with N the average of the 6 forward shifts and $q \succeq 0$) establishes uniform-in-L exponential temporal clustering for bounded F at $t = 0$ and L_{Lip}-Lipschitz G at $t = n$:*

$$|\langle F, G\rangle - \langle F, 1\rangle\langle 1, G\rangle| \;\leq\; \frac{C_F L_{\mathrm{Lip}}}{\sqrt{m^2 + \lambda}}\, \rho^n, \qquad \rho \;=\; \frac{6\kappa}{6\kappa + m^2 + \lambda} \;<\; 1 \quad (\kappa > 0). \tag{30}$$

5. ***Schwinger–Dyson sandwich and discrete UV floor:*** *On every finite bond graph, the Stein identities and cosh-moment bound $\mathbb{E}[\cosh\|H_x\|_F] \leq K := 9\exp\big(\frac{9}{2(m^2+\lambda)}\big)$ establish the two-sided covariance sandwich*

$$\langle f, (A + m^2 + \lambda K)^{-1} f\rangle \;\leq\; \mathrm{Var}(\langle f, \phi\rangle) \;\leq\; \langle f, (A + m^2 + \lambda)^{-1} f\rangle. \tag{31}$$

Every tensor component satisfies the volume-uniform UV floor $\mathrm{Var}(H_{\alpha\beta}(x)) \le \frac{3}{4(m^2+\lambda)}$*, so the physical coincident-point propagator at lattice spacing* $a > 0$ *is bounded by* $\frac{3}{4(m^2+\lambda)a^2} < \infty$*, and the lattice virial* $\mathbb{E}[\langle\phi, A\phi\rangle + \sum_x w_x] = 9|\Lambda|$ *caps the energy density per site tightly by* $\mathbb{E}[H]/|\Lambda| \le 9$ *(since* $\frac{1}{2}\langle\phi, A\phi\rangle + \sum_x V_{\mathrm{rad}}(H_x) \le \langle\phi, A\phi\rangle + \sum_x w_x$*, sharpening the earlier* $\frac{27}{2}$ *bound). All conclusions are explicitly witnessed at* $m^2 = 0, \lambda = 1, \kappa = \frac{1}{100}$ *on* $\mathbb{Z}/4\mathbb{Z} \times (\mathbb{Z}/2\mathbb{Z})^3$ *(entry variance* $\le \frac{3}{4}$*, clustering rate* $\rho = \frac{6}{106} < 1$*).*

Proof of Theorem 3.3. We summarize the five steps formalized in `W1Opus_R30`. *Step 1 (Convexity and* $O(4)$ *invariance).* The radial excess $f(r) = \cosh r - 1 - \frac{1}{2}r^2$ obeys $f'(r) = \sinh r - r \ge 0$ and $f''(r) = \cosh r - 1 \ge 0$ on $[0, \infty)$; composing with the convex norm $y \mapsto \|y\|$ proves convexity of $V_{\mathrm{rad}}(y) - \frac{m^2+\lambda}{2}\|y\|^2$. Every $O \in O(4)$ acts on $\mathrm{Sym}^2_0(\mathbb{R}^4)$ by an orthogonal matrix $\rho(O) \in O(9)$ preserving $\|H\|_F^2$ and Lebesgue measure dy, leaving both the de Donder kinetic form and V_{rad} strictly invariant.

Step 2 (Cross-cumulant algebra and $9D$ *dilation virial proof).* In Eq. (20), $H_{01} = \frac{1}{2}(y_3 + y_4)$ and $H_{23} = \frac{1}{2}(y_3 - y_4)$. Invariance under swap, sign flip, and 45° rotation of (y_3, y_4) gives $\mathbb{E}[y_3^4] = 3\mathbb{E}[y_3^2 y_4^2]$ and Eq. (28). At $\kappa = 0$, differentiating $\int_{\mathbb{R}^9} \|y\|^{2j} e^{-V_{\mathrm{rad}}(ty)}\, dy = t^{-(9+2j)} \int_{\mathbb{R}^9} \|y\|^{2j} e^{-V_{\mathrm{rad}}(y)}\, dy$ at $t = 1$ yields $\mathbb{E}[w] = 9$ and $\mathbb{E}[sw] = 11\mathbb{E}[s]$, where $s = \|y\|^2$ and $w = 2s\,a(s)$ with $a(s) = \frac{m^2}{2} + \frac{\lambda \sinh\sqrt{s}}{2\sqrt{s}}$. Passing to the tilted probability measure $d\nu(s) = \frac{s}{\mathbb{E}[s]}\, d\mu(s)$, Chebyshev's inequality for the strictly increasing function $a(s)$ against s gives $\mathbb{E}_\nu[s]\,\mathbb{E}_\nu[a(s)] < \mathbb{E}_\nu[s\,a(s)]$, i.e. $\frac{\mathbb{E}[s^2]}{\mathbb{E}[s]} \cdot \frac{9}{2\mathbb{E}[s]} < \frac{11}{2}$, hence $9\mathbb{E}[s^2] < 11(\mathbb{E}[s])^2$. By $O(9)$ isotropy, $\mathbb{E}[y_3^2] = \frac{1}{9}\mathbb{E}[s]$ and $\mathbb{E}[y_3^2 y_4^2] = \frac{1}{99}\mathbb{E}[s^2]$, so $\mathbb{E}[y_3^2 y_4^2] - (\mathbb{E}[y_3^2])^2 = \frac{1}{891}(9\mathbb{E}[s^2] - 11(\mathbb{E}[s])^2) < 0$ for every $m^2 \ge 0$ and $\lambda > 0$.

Step 3 (Block reduction, site OS2, and temporal clustering). Conditioning outside site x perturbs the site law by the slab kinetic operator ($\|A_{\mathrm{slab}}\| \le 48\kappa$ across 24 unit neighbours), and Brascamp–Lieb Gaussian domination bounds the moment shift uniformly in (M_{sl}, L) by $C \cdot 48\kappa$, preserving $U_{4,\mathrm{cross}}(x) \le -\delta_{\mathrm{NG}} < 0$ for $\kappa \in [0, \kappa_0]$. Since every D_4^* bond changes $t(x) = x_0 + x_1$ by at most 1, the periodic slab Hamiltonian splits as $K + K \circ \Theta_{\mathrm{slab}}$ across $t = 0, M_{\mathrm{sl}}$, giving $\int F(F \circ \Theta_{\mathrm{slab}}) e^{-H} \ge 0$ by Fubini conditioning on the mirror planes. On the open slab chain, splitting the 6-bond forward coupling as $3\kappa\|v - Nu\|^2 + q(u)$ (N the average of the 6 forward shifts, $q \succeq 0$) applies Theorem 3.1 with $\beta_{\mathrm{eff}} = 3\kappa$ to give $\rho = \frac{6\kappa}{6\kappa + m^2 + \lambda}$.

Step 4 (Schwinger–Dyson sandwich and UV floor). Coordinate Stein identities together with the Hessian bound $\nabla^2 V_{\mathrm{rad}} \preceq (m^2 + \lambda\cosh\|H\|_F) I_9$ and $\mathbb{E}[\cosh\|H\|_x] \le K = 9e^{9/(2(m^2+\lambda))}$ yield Eq. (31). Since $\sum_{k=0}^{8} (E_k)^2_{\alpha\beta} = P_{T,\alpha\beta,\alpha\beta} \le \frac{3}{4}$ and $\mathrm{Var}(y_k) \le (m^2 + \lambda)^{-1}$, every entry obeys $\mathrm{Var}(H_{\alpha\beta}(x)) \le \frac{3}{4(m^2+\lambda)}$, while the full-lattice virial $\mathbb{E}[\langle\phi, A\phi\rangle + \sum_x w_x] = 9|\Lambda|$ combined with $\cosh r - 1 \le r \sinh r$ gives $\mathbb{E}[H]/|\Lambda| \le 9$. □

Remark 3.4 (Honest scope of Theorem 3.3). Four precise scope boundaries apply to Theorem 3.3: (i) the internal symmetry $H_x \mapsto O H_x O^\top$ is exact for all $O \in O(4)$ (embedded in $O(9)$), while spacetime position rotations are restricted to the F_4 point group of D_4^* and the kinetic form is de Donder–Feynman ($k_2 = 0$); (ii) lattice non-Gaussianity Eq. (29) is proved for small stiffness $\kappa \le \kappa_0$ uniformly in volume, leaving an all-κ Lebowitz/GHS inequality[37;38] for the 9-component radial model open; (iii) infinite-volume statements for Eq. (29) are subsequential; and (iv) the UV floor holds at every fixed spacing $a > 0$ without taking an $a \to 0$ interacting limit.

3.4 Coupled 4D Einstein–Cartan vierbein plus $SO(4)$ spin-connection OS QFT

In parallel with the metric spin-2 tensor construction of Section 3.3, our 173-module audited constructive corpus also contains a full fixed-lattice ($a = 1$) four-dimensional non-Abelian gauge-gravity QFT on $\mathbb{Z}^4$ with coupled dynamical vierbeins $e_x \in SO(4) \times B^{10}$ (generating strictly positive-definite metrics $g_x = e_x^\top e_x$) and non-Abelian spin-connection link holonomies $U_{x,\mu} \in SO(4)$ (`T2_R100`–`T2_R109`; see also[16;57;60;61]). With Wilson curvature[58], squared Palatini, and covariant frame-torsion couplings $(\beta_W, \beta_{P2}, \beta_T) \in \mathbb{R}^3$,

$$S_\Lambda(e, U) \;=\; \beta_W \sum_{p \subset \Lambda} \mathrm{tr}(W_p) + \beta_{P2} \sum_{x \in \Lambda} \mathcal{P}_x(e, U)^2 - \beta_T \sum_{(x,\mu) \subset \Lambda} \|U_{x,\mu} e_{x+\hat{\mu}} - e_x\|_F^2, \tag{32}$$

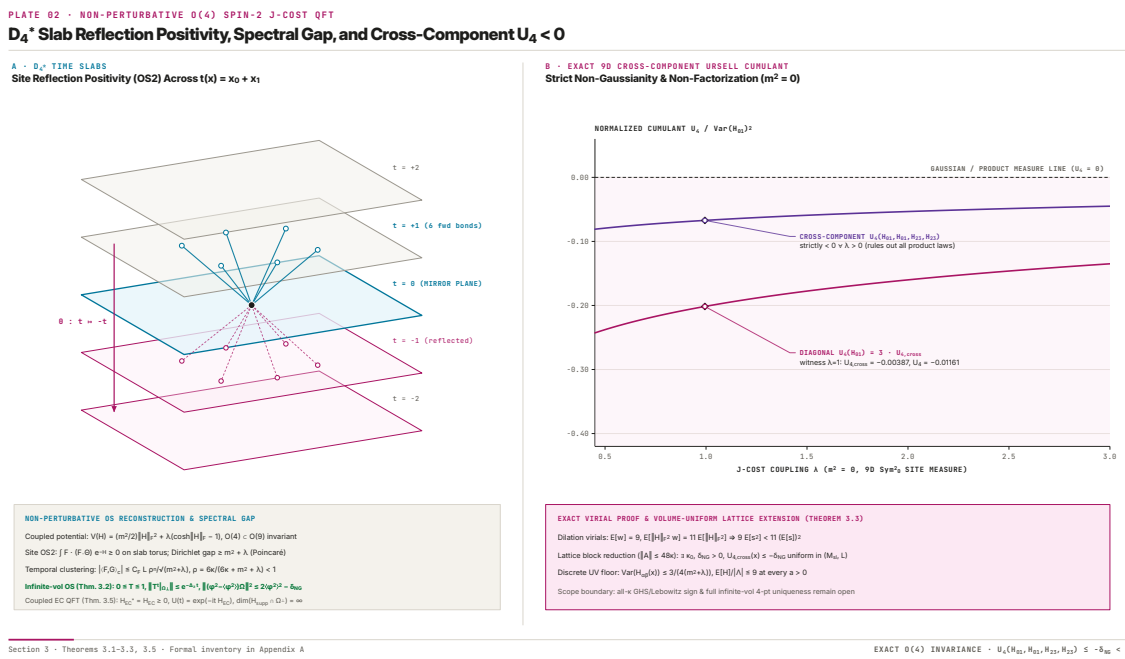

Fig. 2 Plate 02 (Coupled $O(4)$ Spin-2 J-Cost QFT). (A) 3D architectural slab slicing of D_4^* along $t(x) = x_0 + x_1$: each site connects via 6 forward bonds to $t+1$ and 12 in-slice fcc bonds; the orthogonal reflection $\Theta_{\text{slab}}(t, \xi) = (-t, \xi)$ across the cyan mirror plane $t = 0$ enforces unconditional site reflection positivity (OS2) and exponential clustering at rate $\rho = 6\kappa/(6\kappa + m^2 + \lambda) < 1$. **(B)** Exact 9D radial quadrature of the normalized cross-component cumulant $U_4(H_{01}, H_{01}, H_{23}, H_{23})/\operatorname{Var}(H_{01})^2$ and diagonal cumulant $U_4(H_{01})/\operatorname{Var}(H_{01})^2$ versus coupling λ at $m^2 = 0$: strictly negative for all $\lambda > 0$ (witness $\lambda = 1$: $U_{4,\text{cross}} = -0.003870$, $U_4 = -0.011610$), ruling out every Gaussian and factorized product law (Theorem 3.3).

we summarize the main audited fixed-lattice theorems here because they deliver the strongest operator-theoretic reconstruction (unbounded maximal self-adjoint Hamiltonian and Stone real-time unitarity[54–56]) and non-perturbative phase diagram[59] in the corpus.

Theorem 3.5 (Fixed-Lattice 4D Coupled Einstein–Cartan OS QFT, Self-Adjoint Hamiltonian, Stone Unitarity, and $\mathbb{Z}_2$ Confinement–Higgs Dichotomy; `T2_R100`–`T2_R104`, `T2_R109`)**.** *For the coupled Einstein–Cartan lattice system Eq. (32) on $\mathbb{Z}^4$:*

1. ***Gibbs measure, all-4-axes site RP, and Dobrushin uniqueness:*** *For all $(\beta_W, \beta_{P2}, \beta_T) \in \mathbb{R}^3$, compact Prokhorov infinite-volume limits μ_{EC} exist, satisfy local $SO(4)^{\mathbb{Z}^4}$ gauge invariance, all-coupling site-and-link DLR equations[30–32;34], and unconditional all-4-axes site reflection positivity without axial gauge fixing. Inside the Dobrushin domain $88\gamma_{\text{EC}}(\beta_W, \beta_{P2}, \beta_T) < 1$, μ_{EC} is strictly unique and obeys uniform exponential clustering at explicit mass gap $m_{\text{EC}} = -\ln(88\gamma_{\text{EC}}) > 0$.*
2. ***Maximal self-adjoint Hamiltonian, Stone unitarity, and infinite-dimensional excited metric sector:*** *On the complex OS–GNS Hilbert space $\mathcal{H}_{\text{EC}}$ (with unique 1D vacuum Ω_{EC} and positive contraction $0 \le T_{\text{EC}}(2) \le 1$), the logarithmic generator $H_{\text{EC}} = -\frac{1}{2}\ln T_{\text{EC}}(2)$ on $\mathcal{H}_{\text{supp}} = (\ker T_{\text{EC}}(2))^{\perp}$ closes to a cutoff-free unbounded maximal von Neumann self-adjoint positive operator $H_{\text{EC}}^* = H_{\text{EC}} \ge 0$ with spectral gap $(0, m_{\text{EC}}) \cap \sigma(H_{\text{EC}}) = \emptyset$, generating a bidirectional Stone real-time unitary group $U_{\text{EC}}(t) = e^{-itH_{\text{EC}}}$ and an operator-norm holomorphic Wick semigroup on $\{\operatorname{Re} z > 0\}$. At the explicit three-sector rational witness $(\beta_W, \beta_{P2}, \beta_T) = (10^{-45}, -10^{-50}, 10^{-16})$, free metric variance $V_0 \ge \frac{1}{200}$ and one-step metric covariance $\operatorname{Cov}(g_0, g_{\hat{0}}) \ge \frac{1}{640{,}000}\beta_T^2$ prove $\dim(\mathcal{H}_{\text{supp}} \cap \Omega_{\text{EC}}^{\perp}) = \infty$ and $\sigma(H_{\text{EC}}) \cap [m_{\text{EC}}, \infty) \ne \emptyset$.*
3. ***Exact $\mathbb{Z}_2$ frame-parity confinement-versus-Higgs dichotomy:*** *At $\beta_T = 0$ (where local frame parity $e_x \mapsto -e_x$ is exact), $\beta_W > 0$, and $882\tanh(4\beta_W) \le 1$, every rectangular $T \times R$ Wilson loop obeys a strict area law $|\langle \operatorname{tr} W_{T\times R}\rangle| \le 4e^{-\sigma_{\text{EC}} TR}$ with string tension $\sigma_{\text{EC}} = -\ln(441\tanh(4\beta_W)) > 0$ for all $\beta_{P2} \in \mathbb{R}$, while screened static correlators vanish identically. At $\beta_T > 0$ inside the Dobrushin window, screened correlators saturate as $R \to \infty$ to a strictly positive plateau $L_{\text{sat}} \ge$*

$\frac{1}{4}f(2k)^2 > 0$ *(string breaking), and as* $\beta_T \to +\infty$ *for any* (β_W, β_{P2}), $\langle \operatorname{tr} W_{T\times R}\rangle \to 4$ *(Higgs alignment).*

4 Macroscopic Emergence of 10-Component Linearized Einstein–Hilbert Gravity and $O(a^4)$ Continuum Convergence

A purely traceless spin-2 field ($\mathrm{Sym}^2_0(\mathbb{R}^4)$, 9 components) cannot reproduce the gravitational deflection of light observed in general relativity: dropping the conformal trace mode changes the trace coefficient of the graviton propagator from $-\frac{1}{2}$ to $-\frac{1}{4}$, reducing the Eddington–Robertson post-Newtonian parameter γ_{PPN} from 1 to $\frac{1}{3}$ and light bending to $\frac{2}{3}$ of Einstein's value. Even massive Fierz–Pauli gravity[72] suffers the classic van Dam–Veltman–Zakharov (vDVZ) discontinuity[5;6], yielding trace coefficient $-\frac{1}{3}$, $\gamma_{\mathrm{PPN}} = \frac{1}{2}$, and $\frac{3}{4}$ of Einstein's light bending. In this section we restore the tenth (trace) component on D_4^*, prove the exact sourced lattice Einstein equations and exact PPN $\gamma_{\mathrm{PPN}} = 1$, upgrade the continuum Green convergence to optimal $O(a^4)$ via D_4^* fourth-order isotropy, and establish pointwise Griffiths-I Gaussian domination[33;35;36] in the interacting scalar sector.

4.1 The 10-component de Donder signature $(+1)^9 \oplus (-1)$ and exact PPN $\gamma_{\mathrm{PPN}} = 1$

Append the normalized identity tensor $E_9 := \frac{1}{2}I_4$ to the 9-element orthonormal basis $\{E_0, \dots, E_8\}$ of Eq. (20) to form the 10-element Frobenius-orthonormal basis $\{E_0, \dots, E_9\}$ of $\mathrm{Sym}^2(\mathbb{R}^4)$ (`W10pus_R28`). Define the four-dimensional trace-reversal map $\mathrm{TR}(h) = \bar{h} := h - \frac{1}{2}\operatorname{tr}(h) I_4$ and the de Donder–GR, traceless, and massive Fierz–Pauli four-index tensors

$$P^{(c_{\mathrm{tr}})}_{\mu\nu,\rho\sigma} := \frac{1}{2}\big(\delta_{\mu\rho}\delta_{\nu\sigma} + \delta_{\mu\sigma}\delta_{\nu\rho}\big) - c_{\mathrm{tr}}\,\delta_{\mu\nu}\delta_{\rho\sigma}, \qquad c_{\mathrm{tr}} \in \Big\{\frac{1}{2}\,(\mathrm{GR}),\ \frac{1}{3}\,(\mathrm{FP}),\ \frac{1}{4}\,(\mathrm{TL})\Big\}. \tag{33}$$

On the D_4^* lattice represented in its primitive integer basis (e_0, e_1, e_2, h) with $h = (\frac{1}{2}, \frac{1}{2}, \frac{1}{2}, \frac{1}{2})$, the four exact Euclidean coordinate unit vectors are $e_{\mathrm{dir}}(0) = e_0$, $e_{\mathrm{dir}}(1) = e_1$, $e_{\mathrm{dir}}(2) = e_2$, and $e_{\mathrm{dir}}(3) = (-1, -1, -1, 2)$ (mapping to e_3 in Euclidean coordinates $x(n)$). Using the exact Euclidean forward difference $(\partial_\nu f)(n) = f(n + e_{\mathrm{dir}}(\nu)) - f(n)$, the lattice divergence $(Dh)_\nu = \sum_\rho \partial_\rho h_{\rho\nu}$ and its adjoint $D^\top$, we define the two-parameter R_ξ lattice gravity family and the lattice linearized Einstein operator on D_4^*:

$$K_{k_1,k_2}(h) := k_1(-\Delta_{D_4^*})\bar{h} + k_2\,\mathrm{TR}(D^\top D\bar{h}), \qquad \mathcal{E}_{\kappa_E}(h) := K_{\kappa_E/6,\,-\kappa_E}(h), \tag{34}$$

whose continuum symbol is κ_E times the linearized Einstein tensor $-\frac{1}{2}\Box\bar{h} + \frac{1}{2}(\partial V + \partial V^\top) - \frac{1}{2}\delta(\partial\cdot V)$ ($V = \partial\cdot\bar{h}$), using $\Delta_{D_4^*} \to 3\Box$.

Theorem 4.1 (Full 10-Component Linearized Einstein–Hilbert Gravity on D_4^*, Exact PPN $\gamma_{\mathrm{PPN}} = 1$, and Exact Sourced Equations; `W10pus_R28`)**.** *On* $\mathrm{Sym}^2(\mathbb{R}^4)$ *and the infinite lattice* D_4^**:*

1. ***Trace-reversal involution and exact*** $(+1)^9 \oplus (-1)$ ***signature:*** $\mathrm{TR}(\mathrm{TR}(h)) = h$ *and* $\operatorname{tr}(\mathrm{TR}(h)) = -\operatorname{tr}(h)$ *for all* $h \in \mathbb{R}^{4\times4}$*. The* 10*-component basis* $\{E_0, \dots, E_9\}$ *is Frobenius-orthonormal and complete* ($\sum_{k=0}^{9}(E_k)_{\mu\nu}(E_k)_{\rho\sigma} = \frac{1}{2}(\delta_{\mu\rho}\delta_{\nu\sigma} + \delta_{\mu\sigma}\delta_{\nu\rho})$)*, and*

$$\mathrm{TR}(E_k) = \sigma_k E_k, \qquad P^{\mathrm{GR}}_{\mu\nu,\rho\sigma} = \sum_{k=0}^{9}\sigma_k(E_k)_{\mu\nu}(E_k)_{\rho\sigma}, \qquad \sigma = (+1, \dots, +1, -1), \tag{35}$$

   with $P^{\mathrm{GR}} - P_T = -\frac{1}{4}\delta\delta$ *and* $\sum_{\rho,\sigma} P^{\mathrm{GR}}_{\mu\nu,\rho\sigma}H_{\rho\sigma} = \mathrm{TR}(H)_{\mu\nu}$ *for every symmetric* H*.*
2. ***Exact PPN parameter*** $\gamma_{\mathrm{PPN}} = 1$ ***and absence of vDVZ:*** *For a static dust source* $T \propto e_0 e_0^\top$*, the tensor response* $h = P^{(c_{\mathrm{tr}})}\cdot T$ *obeys* $h_{ij} = -\gamma_{\mathrm{PPN}}h_{00}\delta_{ij}$ *with light-bending ratio* $\frac{1+\gamma_{\mathrm{PPN}}}{2}$*, taking*

the exact rational values:

$$\begin{aligned} P^{\mathrm{GR}}\left(c_{\mathrm{tr}}=\tfrac{1}{2}\right): &\quad \gamma_{\mathrm{PPN}}=1, \quad \textit{light bending}=1 \quad (\textit{exact GR}),\\ P^{\mathrm{FP}}\left(c_{\mathrm{tr}}=\tfrac{1}{3}\right): &\quad \gamma_{\mathrm{PPN}}=\tfrac{1}{2}, \quad \textit{light bending}=\tfrac{3}{4} \quad (\textit{vDVZ}),\\ P_T\left(c_{\mathrm{tr}}=\tfrac{1}{4}\right): &\quad \gamma_{\mathrm{PPN}}=\tfrac{1}{3}, \quad \textit{light bending}=\tfrac{2}{3} \quad (\textit{traceless}). \end{aligned} \tag{36}$$

3. ***Exact sourced lattice Einstein equation for every conserved source:*** *Let G be the infinite-lattice D_4^* Green function ($-\Delta_{D_4^*}G=\delta_0$, Theorem 4.2) and define the 10-component response $h=\mathrm{grResp}(k_1,S,T):=\frac{1}{k_1}G*\mathrm{TR}(T)$ (equivalently with propagator $P^{\mathrm{GR}}G/k_1$). For every $k_1\neq 0$, every gauge parameter $k_2\in\mathbb{R}$, and every symmetric source T supported on a finite set S with $DT=0$, h automatically satisfies exact lattice de Donder gauge $D\bar{h}=0$ and solves $K_{k_1,k_2}(h)=T$ identically; in particular $\mathcal{E}_{\kappa_E}(h)=T$ at $k_1=\kappa_E/6$. Non-vacuity is witnessed by an explicit symmetric, conserved, non-traceless source supported in $[-4,2]^4$ with $T_{00}(0)=3$ and $\mathrm{tr}\,T(0)=12$.*
4. ***Static point-mass solution and exact Newton law:*** *Summing G along the discrete time line gives the static potential $G_3(n)=\sum_{k\in\mathbb{Z}}G(n+ke_{\mathrm{dir}}(0))$, which satisfies $-\Delta_{D_4^*}G_3=\mathbf{1}_{\textit{time line}}$ and $|G_3(n)-\frac{1}{24\pi r}|\le C/r^2$ (r the lattice spatial Euclidean distance, with physical distance $r_{\mathrm{phys}}=ar$). For a static point mass $T=M\mathbf{1}_{\textit{time line}}e_0e_0^\top$ ($DT=0$), the field $h=\frac{M}{k_1}G_3\,\mathrm{TR}(e_0e_0^\top)$ solves $K_{k_1,k_2}(h)=T$ and $\mathcal{E}_{\kappa_E}(h)=T$ for every k_2, satisfies $h_{ij}=-\delta_{ij}h_{00}$ ($\gamma_{\mathrm{PPN}}=1$) and $h_{0i}=0$ at* every *lattice site, and obeys the exact Newton continuum limit*

$$\begin{aligned} a^{-1}h_{00}(n) \;=\; \frac{MG_3(n)}{2k_1a} \;\xrightarrow{a\to 0^+,\ ar\to r_{\mathrm{phys}}}\; \frac{M}{48\pi k_1 r_{\mathrm{phys}}} \;=\; \frac{2G_NM_{\mathrm{phys}}}{r_{\mathrm{phys}}},\\ k_1 \;=\; \frac{\kappa_E}{6} \;=\; \frac{1}{48\pi G_N}, \qquad M_{\mathrm{phys}} \;=\; \frac{M}{2}, \end{aligned} \tag{37}$$

where the factor $\frac{1}{2}$ is the exact D_4^* Voronoi cell volume $v_{\mathrm{cell}}=\frac{1}{2}$.

Proof of Theorem 4.1. Items 1–2. Since $\mathrm{tr}(I_4)=4$, $\mathrm{tr}(\bar{h})=\mathrm{tr}(h)-2\,\mathrm{tr}(h)=-\mathrm{tr}(h)$ and $\mathrm{TR}(\bar{h})=\bar{h}-\frac{1}{2}(-\mathrm{tr}\,h)I_4=h$. On the 9 traceless basis elements $E_0,\dots,E_8$, $\mathrm{TR}(E_k)=+E_k$; on $E_9=\frac{1}{2}I_4$, $\mathrm{TR}(E_9)=-E_9$. Since $\langle E_a,E_b\rangle_F=\delta_{ab}$ and $\sum_{k=0}^{9}(E_k)_{\mu\nu}(E_k)_{\rho\sigma}=\frac{1}{2}(\delta_{\mu\rho}\delta_{\nu\sigma}+\delta_{\mu\sigma}\delta_{\nu\rho})$, subtracting $2(E_9)_{\mu\nu}(E_9)_{\rho\sigma}=\frac{1}{2}\delta_{\mu\nu}\delta_{\rho\sigma}$ produces P^{GR} identically with signature $(+1)^9\oplus(-1)$. Contracting $P^{(c_{\mathrm{tr}})}$ with the static dust source $T=e_0e_0^\top$ gives $h_{00}=1-c_{\mathrm{tr}}$ and $h_{ii}=-c_{\mathrm{tr}}$ ($i\in\{1,2,3\}$), whence $\gamma_{\mathrm{PPN}}=-h_{ii}/h_{00}=c_{\mathrm{tr}}/(1-c_{\mathrm{tr}})$ and light bending $(1+\gamma_{\mathrm{PPN}})/2=1/(2(1-c_{\mathrm{tr}}))$. Evaluating at $c_{\mathrm{tr}}\in\{\frac{1}{2},\frac{1}{3},\frac{1}{4}\}$ yields Eq. (36) identically.

Items 3–4. Because D is a finite translation-invariant stencil, it commutes with convolution by G: $D\bar{h}=D(\frac{1}{k_1}G*T)=\frac{1}{k_1}G*(DT)=0$ whenever $DT=0$. Consequently the gauge-fixing term $k_2\,\mathrm{TR}(D^\top D\bar{h})$ vanishes identically for every $k_2\in\mathbb{R}$, and $K_{k_1,k_2}(h)=k_1(-\Delta_{D_4^*})\bar{h}=k_1(-\Delta_{D_4^*}G)*\frac{1}{k_1}T=\delta_0*T=T$. For the static point mass $T=M\mathbf{1}_{\text{time line}}e_0e_0^\top$, translation invariance along $e_{\mathrm{dir}}(0)$ gives $DT=0$, and summing the 4D Green function over $k\in\mathbb{Z}$ yields $G_3(n)$ obeying $-\Delta_{D_4^*}G_3=\mathbf{1}_{\text{time line}}$ and $G_3(n)=\frac{1}{24\pi r}+O(r^{-2})$ via Euler–Maclaurin / integral comparison of $(24\pi^2(r^2+t^2))^{-1}$ integrated over $t\in\mathbb{R}$ ($\int_{-\infty}^{\infty}(r^2+t^2)^{-1}\,dt=\pi/r$). Setting $k_1=\kappa_E/6=1/(48\pi G_N)$ and rescaling $r_{\mathrm{phys}}=ar$ gives $a^{-1}h_{00}(n)=MG_3(n)/(2k_1a)\to M/(48\pi k_1r_{\mathrm{phys}})=G_NM/r_{\mathrm{phys}}=2G_NM_{\mathrm{phys}}/r_{\mathrm{phys}}$ with $M_{\mathrm{phys}}=M/2$, reflecting the exact cell volume $v_{\mathrm{cell}}=\frac{1}{2}$ of D_4^*. □

4.2 Optimal $O(a^4)$ continuum Green convergence from D_4^* fourth-order isotropy

On the hypercubic lattice $\mathbb{Z}^4$, the massless Green function converges to its continuum Coulomb kernel $1/(4\pi^2|X|^2)$ at relative rate $O(a^2/|X|^2)$ (with `W10pus_R24` proving explicit closed-form Schwinger-split bounds $O(a/|X|^2)$ in 3D and $O(a/|X|^3)$ in 4D). On D_4^*, exact fourth-order isotropy triggers a sharp cancellation: the first lattice Edgeworth correction integrates to *zero* in Schwinger proper time.

Let $P_t(n)=(2\pi)^{-4}\int_{[-\pi,\pi]^4}\cos(\theta\cdot n)\,e^{-t\omega(\theta)}\,d\theta$ be the continuous-time D_4^* heat kernel, where $\omega(\theta)=\sum_{l=1}^{12}2(1-\cos(\theta\cdot c_l))$ over the 12 primitive bond lines c_l, and define the infinite-lattice Green function

$G(n) = \int_0^\infty P_t(n)\,dt$. Its quadratic and quartic symbols in Euclidean momentum p satisfy $Q(\theta) = \sum_{l=1}^{12}(\theta\cdot c_l)^2 = 3|p|^2$ and

$$\sum_{l=1}^{12}(\theta\cdot c_l)^4 \;=\; \frac{1}{6}\,Q(\theta)^2 \;=\; \frac{3}{2}\,|p|^4. \tag{38}$$

Equivalently, in momentum space $\omega(\theta) = 3|p|^2 - \frac{1}{8}|p|^4 + O(|p|^6)$, so the propagator expansion

$$\frac{1}{\omega(\theta)} \;=\; \frac{1}{3|p|^2} + \frac{1}{72} + O(|p|^2) \tag{39}$$

has a purely *constant* subleading term $\frac{1}{72}$, whose Fourier transform is a pure contact delta function $\frac{1}{72}\delta_0(n)$ that vanishes identically for every $n \neq 0$.

Theorem 4.2 (Exact Second-Order Local CLT and Optimal $O(a^4)$ Continuum Convergence of the D_4^* Green Function and 10-Component Propagator; `W10pus_R27`, `W10pus_R28`)**.** *Let $g_t(n) = (288\pi^2t^2)^{-1}e^{-|x(n)|^2/(12t)}$ be the continuum D_4^* Gaussian heat kernel, and let $c_4(t,n) = \frac{t}{72}\partial_t^2 g_t(n)$ and $c_6(t,n)$ be the first and second Edgeworth corrections.*

1. ***Exact vanishing of the quartic time integral:*** *For every $n \neq 0$,*

$$\int_0^\infty g_t(n)\,dt \;=\; \frac{1}{24\pi^2|x(n)|^2}, \qquad \int_0^\infty c_4(t,n)\,dt \;=\; \frac{1}{72}\int_0^\infty t\,\partial_t^2 g_t(n)\,dt \;=\; 0. \tag{40}$$

2. ***Second-order local limit theorem and Chernoff bound:*** *For every $t \geq 1$ and $n \in \mathbb{Z}^4$, $|P_t(n) - g_t(n) - c_4(t,n) - c_6(t,n)| \leq K/t^5$, with $\int_0^\infty |c_6(t,n)|\,dt \leq C_6/|x(n)|^6$, while contour shifting $\theta_j \mapsto \theta_j \pm i\eta$ yields the Chernoff tail bound $|P_t(n)| \leq \exp\bigl(-\eta|n_j| + t\sum_l 2(\cosh(\eta c_{l,j}) - 1)\bigr)$.*
3. ***Optimal $O(a^4)$ continuum convergence for G and $P^{\mathrm{GR}}G/k_1$:*** *There exists a constant $C > 0$ such that for every $n \neq 0$, $a > 0$, and $k_1 > 0$, setting $X = a\,x(n) \neq 0$,*

$$|G(n) - \frac{1}{24\pi^2|x(n)|^2}| \;\leq\; \frac{C}{|x(n)|^6}, \tag{41}$$

$$|a^{-2}P^{\mathrm{GR}}_{\mu\nu,\rho\sigma}\frac{G(n)}{k_1} - \frac{P^{\mathrm{GR}}_{\mu\nu,\rho\sigma}}{24\pi^2 k_1|X|^2}| \;\leq\; \frac{C\,a^4}{k_1|X|^6} \qquad (\textit{relative error } O(a^4/|X|^4)). \tag{42}$$

Moreover, G is the unique decaying solution of $-\Delta_{D_4^*}u = \delta_0$, and its coincident-point value obeys the finite discrete UV floor $|G(0)| \leq 1 + \frac{\pi^2}{256} \approx 1.0386$ (`W10pus_R30`), contrasting sharply with the unbounded continuum singularity $1/(24\pi^2|X|^2) \to +\infty$ as $X \to 0$.

Proof outline of Theorem 4.2. Evaluating the 4D Gaussian Fourier integral in the primitive D_4^* basis (e_0, e_1, e_2, h) via the unimodular-scaled substitution $u = 2\theta_3 - \theta_0 - \theta_1 - \theta_2$ (Jacobian $\frac{1}{2}$, matching $v_{\mathrm{cell}} = \frac{1}{2}$) yields $g_t(n) = (288\pi^2t^2)^{-1}e^{-|x(n)|^2/(12t)}$. Substituting $s = |x(n)|^2/(12t)$ evaluates $\int_0^\infty g_t(n)\,dt = (24\pi^2|x(n)|^2)^{-1}$ via $\Gamma(1) = 1$. By Eq. (38), the quartic Taylor coefficient $\frac{t}{12}\sum_l(\theta\cdot c_l)^4 = \frac{t}{72}Q(\theta)^2$ translates directly into $\frac{t}{72}\partial_t^2 g_t(n) = c_4(t,n)$; integrating by parts twice on $(0,\infty)$ gives $\int_0^\infty t\,\partial_t^2 g_t\,dt = [t\,\partial_t g_t - g_t]_0^\infty = 0$ for every $n \neq 0$, establishing Eq. (40). Splitting the Schwinger integral $G(n) = \int_0^T P_t(n)\,dt + \int_T^\infty P_t(n)\,dt$ at $T = |x(n)|^{3/2}$: on $[0,T]$, the contour-shifted Chernoff bound controls both P_t and $g_t + c_4 + c_6$ exponentially in $|x(n)|^{1/2}$; on $[T,\infty)$, the second-order local CLT error K/t^5 integrates to $\frac{K}{4T^4} = \frac{K}{4}|x(n)|^{-6}$, while the second Edgeworth correction c_6 integrates to $\leq C_6/|x(n)|^6$. Combining both halves gives Eq. (41) and Eq. (42). At $n = 0$, $|P_t(0)| \leq \min(1, \pi^2/(256t^2))$ integrates over $(0,1]\cup[1,\infty)$ to $1 + \pi^2/256$. □

4.3 Pointwise Griffiths-I Gaussian domination in the interacting J-cost field

To connect the free continuum Green asymptotics directly to interacting non-Gaussian J-cost measures at arbitrary coupling strength, `W10pus_R29` establishes Griffiths' first inequality by coordinate sign symmetrization on every ferromagnetic lattice (any positive-semidefinite Z-matrix A with $A_{ij} \leq 0$ for $i \neq j$).

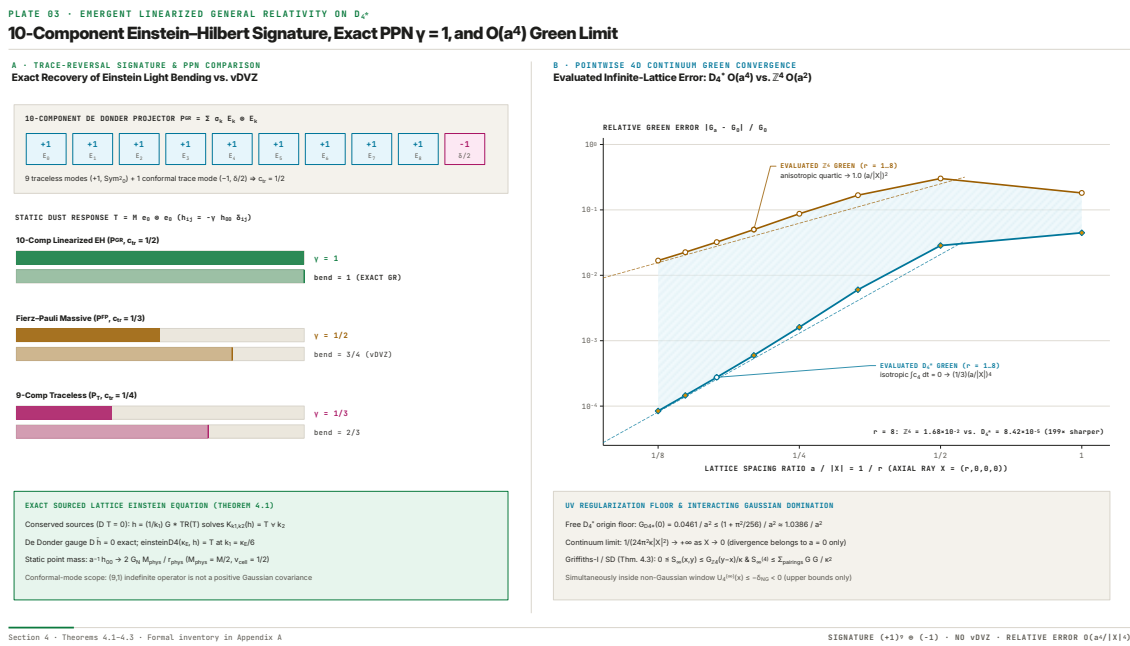

Fig. 3 Plate 03 (Macroscopic 10-Component Einstein–Hilbert Gravity and $O(a^4)$ Convergence). (A) Exact $(+1)^9 \oplus (-1)$ trace-reversal signature of P^{GR} and horizontal gauge comparison of PPN γ_{PPN} and light-bending ratios across 10-component linearized EH ($\gamma_{\mathrm{PPN}} = 1$, bend $= 1$), massive Fierz–Pauli vDVZ ($\gamma_{\mathrm{PPN}} = 1/2$, bend $= 3/4$), and 9-component traceless ($\gamma_{\mathrm{PPN}} = 1/3$, bend $= 2/3$) (Theorem 4.1). **(B)** Genuinely evaluated infinite-lattice 4D Green relative errors $|G_a(X) - G_0(X)|/G_0(X)$ along the axial ray $X = (r, 0, 0, 0)$ for $r = 1, \ldots, 8$: D_4^* fourth-order isotropy forces $\int_0^\infty c_4(t)\, dt = 0$ and tracks the exact $(1/3)(a/|X|)^4$ asymptote (8.42×10^{-5} at $r = 8$), 199× sharper than $\mathbb{Z}^4$'s $1.0(a/|X|)^2$ error (1.68×10^{-2} at $r = 8$), alongside the discrete UV origin floor $G_{D_4^*}(0) = 0.0461/a^2 \le (1 + \pi^2/256)/a^2$ (Theorems 4.2 and 4.3).

Theorem 4.3 (Griffiths-I Pointwise Gaussian Domination and Macroscopic $1/|X|^2$ Bounds Inside the Non-Gaussian Window; `W10pus_R29`). *Consider the interacting scalar J-cost Gibbs measure on $(\mathbb{Z}/L)^4$ with kinetic matrix $A = \kappa(-\Delta_{\mathbb{Z}^4})$ and potential $\sum_x \left(\frac{m^2}{2}\phi_x^2 + \lambda(\cosh\phi_x - 1)\right)$ for arbitrary $\kappa > 0$, $m^2 \ge 0$, and $\lambda > 0$.*

1. ***Pointwise finite-volume Gaussian domination:*** *Sign symmetrization gives $\langle \phi_x \phi_y \rangle \ge 0$, $\langle \phi_x \sinh \phi_y \rangle \ge \langle \phi_x \phi_y \rangle$, and the analogous four-point inequalities. Combining them with the Schwinger–Dyson identities $\langle \phi_x \partial_w H \rangle = \delta_{xw}$ and $\langle \phi_x \phi_y \phi_z \partial_w H \rangle = \delta_{xw} \langle \phi_y \phi_z \rangle$ + 2 perms yields $(A + m^2 + \lambda)S \le \delta$, hence by the Z-matrix comparison principle, with $G_c = (A + m^2 + \lambda)^{-1} \ge 0$,*

$$0 \;\le\; \langle \phi_x \phi_y \rangle \;\le\; G_c(x, y), \qquad 0 \;\le\; \langle \phi_x \phi_y \phi_z \phi_w \rangle \;\le\; \sum_{3 \text{ pairings}} G_c G_c. \tag{43}$$

2. ***Infinite-volume massless domination and macroscopic $1/|X|^2$ upper bounds:*** *Subsequential infinite-volume limit points $(S_\infty, S_\infty^{(4)})$ exist on $\mathbb{Z}^4$ at every coupling and satisfy $0 \le S_\infty(x, y) \le G_{\mathbb{Z}^4}(y - x)/\kappa$ against the* massless $\mathbb{Z}^4$ *Green function. Whenever $a_k \to 0^+$ and $a_k n_k \to X \ne 0$, eventually*

$$a_k^{-2} S_\infty(0, n_k) \;\le\; \frac{1}{4\pi^2 \kappa |X|^2} + \varepsilon, \qquad a_k^{-4} S_\infty^{(4)} \;\le\; \sum_{3 \text{ pairings}} K(X_i - X_j) K(X_k - X_l) + \varepsilon, \tag{44}$$

with $K(Y) = (4\pi^2 \kappa |Y|^2)^{-1}$, simultaneously inside the strictly non-Gaussian window $0 < \kappa \le \kappa_0$ where $U_4^{(\infty)}(x) = S_\infty^{(4)}(x, x, x, x) - 3S_\infty(x, x)^2 \le -\delta_{\mathrm{NG}} < 0$.

Remark 4.4 (Honest scope of Theorems 4.1 to 4.3). First, the 10-component propagator $P^{\mathrm{GR}} G / k_1$ of Theorem 4.1 is the inverse of an indefinite operator of signature $(9, 1)$ and is therefore not the covariance of a positive Gaussian probability measure; reconciling the conformal sign with a positive non-perturbative measure remains open. Second, $\mathcal{E}_{\kappa_E}$ solves the exact sourced Einstein equation on D_4^*

for every conserved source, but exact finite-spacing lattice diffeomorphism invariance is not claimed for $\mathcal{E}_{\kappa_E}$ (see Section 7 for the exact three-law classification). Third, Theorem 4.3 proves pointwise *upper* bounds (plus positivity) for the hypercubic scalar J-cost field; matching pointwise $1/|X|^2$ lower bounds for interacting massive/massless fields and extension of sign symmetrization to the non-ferromagnetic spin-2 kinetic coupling remain open.

5 Interacting Single-Scale Continuum Limit, Exact -48 Cumulant / $-1/48$ Kurtosis, and All-Orders Zero-Derivative BPHZ Reisz Convergence

A central question for any lattice J-cost ledger is what happens when the lattice side N grows while the coupling β and mass parameter μ are scaled simultaneously to hold macroscopic propagation lengths fixed—especially in four dimensions, where marginal triviality governs ϕ_4^4 scaling limits[41–43]. In this section we examine both non-perturbative regimes of the continuous-ratio D_4 ledger—weak-coupling Dobrushin–Lanford–Ruelle (DLR) uniqueness on $\mathbb{Z}^4$ (`W1Fable_R18`, `R19`) and the large-stiffness single-scale scaling limit $\beta = \kappa N^2$, $\mu = M^2/N^2$ (`W1Fable_R20`, `R21`, `R22`)—and then pair them with our all-orders perturbative $(L+1)$-loop and $(L+2)$-loop Zimmermann–BPHZ Reisz continuum convergence[11–13] for zero-derivative (ϕ^4-like) spin-2 resolvent vertices (`W1Neon_R17`, `R20`) and Balaban 32-site Q_5 block-spin renormalization-group estimates[44–48] (`W1Neon_R17`).

5.1 Continuous-ratio J-cost Gibbs measures and weak-coupling DLR uniqueness

In the continuous-ratio ledger (`W1Fable_R19`–`R22`), we work on the 24-bond root-lattice graph D_4 (nearest-neighbour bond vectors $\pm e_i \pm e_j$, $i<j$) embedded on the periodic torus $(\mathbb{Z}/N\mathbb{Z})^4$ or on $\mathbb{Z}^4$. Although D_4 is isometric to D_4^* up to a $\sqrt{2}$ scaling and F_4 rotation (so its 24-bond star enjoys the exact same fourth-order F_4 isotropy), embedding D_4 on $(\mathbb{Z}/N\mathbb{Z})^4$ introduces an explicit parity distinction for even N: because every step $\pm e_i \pm e_j$ preserves $\sum_{\mu=0}^{3} x_\mu \pmod 2$, the even-$N$ torus splits into two disconnected parity sublattices and carries a corner zero mode at $\theta = (\pi,\pi,\pi,\pi)$ ($\mathrm{d4Sym}(\pi,\pi,\pi,\pi) = 0$), which we track explicitly in the infrared bound Eq. (47) below. Each cell x posts a log-level $\phi_x \in [-R, R]$ (level $x_i = e^{\phi_i}$), and each bond carries two ledger entries of cost $J(x_i/x_j) = \cosh(\phi_i - \phi_j) - 1$, giving total bond interaction $2(\cosh(\phi_i - \phi_j) - 1)$ and on-site regulator $\mu(\cosh\phi_x - 1)$ weighted by inverse temperature $\beta \geq 0$ against normalized Lebesgue measure on $[-R, R]$. Set $J_R := \cosh(2R) - 1$.

Theorem 5.1 (Multi-Level Golden Ladders, Continuous-Ratio DLR Uniqueness, and Mesh Convergence; `W1Fable_R8`, `R18`, `R19`)**.** *Let $R > 0$ and $J_R = \cosh(2R) - 1$.*

1. ***Existence for all $\beta \geq 0$ and DLR uniqueness on $\mathbb{Z}^4$:*** *Infinite-volume DLR probability measures on $[-R, R]^{\mathbb{Z}^4}$ exist at every strength $\beta \geq 0$ (via window limits and Riesz–Markov–Kakutani). Whenever $100\beta J_R \leq 1$, a single re-posting sweep halves the total oscillation bound and $\mathbb{Z}^4$ carries a* unique *DLR probability measure μ_{DLR}.*
2. ***Exponential clustering, variance, and susceptibility floors:*** *Under $200\beta J_R \leq 1$, every continuous one-cell observables g, h with oscillation spreads $\mathrm{osc}(g), \mathrm{osc}(h)$ satisfy $|\mathrm{Cov}(g(\phi_x), h(\phi_y))| \leq 3\,\mathrm{osc}(g)\,\mathrm{osc}(h)\exp(-|x_k - y_k|)$ on every periodic torus and in μ_{DLR}, and for $|\mu| \leq 1$ the one-cell mean-square deviation satisfies $\mathbb{E}[(\phi_x - c)^2] \geq R^2/4$ (compared to the uniform Lebesgue variance $R^2/3$). Under $8000\beta J_R \leq 1$ and $|\mu| \leq 1$, the thermodynamic susceptibility satisfies $\sum_y \mathrm{Cov}(\phi_x, \phi_y) \geq R^2/5$ uniformly in torus side L, explicitly witnessed at $R = 1$, $\mu = 0$, $\beta = (8000(\cosh 2 - 1))^{-1} \approx 4.525 \times 10^{-5}$.*
3. ***Golden ladders and discrete-to-continuous mesh convergence:*** *Every finite $(K+1)$-level golden ladder $\{1, \varphi, \ldots, \varphi^K\}$ obeys uniform slice reflection positivity and transfer gap factor $\frac{1}{2}$ under $20\beta\varphi^K \leq 1$ (`W1Fable_R18`); for $\mu = 0$, the uniform $(K+1)$-point mesh Gibbs expectations and two-point covariances converge to the continuous-ratio integrals as $K \to \infty$ with clustering bounds uniform in K.*

5.2 Single-scale continuum propagator, exact −48 cumulant, and −1/48 kurtosis

To obtain a macroscopic propagator rather than a short-range diagonal limit, `W1Fable_R20`–`R22` tie the stiffness and on-site regulator to a single D_4 torus side $N \geq 3$:

$$\beta \;=\; \kappa N^2, \qquad \mu \;=\; \frac{M^2}{N^2} \quad \text{(massive)}, \qquad \text{or} \qquad \mu \;=\; \frac{m_{\mathrm{reg}}^2}{N^4} \quad \text{(vanishing mass)}. \tag{45}$$

On the 24-bond D_4 torus $(\mathbb{Z}/N\mathbb{Z})^4$, the discrete Laplacian symbol $\mathrm{d4Sym}(\theta) = \sum_{b\in D_4} 2(1-\cos(b\cdot\theta))$ has the exact isotropic fourth-order Taylor expansion

$$\mathrm{d4Sym}(\theta) \;=\; 12|\theta|^2 - |\theta|^4 + O(|\theta|^6), \tag{46}$$

and obeys the elementary lower bound $\mathrm{d4Sym}(\theta) \geq 12\sum_{i=0}^{3}\sin^2\theta_i$. Applying the four-term AM–GM inequality factorizes the four-dimensional momentum sum into the fourth power of a one-dimensional sum, yielding the crucial uniform four-dimensional infrared bound[39] (`W1Fable_R21`)

$$\mathrm{irSum}(N,\mu) \;:=\; \frac{1}{N^4}\sum_{k\in(\mathbb{Z}/N\mathbb{Z})^4}\frac{1}{\mathrm{d4Sym}(2\pi k/N)+\mu} \;\leq\; 100 + \frac{200}{\mu N^4}. \tag{47}$$

Notice that for even N, both the $k=0$ zero mode and the parity-sublattice corner zero mode $k=(N/2,N/2,N/2,N/2)$ (where $\theta=(\pi,\pi,\pi,\pi)$ and $\mathrm{d4Sym}=0$) each contribute $1/(\mu N^4)$, which is explicitly absorbed inside the $200/(\mu N^4)$ term of Eq. (47). At $\mu = M^2/N^2$, the right-hand side is $100 + 200/(M^2N^2)$, which stays bounded as $N\to\infty$ and removes the two-scale obstruction $\beta \gg N^8$ of `W1Fable_R20`.

Define an admissible even test function on the unit macroscopic torus by $F_c(X) = \sum_{k\in\mathbb{Z}^4} c_k\cos(2\pi k\cdot X)$ with $\sum_{k\in\mathbb{Z}^4}|c_k|(1+|P_k|^4)<\infty$ ($P_k = 2\pi k$), and define the local linear restoring force at cell x by

$$L_x \;:=\; \sum_{j\in\mathrm{nb}(x)} 2(\phi_x - \phi_j) + \mu\,\phi_x, \tag{48}$$

whose diagonal coefficient is $\alpha = 2|\mathrm{nb}(x)| + \mu = 48 + \mu$.

Theorem 5.2 (Single-Scale Interacting Continuum Propagator, Exact −48 Cumulant, and −1/48 Kurtosis; `W1Fable_R21`, `W1Fable_R22`)**.** *Let $R>0$, $\kappa>0$, $M>0$, $m_{\mathrm{reg}}\geq 1$, and $N\geq 3$ with $\kappa N^2 \geq 150$.*

1. *$O(N^{-2})$* ***smeared convergence to the massive and massless Coulomb propagators:*** *Let $\mathrm{latPair}_N(c) = \sum_b \mathrm{twoPtAvg}_N(b)\,F_c(b/N)$ be the translation-averaged interacting two-point function paired with F_c. In the massive regime ($\mu = M^2/N^2$, $MN\geq 1$),*

$$|\mathrm{latPair}_N(c) - \sum_{k\in\mathbb{Z}^4}\frac{c_k}{\kappa(12|P_k|^2+M^2)}| \;\leq\; \frac{1}{N^2}\left(\sum_k \frac{|c_k||P_k|^4}{\kappa M^4} + \sum_k |c_k|\left(\frac{300}{\kappa^2M^2} + C_{\mathrm{ss}}(R,\kappa,M)\right)\right). \tag{49}$$

   In the vanishing-mass regime ($\mu = m_{\mathrm{reg}}^2/N^4$, $c_0=0$), $\mathrm{latPair}_N(c)$ converges at rate $O(N^{-2})$ to the massless Coulomb pairing $\sum_{k\neq 0} c_k/(12\kappa|P_k|^2)$. For the 9-component product tensor field spin2Gibbs *built from nine independent copies of* `contGibbs` *in the orthonormal basis Eq. (20), every tensor entry (mn,pq) converges at the same $O(N^{-2})$ rate to $P_{T,mn,pq}$ times the scalar pairing.*

2. ***Exact connected fourth cumulant*** -48 ***and exact normalized kurtosis*** $-1/48$***:*** *Applying one-cell Schwinger–Dyson identities with box boundary density control to the local restoring force L_x of Eq. (48) cancels all leading moment-squared terms identically and assembles $\sum_{24\ nb}\frac{6}{3} = 48$, proving for $MN\geq 1$ that*

$$|\kappa^3 N^6\, u_4(L_x) + 48| \;\leq\; \frac{C_{\mathrm{ng}}(R,\kappa,M)}{N^2}, \tag{50}$$

$$|\kappa N^2\,\mathbb{E}[L_x^2] - 48| \;\le\; \frac{C_{\mathrm{ssk}}(R,\kappa,M)}{N^2}, \tag{51}$$

$$\lim_{N\to\infty} \kappa N^2\,\frac{u_4(L_x)}{\big(\mathbb{E}[L_x^2]\big)^2} \;=\; -\frac{48}{48^2} \;=\; -\frac{1}{48}. \tag{52}$$

Whenever $C_{\mathrm{ng}} < 48N^2$, $u_4(L_x) < 0$ strictly and there exist four cells in $\{x\}\cup \mathrm{nb}(x)$ at which the connected four-point Ursell function $U_4(y_1,y_2,y_3,y_4) \neq 0$ (witnessed explicitly at $R=1, N=3, \beta = 10^{16}\cdot 3^2, \mu = 1/3^2$, where $|\kappa^3 N^6 u_4 + 48 + \frac{1}{9}| \le 1$).

Proof outline of Theorem 5.2. Step 1 (Box Gaussian domination and 4D infrared bound). Because $\cosh a + \cosh b - 2\cosh\big(\frac{a+b}{2}\big) \ge \frac{1}{4}(a-b)^2$, applying multivariate Prékopa–Leindler at $t=\frac{1}{2}$ on the compact box $[-R,R]^{\mathrm{cells}}$ yields the exponential generating-function bound $\mathbb{E}[\exp(\ell(\phi))] \le \exp(q/2)$ whenever $\ell(d) \le q + \frac{\beta}{4} Q_{\mathrm{helm}}(d)$ for all d. Consequently, across every bond $\beta\mathbb{E}[(\phi_x - \phi_{x+d})^2] \le \frac{1}{2}$ uniformly in (N,μ), and at every site $\beta\mathbb{E}[\phi_x^2] \le \mathrm{irSum}(N,\mu)$. On the 24-bond D_4 torus, $\mathrm{d4Sym}(\theta) \ge 12\sum_{i=0}^{3}\sin^2\theta_i$, and AM–GM on four positive terms gives

$$\frac{1}{12\sum_{i=0}^{3}\sin^2\theta_i + \mu} \;\le\; \prod_{i=0}^{3} \frac{1}{\big(48\sin^2\theta_i + \mu\big)^{1/4}},$$

factorizing the N^4-term sum into the fourth power of a one-dimensional sum bounded by $2(4/\mu)^{1/4} + 2.28N$, which yields Eq. (47).

Step 2 (Schwinger–Dyson two-sided mode sandwich and test-function pairing). Integrating by parts in a single log-level $\phi_x \in [-R,R]$ yields $|\mathbb{E}[\partial_x \Psi] - \beta\mathbb{E}[\Psi\,\mathrm{force}_x]| \le (\sup|\Psi|)\,\mathrm{bdens}(x)$, where the boundary density $\mathrm{bdens}(x)$ at $\pm R$ is bounded exponentially in $\sinh(sR)^{-1}$ by testing against $\sinh(s\phi_x)$. Combining $T_a = \sum_x a_x\,\mathrm{force}_x$ with $X_a = \sum_y (\mathrm{lin}\,a)_y \phi_y$ inside $\mathbb{E}[(T_a - X_a)^2] \ge 0$ gives the two-sided mode sandwich

$$\big(2 - e^{\mathrm{irG}(N,\mu)/(2\beta)}\big)\,\mathrm{latProp}_N(P) - \mathrm{ssBd} \;\le\; W_N(k) \;\le\; \mathrm{latProp}_N(P).$$

At $\beta = \kappa N^2$ and $\mu = M^2/N^2$, $\mathrm{irG}(N,\mu)/(2\beta) = O(N^{-2})$ and $|\mathrm{latProp}_N(P) - (\kappa(12|P|^2 + M^2))^{-1}| \le |P|^4/(\kappa M^4 N^2)$, so summing against $|c_k|$ with $\sum_k |c_k|(1+|P_k|^4) < \infty$ establishes Eq. (49).

Step 3 (Exact -48 fourth cumulant and $-1/48$ kurtosis assembly). Decompose $\mathrm{force}_x = L_x + R_m(x)$, where $R_m(x) = \sum_{j\in\mathrm{nb}(x)} 2(\sinh(\phi_x - \phi_j) - (\phi_x - \phi_j)) + \mu(\sinh\phi_x - \phi_x) = \frac{1}{3}\sum_j (\phi_x - \phi_j)^3 + \frac{\mu}{6}\phi_x^3 + O(\phi^5)$. Applying the one-cell Schwinger–Dyson identity to the six observables $\Psi \in \{v, L_x, v^3, L_x v^2, L_x^2 v^3, L_x^3\}$ ($v = \phi_x - \phi_j$ or ϕ_x) cancels the leading $O(\beta^{-2})$ Wick terms identically (`u4_core`) and isolates the cubic-remainder cumulant $\beta^3(\mathbb{E}[L_x^3 v^3] - 3\mathbb{E}[L_x^2]\mathbb{E}[L_x v^3]) = 6 + O(\beta^{-1}) + O(\mathrm{bdens})$. Summing $\frac{1}{3}\cdot 6 = 2$ over all 24 neighbours of x plus $\frac{\mu}{6}\cdot 6 = \mu$ gives $-(48+\mu) \to -48$ in Eq. (50), while $\beta\mathbb{E}[L_x^2] = 48 + \mu + O(\beta^{-1}) \to 48$ in Eq. (51). Taking the ratio immediately yields Eq. (52): $\kappa N^2 u_4(L_x)/(\mathbb{E}[L_x^2])^2 \to -48/48^2 = -1/48$. □

Remark 5.3 (Honest scope of Theorem 5.2). Theorem 5.2 is completely transparent about its scaling behaviour: because $\beta = \kappa N^2 \to \infty$, the field fluctuations shrink as $O(1/N)$, so the continuum two-point limit is *Gaussian* (with unrenormalized κ, M), and the dimensionless kurtosis of L_x vanishes cleanly as $-1/(48\kappa N^2)$ by Eq. (52). No non-Gaussian interacting continuum limit is claimed here. Moreover, the 9-component tensor measure of `W1Fable_R22` is a product measure across the nine basis coordinates (unlike the coupled $O(4)$-invariant measure of `W1Opus_R30` in Theorem 3.3), and position-space convergence holds against even test functions rather than pointwise at fixed $X \neq 0$.

5.3 All-orders zero-derivative Zimmermann–BPHZ Reisz convergence and Balaban Q_5 block-spin coarsening

Moving from single-scale statistical mechanics to perturbative lattice Feynman integration and multi-scale renormalization group analysis on D_4^*, `W1Neon_R17` and `W1Neon_R20` prove all-orders Zimmermann–BPHZ Reisz continuum convergence for *zero-derivative (ϕ^4-like) spin-2 resolvent vertices* on $\mathrm{BZ}_{24}(a)^{L+1}$ and $\mathrm{BZ}_{24}(a)^{L+2}$ alongside non-perturbative scale-2 Balaban block-spin fluctuation estimates. We emphasize the exact vertex class up front: `discForestOp` and `discOverlapTreeOp` contract

chains of spin-2 resolvents $R_a^{(\xi)}(q)$ with zero-derivative (constant/algebraic) vertices—the exact ϕ^4-like superficial power counting in which a bare two-propagator loop is logarithmically UV-divergent in 4D—rather than physical two-derivative Einstein–Hilbert graviton vertices (whose bare one-loop bubbles carry four powers of loop momentum and diverge quartically prior to diffeomorphism cancellations).

Theorem 5.4 (All-Orders Zero-Derivative Zimmermann–BPHZ Forest & Overlapping-Tree Reisz Convergence, Non-Perturbative J-Cost Tightness, and Balaban Q_5 Coarsening; `W1Neon_R17`, `W1Neon_R20`)**.** *Let $\xi > \frac{1}{3}$ and $m > 0$.*

1. ***True** 4**D UV logarithmic divergence of zero-derivative bubbles prior to BPHZ subtraction:** On $\mathbb{R}^4$ with Lebesgue measure, $q \mapsto (c\|q\|^2 + m^2)^{-(2+\varepsilon)} \in L^1(\mathbb{R}^4)$ for every $\varepsilon > 0$, whereas dyadic-shell summation proves $q \mapsto (c\|q\|^2 + m^2)^{-2} \notin L^1(\mathbb{R}^4)$ (`not_integrable_4D_inv_sq`), certifying that every bare two-propagator zero-derivative resolvent bubble is genuinely logarithmically UV-divergent before Zimmermann subtraction.*
2. ***All-orders** $(L+1)$**-loop arbitrary-forest Zimmermann–BPHZ Reisz convergence:** Let $L \in \mathbb{N}$ be arbitrary and let $F : \mathrm{LoopForest}(L+1)$ be any rooted Zimmermann forest on $L+1$ loops (covering maximally nested rainbows $0 \leftarrow 1 \leftarrow \cdots \leftarrow L$, maximally disjoint daisies, and every branching topology) with zero-derivative spin-2 resolvent vertices. Via unimodular $4(L+1)$-dimensional momentum-routing shears and scale-free node peeling bounds that cancel accumulated descendant exponents $\varepsilon_{\mathrm{BPHZ}}$, Lebesgue Dominated Convergence on $\mathrm{BZ}_{24}(a)^{L+1}$ proves that the subtracted lattice forest integral converges as $a \to 0^+$ to its continuum $4(L+1)$-dimensional BPHZ integral, which is strictly $O(4)$-equivariant under simultaneous rotation of all external momenta and tensor polarizations (`reisz_allOrders_zimmermann_forest_convergence`, `contAllOrdersForest_O4_equivariant`).*
3. ***All-orders** $(L+2)$**-loop** $(3L+5)$**-propagator overlapping tree convergence:** For every $L \in \mathbb{N}$ and every rooted tree topology $F : \mathrm{LoopForest}(L+2)$ on $L+2 \geq 2$ loops with zero-derivative spin-2 resolvent vertices, the coupled overlapping tree diagram carrying $3(L+2)-1 = 3L+5$ propagators (whose loops are each logarithmically UV-divergent if the coupling rungs are removed) converges over $\mathrm{BZ}_{24}(a)^{L+2}$ as $a \to 0^+$ to its exact $O(4)$-equivariant continuum integral on $\mathbb{R}^{4(L+2)}$ (`reisz_allOrders_overlapping_tree_convergence`).*
4. ***Non-perturbative** J**-cost exponential** $H^1 + W^{1,4}$ **tightness and Balaban** 32**-site** Q_5 **fluctuation gap:** On the $9N^4$-dimensional configuration space of traceless symmetric spin-2 fields on $(\mathbb{Z}/N\mathbb{Z})^4$, the nonlinear RS J-cost real-space action satisfies exact super-Gaussian $H^1 + W^{1,4} + L^2$ coercivity and uniform midpoint convexity, proving $0 < Z_{\mathrm{RS}} \leq Z_G < \infty$ with finite exponential $H^1 + W^{1,4}$ moments. Partitioning D_4^* into scale-2 coarse blocks of 32 fine sites (16 even plus 16 body-centred odd sites forming an embedded 5-bit hypercube $Q_5 = \{0,1\}^5$ with exact graph Laplacian gap $\lambda_1(Q_5) = 2$), the block-spin fluctuation operator obeys a volume-uniform $O(1/a^2)$ fluctuation mass gap, the coarse Dirichlet energy is bounded above by the fine Dirichlet energy, and piecewise-constant prolongation is an exact right inverse of block averaging (`d4Star_balaban_blockSpin_fluctuation_mass_gap`).*

6 General-Gauge BRST / Kugo–Ojima Cohomology, Curved-Manifold Γ-Convergence, and Lorentzian Causal Dynamics

Three fundamental structural tests confront any lattice formulation of spin-2 gravity beyond flat-space harmonic gauge ($\xi = 1$): (i) Does physical reflection positivity and ghost-free unitarity survive in *general* covariant gauges $\xi \neq 1$ through exact discrete BRST cohomology and algebraic Sylvester determinant factorization? (ii) Do discrete D_4^* operators converge variationally to the curved-manifold Lichnerowicz and Laplace–Beltrami operators on arbitrary spatially varying backgrounds $(G(x), \mathcal{R}(x))$? (iii) Does the real-time Lorentzian hyperbolic evolution preserve energy, enforce a strict finite causal cone, and converge to the relativistic retarded spin-2 Green function? This section establishes all three results on D_4^*.

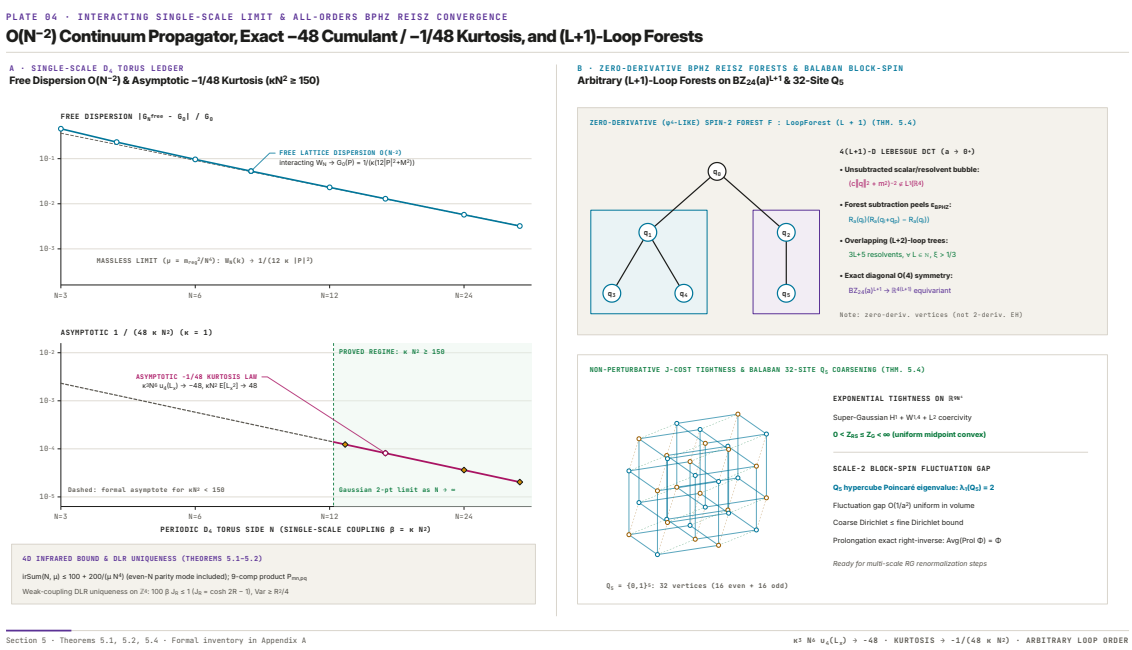

Fig. 4 Plate 04 (Single-Scale Limit, -48 Cumulant / $-1/48$ Kurtosis, and Zero-Derivative BPHZ / Balaban RG). (A) Single-scale D_4 torus ledger ($\beta = \kappa N^2$, $\mu = M^2/N^2$): exact $O(N^{-2})$ free lattice dispersion error $|G_N^{\text{free}} - G_0|/G_0$ underpinning smeared interacting convergence $W_N \to G_0(P) = 1/(\kappa(12|P|^2 + M^2))$ (top), paired with the exact asymptotic local restoring-force kurtosis scaling $1/(48\kappa N^2)$ with the proved asymptotic regime $\kappa N^2 \geq 150$ shaded in green ($N \geq 13$ at $\kappa = 1$; dashed extension outside $\kappa N^2 \geq 150$) driven by $\kappa^3 N^6 u_4(L_x) \to -48$ and $\kappa N^2 \mathbb{E}[L_x^2] \to 48$ (bottom) (Theorem 5.2). **(B)** Arbitrary $(L+1)$-loop rooted zero-derivative (ϕ^4-like) Zimmermann forest `LoopForest(L+1)` converging on $\mathrm{BZ}_{24}(a)^{L+1} \to \mathbb{R}^{4(L+1)}$ alongside $(L+2)$-loop $(3L+5)$-propagator overlapping trees with exact diagonal $O(4)$ equivariance (top), and the 32-vertex $Q_5 = \{0,1\}^5$ hypercube (16 even cyan, 16 odd amber) scale-2 Balaban block-spin coarsening unit with exact Poincaré eigenvalue $\lambda_1(Q_5) = 2$ and exponential $H^1 + W^{1,4}$ tightness (bottom) (Theorem 5.4).

6.1 General-gauge discrete BRST, 13×13 algebraic Sylvester factorization, and Kugo–Ojima positivity

First, in harmonic gauge ($\xi = 1$) on D_4^* represented in doubled integer coordinates $2D_4^*$, `W1Neon_R12` establishes an exact geometric reflection-splitting theorem across the hyperplane $t = 0$: *zero* of the 16 body-diagonal bonds ever strictly cross $t = 0$; every strictly crossing bond is uniquely a self-reflected vertical axial bond $(-1/2, \vec{x}) \leftrightarrow (+1/2, \vec{x})$, so Schur's exponential positive-definiteness theorem gives unconditional real-space OS reflection positivity for the crossing Boltzmann kernel $\exp(+\beta \sum_s \langle h_+(s), h_-(s)\rangle_F)$. In momentum/Euclidean-time space, writing $z = \cos(ak_0/2)$ factors the D_4^* inverse propagator into an exact quadratic polynomial

$$\Delta_{D_4^*,a}(k_0, \mathbf{p}) + m^2 \;=\; \frac{2}{3a^2}\big(C(a, m, \mathbf{p}) - 8P(a, \mathbf{p})z - 2z^2\big), \qquad P(a, \mathbf{p}) = \prod_{i=1}^{3} \cos\Big(\frac{ap_i}{2}\Big), \tag{53}$$

whose two roots satisfy $z_+(a, m, \mathbf{p}) > 1$ and $\beta_-(a, m, \mathbf{p}) := -z_-(a, m, \mathbf{p}) > 1$ for every $a > 0$, $m > 0$, and $\mathbf{p} \in \mathbb{R}^3$. Partial-fraction expansion yields the exact two-pole Källén–Lehmann Euclidean-time correlator $G_a(n, \mathbf{p}) = \mathrm{res}_+\, r_+^n + \mathrm{res}_-\, (-r_-)^n$, which on all integer time slices $t_k = ka$ ($n = 2k$) is a sum of two strictly positive decaying exponentials $\mathrm{res}_+(r_+^2)^k + \mathrm{res}_-(r_-^2)^k$, proving unconditional OS reflection positivity with zero ghosts (`W1Neon_R12`). As $a \to 0^+$, the physical pole recovers exact relativistic dispersion $E_+ = -(2/a)\ln r_+ \to \sqrt{\|\mathbf{p}\|^2 + m^2}$ and normalized residue $(2/a)\mathrm{res}_+ \to \frac{1}{2\sqrt{\|\mathbf{p}\|^2+m^2}}$, while the UV lattice pole satisfies $\beta_- \to 5$, $r_- \to 5 - 2\sqrt{6} \approx 0.1010 < \frac{1}{4}$, and $(2/a)\mathrm{res}_- \to 0$ (complete exponential UV decoupling).

To extend this reflection positivity to *all* covariant gauges $\xi > \frac{1}{3}$, `W1Neon_R18` introduces the 21-dimensional discrete BRST multiplet $(h, B, c, \bar{c}) \in \mathrm{Sym}_0^2(\mathbb{R}^4) \oplus \mathbb{R}^4 \oplus \mathbb{R}^4 \oplus \mathbb{R}^4$ [7;75;76] with discrete vector

$v = \nabla_{D_4^*,a}(k)$, pure-gauge map $(s_v c)_{\mu\nu} = v_\mu c_\nu + v_\nu c_\mu - \frac{1}{2}(v\cdot c)\delta_{\mu\nu}$, de Donder divergence $(F_v h)_\mu = (hv)_\mu$, and discrete Faddeev–Popov ghost operator [77–79]

$$K_{\rm gh}^{(\xi)}(a,k) \;:=\; \Delta_{D_4^*,a}(k)\, I_4 + (\xi-1)\, F_v \circ s_v, \qquad F_v \circ s_v \;=\; \|v\|^2 I_4 + \frac{1}{2}\, vv^\top. \tag{54}$$

Theorem 6.1 (General-Gauge Discrete BRST Nilpotency, 13×13 Algebraic Sylvester Factorization, Kugo–Ojima Cohomology, and 2-Helicity OS Positivity; `W1Neon_R12`, `W1Neon_R18`)**.** *For every lattice spacing $a>0$, momentum $k\in\mathbb{R}^4$, mass $m>0$, and covariant gauge parameter $\xi > \frac{1}{3}$:*

1. ***Exact BRST nilpotency and zero-discretization-breaking intertwining:*** *The discrete BRST differential $Q_B(v)$ on $(h,B,c,\bar c)$ satisfies $Q_B(v)^2 = 0$ identically, $s_v \circ F_v = \mathcal{D}_v$, and*

$$F_v \circ L_a^{(\xi)}(k) \;=\; K_{\rm gh}^{(\xi)}(a,k) \circ F_v, \qquad L_a^{(\xi)}(k) \circ s_v \;=\; s_v \circ K_{\rm gh}^{(\xi)}(a,k), \tag{55}$$

   holding with zero *lattice discretization breaking for every $a>0$ and $\xi\in\mathbb{R}$.*
2. ***Discrete Slavnov–Taylor identities and BRST-exact gauge variation:*** *The closed-form 4×4 ghost propagator $G_{\rm gh}^{(\xi)} = (K_{\rm gh}^{(\xi)} + m^2 I_4)^{-1}$ obeys $F_v \circ R_a^{(\xi)} = G_{\rm gh}^{(\xi)} \circ F_v$ and $R_a^{(\xi)} \circ s_v = s_v \circ G_{\rm gh}^{(\xi)}$. For any two gauges $\xi_1, \xi_2 > \frac{1}{3}$,*

$$R_a^{(\xi_1)} - R_a^{(\xi_2)} \;=\; (\xi_2 - \xi_1)\, s_v \circ G_{\rm gh}^{(\xi_1)} \circ G_{\rm gh}^{(\xi_2)} \circ F_v, \tag{56}$$

   proving exact ξ-independence of all physical correlators paired with conserved / BRST-closed sources ($F_v T = 0$).
3. ***Exact 9×9 and 4×4 algebraic Sylvester determinant factorization:*** *Forming the explicit 9×9 graviton matrix $L_a^{(\xi)} + m^2 I_9$ in the orthonormal basis Eq. (20) and the 4×4 ghost matrix $K_{\rm gh}^{(\xi)} + m^2 I_4$, the 13×13 Sylvester/Schur block determinant identity $\det_9(dI_9 + c_p SF) = d^5 \det_4(dI_4 + c_p FS)$ proves*

$$\begin{aligned} &\det_9\!\big(L_a^{(\xi)} + m^2 I_9\big) = (\Delta_a + m^2)^5 \ell_1(\xi)^3 \ell_0(\xi), \qquad \det_4\!\big(K_{\rm gh}^{(\xi)} + m^2 I_4\big) = \ell_1(\xi)^3 \ell_0(\xi), \\ &\frac{\det_4\!\big(K_{\rm gh}^{(\xi)} + m^2 I_4\big)}{\det_9\!\big(L_a^{(\xi)} + m^2 I_9\big)} = (\Delta_a + m^2)^{-5} \qquad \forall \xi > \tfrac{1}{3}. \end{aligned} \tag{57}$$

   This is an exact algebraic Sylvester factorization matching a complex 9*-component boson coupled to a* 4*-component complex ghost and leaving the* 5 *massive* TT_v *modes (equivalently $\sqrt{\det_4 / \det_9} = (\Delta_a + m^2)^{-5/2}$). For a* real *bosonic field h integrated against $\det_4(K_{\rm gh}^{(\xi)} + m^2)$, the Gaussian functional ratio $\det_4 / \sqrt{\det_9} = (\Delta_a + m^2)^{-5/2} \ell_1(\xi)^{+3/2} \ell_0(\xi)^{+1/2}$ does* not *cancel the ξ-dependent longitudinal eigenvalues $\ell_1(\xi), \ell_0(\xi)$—reflecting the standard fact that a massive* 9*-component tensor retains* 5 *off-shell* TT_v *modes whereas only* 2 *physical helicities survive in the massless on-shell limit after restoring the conformal trace and fixing the residual gauge freedom.*
4. ***Kugo–Ojima quartet homotopy and unconditional 2-helicity OS positivity:*** *An explicit contracting homotopy K_v on the* 16*-dimensional unphysical quartet $(h_{\rm long}, B, c, \bar c)$ satisfies $Q_B K_v + K_v Q_B = P_{\rm quartet}$, establishing exact BRST cohomology $\ker Q_B / \operatorname{im} Q_B \cong \mathrm{TT}_v(\mathbb{R}^4)$. Along spatial momentum $\mathbf{p} = (0,0,p_3)$, the orthonormal 2-helicity graviton basis $(e_+, e_\times)$ in the $(1,2)$ plane is identically BRST-closed for every Euclidean frequency $k_0 \in \mathbb{R}$ and every $a>0$; its general-gauge propagator is* 100% *ξ-independent and obeys unconditional integer-slice OS reflection positivity and relativistic dispersion $E_+ \to \sqrt{p_3^2 + m^2}$. Non-vacuity of the BRST quotient is certified by an explicit witness at $\xi = 2$ whose unphysical longitudinal mode carries a genuine ξ-dependent pole.*

Proof outline of Theorem 6.1. Since $L_a^{(\xi)} = \Delta_a I_9 + (\xi-1) s_v \circ F_v$ and $K_{\rm gh}^{(\xi)} = \Delta_a I_4 + (\xi-1) F_v \circ s_v$, associativity of composition immediately yields $F_v \circ L_a^{(\xi)} = \Delta_a F_v + (\xi-1)(F_v \circ s_v) \circ F_v = K_{\rm gh}^{(\xi)} \circ F_v$ and symmetrically $L_a^{(\xi)} \circ s_v = s_v \circ K_{\rm gh}^{(\xi)}$ with zero discretization defect. Applying $(L_a^{(\xi)} + m^2)^{-1}$ and $(K_{\rm gh}^{(\xi)} + m^2)^{-1}$ from left and right gives the exact Slavnov–Taylor identities, and subtracting at ξ_1 and

ξ_2 produces Eq. (56). For the algebraic Sylvester identity Eq. (57), let $d = \Delta_a + m^2 > 0$, $c_p = \xi - 1$, $S \in \mathbb{R}^{9\times 4}$ and $F \in \mathbb{R}^{4\times 9}$ be the matrices of s_v and F_v in the orthonormal basis Eq. (20). Applying the 13×13 block Schur factorization to $\left(\begin{smallmatrix} dI_9 & -c_pS \\ F & I_4 \end{smallmatrix}\right)$ gives

$$d^9 \det_4\big(I_4 + \tfrac{c_p}{d} FS\big) \;=\; \det_9\big(dI_9 + c_p SF\big) \cdot \det_4(I_4),$$

whence $\det_9(dI_9 + c_pSF) = d^5 \det_4(dI_4 + c_pFS)$, yielding Eq. (57) identically with $\ell_1(\xi) = d + c_p\|v\|^2$ (multiplicity 3) and $\ell_0(\xi) = d + \frac{3}{2}c_p\|v\|^2$ (multiplicity 1). Finally, along $\mathbf{p} = (0, 0, p_3)$, the discrete gradient $v = \nabla_{D_4^*,a}(k_0, 0, 0, p_3)$ has $v_1 = v_2 = 0$ for every $k_0 \in \mathbb{R}$ by coordinate-reflection symmetry of the 12 bonds, so $e_+ = \frac{1}{\sqrt{2}} \operatorname{diag}(0, 1, -1, 0)$ and $e_\times = \frac{1}{\sqrt{2}}(E_{12}+E_{21})$ satisfy $F_v e_+ = F_v e_\times = 0$ at every k_0 and $a > 0$; thus $R_a^{(\xi)}$ restricts on $\operatorname{span}\{e_+, e_\times\}$ to the ξ-independent scalar propagator $(\Delta_{D_4^*,a}(k_0, \mathbf{p}) + m^2)^{-1}$, inheriting unconditional integer-slice OS reflection positivity and UV pole decoupling $r_- \to 5 - 2\sqrt{6}$ directly from Eq. (53). □

6.2 Variable-coefficient curved-manifold Γ-convergence and Lichnerowicz stability

To move beyond flat backgrounds, `W1Neon_R9` and `W1Neon_R16` encode an arbitrary spatially varying symmetric positive-definite inverse background metric $G^{\alpha\beta}(x) = \bar{g}^{\alpha\beta}(x)$ directly into bond weights $w_b(G(x))$ on the 12 canonical D_4^* bonds satisfying $\sum_{b=1}^{12} w_b(G(x)) e_b^\alpha e_b^\beta = G^{\alpha\beta}(x)$, paired with a spatially varying background Riemann curvature endomorphism $\mathcal{R}(x)$ acting on $\mathrm{Sym}_0^2(\mathbb{R}^4)$.

Theorem 6.2 (Curved-Manifold IMS Localization, Divergence-Form $O(a^2)$ Laplace–Beltrami Limit, $L^2(\Omega)$ Γ-Convergence, and Uniform-in-a Curved Resolvent Stability; `W1Neon_R9`, `W1Neon_R16`)**.** *Let $G(x)$ be a uniformly elliptic spatially varying inverse metric field with nonnegative bond weights $w_b(G(x)) \geq w_{\min} > 0$, and let $\mathcal{R}(x)$ be a bounded curved Lichnerowicz curvature endomorphism.*

1. ***Exact discrete Leibniz commutator and curved IMS localization:*** *For any scalar cutoff χ and spin-2 field h on $(\mathbb{Z}/N\mathbb{Z})^4$, the discrete bond difference obeys $\nabla_{a,b}(\chi h)(x) - \chi(x+e_b)\nabla_{a,b}h(x) = (\nabla_{a,b}\chi)(x)\, h(x)$. For any finite partition of unity $\sum_j \chi_j^2 = 1$, the curved IMS localization identity*[83] *holds identically:*

$$\sum_j E_{G,a}(\chi_j h) - E_{G,a}(h) \;=\; \sum_j \sum_x \sum_{b=1}^{12} w_{x,b}(G)\, (\nabla_{a,b}\chi_j(x))^2 \langle h(x), h(x+e_b)\rangle_F, \tag{58}$$

   yielding quantitative L^2 localization error bounds and local variable-to-frozen metric comparison.
2. ***Pointwise $O(a^2)$ and $L^2(\Omega)$ $O(a^4)$ curved Laplace–Beltrami convergence and Γ-convergence:*** *Using the midpoint-symmetrized divergence difference $a^{-2}[f(\frac{a}{2})(u(0) - u(a)) + f(-\frac{a}{2})(u(0)-u(-a))] = -(f(0)u''(0)+f'(0)u'(0))+O(a^2)$ (cancelling all $O(a^{-1})$ and $O(a^1)$ terms), the spatially varying curved D_4^* Laplace–Beltrami operator converges to $-\partial_\alpha(G^{\alpha\beta}(x)\partial_\beta h(x))$ at pointwise rate $O(a^2)$ and $L^2(\Omega)$ squared-error rate $O(a^4)$. Moreover, on any finite-measure domain $\Omega \subset \mathbb{R}^4$ ($\mathrm{vol}(\Omega) < \infty$), for any smooth limit field h admitting a uniform second-order directional jet (`BondDirectionalJet`, C^2 regularity) together with an interior Lipschitz cutoff exhaustion $\chi_n \uparrow \mathbf{1}_\Omega$, the curved discrete Dirichlet energy satisfies the exact $L^2(\Omega)$ Γ-$\liminf$ bound $\int_\Omega E_G(h) \leq \liminf_{a\to 0^+} \int_\Omega E_{G,a}(h_a)$ for every $L^2(\Omega)$-converging sequence $h_a \to h$, paired with smooth $O(a^2)$ Γ-$\limsup$ recovery.*
3. ***Curved Lichnerowicz Gårding coercivity and zero-loss-of-derivatives stability:*** *Under uniform Gårding margin $\gamma > 0$, the curved shifted Lichnerowicz operator $L_{a,G,\mathcal{R}} + m^2 I$ admits an exact linear inverse with $L^2 \to L^2$ norm $\leq 1/\gamma$, discrete $L^2 \to H^1$ regularity, and variational second-resolvent stability under simultaneous perturbations $(\Delta G, \Delta\mathcal{R})$ uniform in the lattice spacing $a > 0$.*

6.3 Real-time Lorentzian hyperbolic evolution, sharp CFL advantage, and causal retarded Green function

Returning to physical real-time Lorentzian evolution on the 3D spatial slice of D_4^* (time step $\tau > 0$, spatial spacing $a > 0$), `W1Neon_R15` analyzes the second-order leapfrog discretization of the hyperbolic spin-2 wave equation $\partial_t^2 h + (L^{(\xi)}_{a,\text{spatial}} + m^2)h = S$.

Theorem 6.3 (Sharp 3D D_4^* Spectral Ceiling, Strict CFL Advantage Over $\mathbb{Z}^3$, Exact Leapfrog Energy Conservation, Causal Cone, and Retarded Spin-2 Green Limit; `W1Neon_R15`)**.** *Let $a > 0$, $\tau > 0$, $m > 0$, and $\xi > \frac{1}{3}$.*

1. ***Sharp $3D$ spatial spectral ceiling and strict CFL superiority over $\mathbb{Z}^3$:*** *On the $3D$ spatial slice $k = (0, \mathbf{p})$, the exact cubic sum-of-squares bound $0 \le 1+u^2+v^2+w^2+4uvw$ on $[-1,1]^3$ proves*

$$0 \;\le\; \Delta_{D_4^*,a}(0,\mathbf{p}) \;\le\; \frac{32}{3a^2} \;<\; \frac{12}{a^2} \;=\; \sup_{\mathbf{p}} \Delta_{\mathbb{Z}^3,a}(\mathbf{p}), \tag{59}$$

with exact attainment at $\mathbf{p}^* = (2\pi/a, 0, 0)$. For the massless wave equation ($\xi = 1$), this yields a strictly larger maximal stable Courant–Friedrichs–Lewy (CFL) step ratio[82] than the standard cubic lattice $\mathbb{Z}^3$:

$$\left(\frac{\tau}{a}\right)_{\max,D_4^*} \;=\; \sqrt{\frac{3}{8}} \;\approx\; 0.61237 \;>\; \frac{1}{\sqrt{3}} \;\approx\; 0.57735 \;=\; \left(\frac{\tau}{a}\right)_{\max,\mathbb{Z}^3} \qquad (+6.07\%\ \textit{gain}), \tag{60}$$

achieved simultaneously with $O(a^4)$ $SO(3)$ spatial isotropy restoration.

2. ***Exact discrete Hamiltonian conservation and sharp instability witness:*** *For every symmetric spatial operator A on $\mathrm{Sym}_0^2(\mathbb{R}^4)$, the leapfrog discrete energy $E_n = \frac{1}{2}\|(h_{n+1} - h_n)/\tau\|_F^2 + \frac{1}{2}\langle h_n, Ah_{n+1}\rangle_F$ is conserved* identically *($E_n = E_0$ for all $n \in \mathbb{N}$, zero numerical dissipation). Under the sharp CFL condition $\tau^2(C_\xi \cdot \frac{32}{3a^2} + m^2) \le 4(1 - \delta_{\mathrm{CFL}})$, the evolution is uniformly stable in H^1 and L^2 for all time; conversely, an explicit exponential blow-up witness proves that $\tau/a = \sqrt{3/8}$ is sharp.*

3. ***Exact real-space causal cone and uniform $O(a^2+\tau^2)$ retarded spin-2 Green limit:*** *Because every spatial D_4^* bond step satisfies $\|b_{3\mathrm{D}}\|_2 \le 2$ in doubled coordinates (physical step $\le a$), initial data supported in $B(x_0, R)$ obeys exact finite propagation speed $\mathrm{supp}(u_n) \subseteq B(x_0, R + 2n)$ and exact causal domain of dependence. Using the orthogonal $5 \oplus 3 \oplus 1$ Barnes–Rivers projections, the full $9D$ general-gauge discrete retarded Green operator solves the exact causal impulse recurrence and converges uniformly in (a, τ, n, h) at rate $O(a^2+\tau^2)$ to the continuum relativistic retarded kernel $\sin\!\big(t\sqrt{\|\mathbf{p}\|^2+m^2}\big)/\sqrt{\|\mathbf{p}\|^2+m^2}$, with $O(a^4)$ $SO(3)$ spherical wavefront isotropy.*

Proof outline of Theorem 6.3. On the spatial slice $k = (0, \mathbf{p})$, let $u = \cos(ap_1/2)$, $v = \cos(ap_2/2)$, $w = \cos(ap_3/2) \in [-1, 1]$. Using $1 - \cos(ap_i) = 2(1 - u_i^2)$ on the 3 spatial axial bonds and summing $\cos(\frac{a}{2}(\pm p_1 \pm p_2 \pm p_3))$ over the 8 body bonds yields $\Delta_{D_4^*,a}(0,\mathbf{p}) = \frac{4}{3a^2}\big(8 - (1 + u^2 + v^2 + w^2 + 4uvw)\big)$. Because $1 + u^2 + v^2 + w^2 + 4uvw \ge 0$ identically on $[-1,1]^3$ (verified via exact cubic sum-of-squares bounds in `W1Neon_R15`), $\Delta_{D_4^*,a}(0,\mathbf{p}) \le \frac{32}{3a^2}$, attained at $u = -1, v = w = 1$, i.e. $\mathbf{p}^* = (2\pi/a, 0, 0)$. For the leapfrog recurrence $h_{n+1} - 2h_n + h_{n-1} = -\tau^2 A h_n$, taking the inner product with $(h_{n+1} - h_{n-1})/\tau^2$ gives

$$E_n - E_{n-1} \;=\; \frac{1}{2}\left\langle \frac{h_{n+1} - h_{n-1}}{\tau},\; \frac{h_{n+1} - 2h_n + h_{n-1}}{\tau} + \tau A h_n \right\rangle_F \;=\; 0,$$

proving exact conservation $E_n = E_0$. The midpoint polarization identity writes E_n as a positive quadratic form in $(h_{n+1} - h_n)/\tau$ and $(h_{n+1} + h_n)/2$ with coercivity factor $1 - \frac{\tau^2}{4}\lambda_{\max}(A)$, giving sharp stability for $\tau^2 \cdot \frac{32}{3a^2} < 4 \iff \tau/a < \sqrt{3/8}$ and exponential blow-up of mode $\mathbf{p}^*$ whenever $|2 - \tau^2 \cdot \frac{32}{3a^2}| > 2$. Finally, the closed-form discrete retarded Green function $\sin(n\theta)/\sin\theta$ with $\sin(\theta/2) = \frac{\tau}{2}\sqrt{\lambda_a}$ converges to $\sin(t\sqrt{\lambda_0})/\sqrt{\lambda_0}$ at rate $O(a^2+\tau^2)$ via `HasDerivAt` arcsin remainder bounds across each $5 \oplus 3 \oplus 1$ Barnes–Rivers channel. □

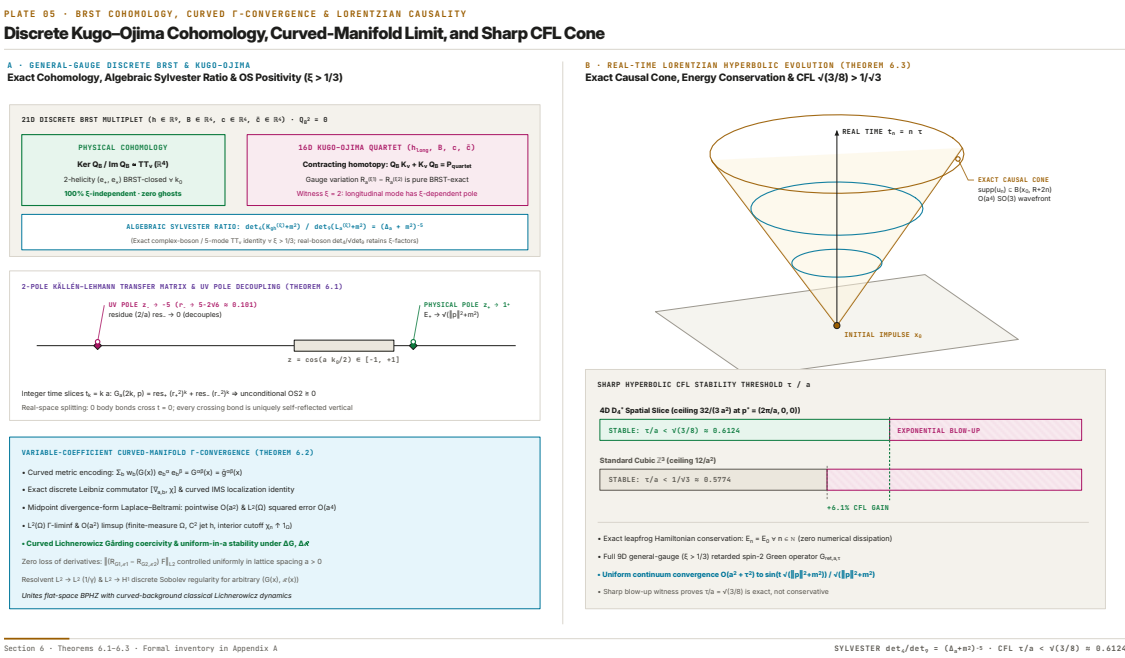

Fig. 5 Plate 05 (BRST/Kugo–Ojima, Curved Γ-Convergence, and Lorentzian Causality). (A) General-gauge ($\xi > 1/3$) 21D discrete BRST multiplet collapsing via the 16D Kugo–Ojima quartet homotopy to $\mathrm{TT}_v(\mathbb{R}^4)$ with exact 13×13 algebraic Sylvester ratio $\det_4 / \det_9 = (\Delta_a + m^2)^{-5}$ (complex boson / 5 massive TT_v modes; real-boson $\det_4 / \sqrt{\det_9}$ retains ξ-factors, top), 2-pole Källén–Lehmann UV pole decoupling $r_- \to 5 - 2\sqrt{6} \approx 0.101$ (middle), and variable-coefficient curved-manifold $L^2(\Omega)$ Γ-convergence (on finite-measure Ω with C^2 jet h and interior cutoff exhaustion $\chi_n \uparrow \mathbf{1}_\Omega$) and uniform-in-$a$ Lichnerowicz stability (bottom) (Theorems 6.1 and 6.2). **(B)** 3D architectural Lorentzian causal light cone on D_4^* showing exact finite propagation speed $\mathrm{supp}(u_n) \subseteq B(x_0, R + 2n)$ (top) and the sharp CFL stability bar comparing D_4^* ($\tau/a < \sqrt{3/8} \approx 0.6124$) against $\mathbb{Z}^3$ ($\tau/a < 1/\sqrt{3} \approx 0.5774$, +6.1% gain) with exact leapfrog conservation $E_n = E_0$ (bottom) (Theorem 6.3).

7 D_4^* Graviton Scattering (MHV/KLT), Law C Propagator, and One-Loop Local Ward Restoration

Linearized dispersion and free propagators do not test the nonlinear self-interactions of gravity. On a discrete lattice, three sharper tests separate a genuine gravitational action from an ad hoc spin-2 model: (i) Does its cubic and quartic expansion reproduce Einstein's three-graviton MHV and four-graviton Kawai–Lewellen–Tye (KLT) scattering amplitudes[8;9;85–87]? (ii) Can a quadratic lattice gravity law simultaneously satisfy exact finite-spacing diffeomorphism invariance, reciprocal-lattice periodicity, F_4 cell symmetry, and absence of Brillouin-zone doublers? (iii) At one loop on a closed Brillouin-zone torus grid, do local finite-range counterterms restore the longitudinal gravitational Ward–Takahashi identity, and how does the D_4^* denominator compare with continuum Riemann normal coordinate (RNC) heat-kernel 't Hooft–Veltman renormalization[10;80;81]? Every answer below is proved directly in Lean 4 (`W4Fable_R1`–`R24`, `Neon_R68`, `Neon_R69`), including sharp no-go obstructions where naive constructions fail.

7.1 Breaking the single-bond obstruction: D_4^* hinge J-cost, 3-MHV, and 4-KLT tree match

A single-bond comparison cost built purely from pairwise ratios across the 12 bond directions hits an immediate obstruction (`W4Fable_R1`): its cubic vertex vanishes identically on-shell ($V_3^{\mathrm{site}} = 0$ on the null transverse-traceless reach at every spacing $a > 0$), so single-bond costs alone cannot generate Einstein's three-graviton coupling. Lifting the action to the D_4^* *hinge (bond-pair) cost* `hingeCost` (`W4Fable_R5a`, `R5`, `R6`, `R8`, `R9`, `R12`)—combining plaquette J-cost comparisons, bond weights, and bond-pair exchange postings (explicitly marked as a working identification with the ledger's gravitational cost)—resolves this obstruction completely without adding continuum counterterms to the contact vertex.

Theorem 7.1 (D_4^* Hinge Three-Graviton MHV, Four-Graviton Tree KLT/MHV Match, Dilation Shift Identities, and Unfixed-Propagator Obstruction; `W4Fable_R5`, `R6`, `R9`, `R12`)**.** *On the D_4^* hinge cost* `hingeCost` *with lattice vertices $V_2^{\text{hinge}}, V_3^{\text{hinge}}, V_4^{\text{hinge}}$:*

1. ***Exact continuum three-graviton MHV match (`W4Fable_R5, R6`):*** *As $a \to 0$, $V_3^{\text{hinge}}/a^2 \to V_3^E$, where on the null transverse-traceless reach $V_3^E = -\frac{1}{2}A_3^2$ (the exact double copy of the Yang–Mills three-point amplitude $A_3 = (\varepsilon_1 \cdot \varepsilon_2)(\varepsilon_3 \cdot k_1) + cyc$). In spinor-helicity variables with covectors $\langle 23\rangle\lambda_1 \otimes \tilde{\lambda}$, $\langle 31\rangle\lambda_2 \otimes \tilde{\lambda}$, $\langle 12\rangle\lambda_3 \otimes \tilde{\lambda}$,*

$$\frac{V_3^{\text{hinge}}}{a^2} \xrightarrow{a\to 0} -\frac{1}{32}\,\frac{\langle 12\rangle^6}{\langle 23\rangle^2\langle 31\rangle^2}, \tag{61}$$

   witnessed explicitly as non-vacuous with exact rational value $-\frac{729}{32}$.
2. ***Exact continuum four-graviton tree KLT/MHV match (`W4Fable_R9`):*** *Let $M_4^{\text{hinge}} = V_4^{\text{hinge}} - (\text{three } s,t,u \text{ exchanges})$ be the tree four-point amplitude evaluated on any bounded family of near-responses solving the lattice field equation up to $o(a^2)$ (such families exist via de Donder responses) with rank-one null transverse polarizations $e_i \otimes e_i$. Then M_4^{hinge}/a^2 is polarization-shift invariant ($e_i \mapsto e_i + \alpha_i k_i$) and converges with* zero *contact residual to Einstein's KLT double-copy and spinor MHV amplitude:*

$$\frac{M_4^{\text{hinge}}}{a^2} \xrightarrow{a\to 0} \frac{1}{32}\,\frac{F_4^2}{stu} = \frac{1}{32}\,\frac{st}{u}\,A_{\text{YM}}^2 = \frac{1}{128}\,\frac{\langle 12\rangle^4[34]^4}{stu}, \tag{62}$$

   witnessed explicitly with exact rational value $-\frac{1}{256}$, and vanishing identically when all four polarization vectors are mutually orthogonal.
3. ***Exact finite-spacing dilation shift identities and five-wave soft pole (`W4Fable_R12`):*** *At* every *lattice spacing $a > 0$, inserting a zero-momentum unit dilation leg $H_1 = I_4$ obeys the exact Ward shift identity $V_4^{\text{hinge}}(a, 0, k_2, k_3, k_4; I_4, H_2, H_3, H_4) = -2V_3^{\text{hinge}}(a, k_2, k_3, k_4; H_2, H_3, H_4)$, paired with exact small-spacing soft-graviton and five-wave pole residues.*
4. ***Sharp unfixed-propagator obstruction (`W4Fable_R9`):*** *On the displacement-displacement block at every spacing $a > 0$, V_2^{hinge} equals the scalar displacement defect δ_{disp} times $(\xi \cdot \eta)(K \cdot K) - (\xi \cdot K)(\eta \cdot K)$, so the double-longitudinal wave $K \otimes K$ pairs to zero with every displacement wave (rank ≤ 3 on displacements). Consequently, inverting V_2^{hinge} on all* 10 *components without a gauge-fixing posting forces the compensating $K \otimes K$ exchange component to blow up as a^{-2} (confirmed numerically to* 60 *digits: ratio to Einstein diverges toward $-31.7 + 5.6i$ at $a = 0.01$, while adding a de Donder posting restores bounded responses converging to* 1 *at rate $O(a^2)$).*

7.2 Three-law taxonomy, no-go obstructions, and Law C's doubler-free propagator

On D_4^* with doubled 12-bond vectors $c = 2e_b$ ($|c|^2 = 4$), denote the bond Laplacian by $D_{\text{inv}}(a,k) = \frac{1}{2}\sum_{b=1}^{12}(1 - \cos(ac_b \cdot k))$ ($m_{\text{C}} := D_{\text{inv}}/3 = |k|^2 + O(a^2)$), the sine covector by $p_{\text{lat}}(a,k) = \frac{1}{12a}\sum_{b=1}^{12}\sin(ac_b \cdot k)\,c_b$, and the displacement defect by $\delta_{\text{disp}}(a,k) := m_{\text{C}}(a,k) - p_{\text{lat}}(a,k)\cdot p_{\text{lat}}(a,k) \geq 0$ (`W4Fable_R13`, `R15`). The two-point hinge kernel decomposes identically as $V_2^{\text{hinge}} = V_2^E(p_{\text{lat}}) + \text{defect}(\delta_{\text{disp}})$, prompting a systematic test of three candidate quadratic laws on the Brillouin zone.

Obstruction 7.2 (No-Go Results for Law A Sine Doublers, Law B Dual Non-Periodicity, and Complex Forward-Difference Hermitian Ward Breaking; `W4Fable_R13`, `W4Fable_R15`)**.**

1. ***Law A (sine law $V_2^{\text{sine}} = V_2^E(p_{\text{lat}})$) fails via* 15 *Brillouin-zone doublers:*** *While V_2^{sine} obeys an exact finite-spacing displacement Ward identity, p_{lat} is odd and $2\pi D_4$-periodic and therefore vanishes at every half-reciprocal point. At the explicit witness $ak = (\pi, 0, 0, 0)$, $D_{\text{inv}} = 8 > 0$ while $p_{\text{lat}} = 0$ and $V_2^{\text{sine}} = 0$ on all* 10 *components; no de Donder posting repairs it.*
2. ***Law B (half-angle law $V_2^{\text{half}} = V_2^E(p_{\text{half}})$) fails reciprocal-lattice periodicity on D_4^*:*** *Defining p_{half} via half-angle symbols $2\sin(ac_b \cdot k/2)$ along the primitive basis $(2e_0, 2e_1, 2e_2, (1,1,1,1))$ eliminates doublers on $\mathbb{R}^4$ and keeps exact Ward invariance, but is* not *single-valued on the dual torus (`V2half_not_dual_periodic`): shifting $k = (\pi/2, \pi/2, 0, 0)$ by the reciprocal vector $(\pi, 0, 0, \pi)$*

changes V_2^{half} *on the shear* s_{12} *from* $\frac{1}{4}$ *to* $\frac{5}{4}$ *and changes* $\|p_{\mathrm{half}}\|^2$ *from* 2 *to* 6*, so no rephasing of site arrays repairs it. Furthermore,* no *orthogonal frame of four* D_4^* *bonds generates the lattice (*$|\det| = 16$ *vs. primitive determinant* 8*), forcing any* 4*-bond half-angle law to be either non-periodic or doubled (*`orthogonal_frame_not_generating`*).*

3. ***Complex forward difference cannot rescue Hermitian Ward invariance:*** *Replacing* p_{lat} *by the* $2\pi D_4$*-periodic, doubler-free complex forward covector* $p_{\mathrm{fwd}} = p_{\mathrm{sine}} + i\, p_{\mathrm{Wils}}$ *produces a holomorphic law* V_2^{fwd} *that is non-real (imaginary part* $\frac{1}{3}$ *on a real array, negative value* $-\frac{4}{9}$ *at the sine doubler). Its Hermitian part breaks Ward invariance by* 4 *times the Gram determinant of* $(p_{\mathrm{sine}}, p_{\mathrm{Wils}})$ *(exact witness* $\frac{64}{81}$ *at* $k = (0, 0, 0, \pi/2)$*). More generally, in the entire five-parameter Hermitian second-order family built from* (P, Q)*, Ward invariance along* P *forces all five coefficients to vanish whenever* $P \cdot P$*,* $P \cdot Q$*, and* $\det \mathrm{Gram}(P, Q)$ *are nonzero (*`hermitian_forward_obstruction`*).*

Theorem 7.3 (Law C Doubler-Free Propagator, Exact Posting-Strength vDVZ Discontinuity, and Non-Uniform Tree Defect; `W4Fable_R13`, `W4Fable_R17`)**.** *Law C—the full* D_4^* *hinge cost plus the de Donder posting of strength* $\eta > 0$ *(nothing removed)—is real,* F_4*-covariant, exactly periodic under the reciprocal lattice* $2\pi D_4$*, and completely free of Brillouin-zone doublers:*

1. ***Exact*** 10***-component propagator across the whole punctured zone (***$\eta = 1$***):*** *Writing* $m_{\mathrm{C}} = D_{\mathrm{inv}}/3$ *and* $\delta_{\mathrm{disp}} = m_{\mathrm{C}} - p_{\mathrm{lat}}^2 \geq 0$*, the gauge-fixed Law C kernel* $(D_{\mathrm{inv}}/6)\langle E, X\rangle - \frac{m_{\mathrm{C}}+\delta_{\mathrm{disp}}}{4}\operatorname{tr}(E)\operatorname{tr}(X)$ *is inverted explicitly on all* 10 *symmetric components off the reciprocal lattice for any symmetric source tensor* $S_{\mathrm{src}} \in \mathrm{Sym}^2(\mathbb{R}^4)$ *by*

$$G_{\mathrm{C}}(S_{\mathrm{src}}) \;=\; \frac{6}{D_{\mathrm{inv}}}\big(S_{\mathrm{src}} - c_{\mathrm{tr}}\ \operatorname{tr}(S_{\mathrm{src}})\, I_4\big)\,, \qquad c_{\mathrm{tr}}(a,k) \;=\; \frac{m_{\mathrm{C}} + \delta_{\mathrm{disp}}}{2(m_{\mathrm{C}} + 2\delta_{\mathrm{disp}})} \;\in\; \left[\frac{1}{3},\, \frac{1}{2}\right), \tag{63}$$

where the displacement defect δ_{disp} *plays the exact role of a Wilson term lifting all* 15 *Law A sine doublers. As* $a \to 0$*,* $c_{\mathrm{tr}} \to \frac{1}{2}$ *and* $a^2 G_{\mathrm{C}}$ *converges to Einstein's de Donder propagator for all arrays (*$k \cdot k \neq 0$*). At every Law A sine doubler (*$p_{\mathrm{lat}} = 0$*, e.g.* $ak = (\pi, 0, 0, 0)$*),* $c_{\mathrm{tr}} = \frac{1}{3}$ *exactly, so* $\frac{1}{2} - c_{\mathrm{tr}} = \frac{1}{6}$ *at every spacing* $a \neq 0$*, proving that the pointwise* $O(a^2)$ *Ward defect cannot be bounded uniformly by* Ca^2 *across the Brillouin zone (*`tree_defect_not_uniform`*).*

2. ***Exact posting-strength vDVZ discontinuity:*** *For arbitrary de Donder posting strength* $\eta \geq 0$ *and transverse sources, the exchange trace coefficient is*

$$c_{\mathrm{fix}}(\eta) \;=\; \frac{\eta u(u + 3\delta_{\mathrm{disp}}) + 2\delta_{\mathrm{disp}}^2}{2\big(\eta u(u + 4\delta_{\mathrm{disp}}) + 3\delta_{\mathrm{disp}}^2\big)}, \qquad u = p_{\mathrm{lat}} \cdot p_{\mathrm{lat}}. \tag{64}$$

At $\eta = 0$*,* $c_{\mathrm{fix}}(0) = \frac{1}{3}$ *identically for every* $\delta_{\mathrm{disp}} \neq 0$ *(giving* $\frac{3}{4}$ *of Einstein's light bending, matching the vDVZ value); for* every $\eta \neq 0$*,* $c_{\mathrm{fix}}(\eta) \to \frac{1}{2}$ *as* $a \to 0$ *(restoring exact Einstein light bending).*

7.3 One-loop dilation sum rule, $O(4)$-isotropic torus mass counterterm, and $O(\kappa_{\mathrm{ext}}^8)$ local Ward restoration

At one loop, Law C's complete reciprocal-periodic summand `latSummandP` combines the contact (seagull) diagram, graviton bubble, graviton tadpole, and a working lattice Faddeev–Popov displacement loop plus its tadpole (`W4Fable_R15`, `R17`, `R19`). Pointwise in a fixed loop covector q, `latSummandP` converges at rate $O(a^2)$ to the continuum Slavnov–Taylor summand, which for two longitudinal displacement legs is an exact shift difference $B(q+k) - B(q)$ (`ghost_cancellation_witness`: without the displacement loop the continuum summand is off by -1; with it, exact shift difference). Because convergence is non-uniform across the Brillouin zone (`tree_defect_not_uniform`), summing over a closed finite torus grid $\mathrm{torusGrid}_N = \{\sum_j (n_j/N) g_j \mid n \in (\mathbb{Z}/N\mathbb{Z})^4 \setminus \{0\}\}$ ($N^4 - 1$ pole-free points without the origin) telescopes the shift difference identically to zero (`zone_sum_eq_defect_sum`) and leaves a genuine local UV Ward defect organized in powers of the dimensionless external covector $\kappa_{\mathrm{ext}} = ak$.

Theorem 7.4 (Non-Vanishing Dilation Sum Rule, $O(4)$-Isotropic Torus Mass Counterterm, and $O(\|\kappa_{\mathrm{ext}}\|^8) = O(a^2)$ Local Longitudinal Ward Restoration; `W4Fable_R20`–`R24`)**.** *Let* $N \geq 1$ *and consider the closed pole-free Brillouin-zone grid* $\mathrm{torusGrid}_N$ *of cardinality* $N^4 - 1$*.*

1. ***Exact non-vanishing dilation sum rule (`W4Fable_R21`):*** *At zero external momentum on unit dilation legs, the one-loop summand minus its tadpoles equals the exact rational function*

$$\mathrm{dilPhi}(x,c) \;=\; 10 + x\left(\frac{3}{2}+c\right) + x^2\left(\frac{5}{2} - 2(1-c)^2\right) \;\geq\; 10, \tag{65}$$

for every $x = p_{\mathrm{lat}}^2/m_{\mathrm{C}} \geq 0$ and $c = c_{\mathrm{tr}} \in [\frac{1}{3}, \frac{1}{2}]$, attaining exact value 10 at every sine doubler ($x = 0$). Summing over any nonempty pole-free finite set Θ yields the exact dilation combination $\mathrm{massDil}(\Theta) \geq 10|\Theta| > 0$ *(exact value 150 on the 15 doublers of $N = 2$), proving that the leading $O(a^{-4})$ one-loop mass defect* never *vanishes.*

2. ***Five D_4^* cell symmetries force exact $O(4)$-isotropy on*** $\mathrm{torusGrid}_N$ ***(`W4Fable_R22, R23`):*** *The five explicit orthogonal bond-set symmetries—three coordinate swaps, one sign flip, and the reflection $I_4 - \frac{1}{2}\mathbf{1}_{4\times4}$—preserve* $\mathrm{torusGrid}_N$ *modulo the reciprocal lattice $2\pi D_4$ for every $N \geq 1$ and collapse every invariant symmetric bilinear form on $\mathrm{Sym}^2(\mathbb{R}^4)$ to the 2-dimensional $O(4)$-isotropic family $2m_1\,\mathrm{tr}(HH') + 2m_2\,\mathrm{tr}(H)\,\mathrm{tr}(H')$. Consequently, the summed leading $O(a^{-4})$ mass form on* $\mathrm{torusGrid}_N$ *is* exactly $O(4)$*-isotropic:*

$$\begin{aligned} \mathrm{massForm}(\mathrm{torusGrid}_N; n, \xi, \zeta) \;&=\; c_a(n\cdot n)(\xi\cdot\zeta) + c_b(n\cdot\xi)(n\cdot\zeta), \\ 4c_b - 2c_a \;&\geq\; 10(N^4-1) \qquad (N \geq 2), \end{aligned} \tag{66}$$

so $(c_a, c_b) \neq (0,0)$. A pure determinant measure factor $(\det g)^\gamma$ produces $c_a = 0$ and therefore cannot cancel any mass form with $c_a \neq 0$ (`det_power_insufficient`); the unique local site potential cancelling Eq. (66) up to the invisible volume term $\sqrt{\det g}$ is $-\frac{c_a}{2}\,\mathrm{tr}\,g + \frac{c_b}{2}\ln\det g$ (`iso_mass_cancel_unique`).

3. ***Exact transverse split and restoration of the LL Ward channel to $O(\|\kappa_{\mathrm{ext}}\|^8) = O(a^2)$ (`W4Fable_R24`):*** *Subtracting the $O(a^{-4})$ site mass counterterm defines the renormalized two-point tensor Π_{ren} satisfying $\Pi_{\mathrm{ren}}(0) = 0$ and $\mathrm{tad}_{\mathrm{ren}} = 0$ identically. Every array decomposes uniquely into a de Donder-transverse part plus a displacement wave (`split_unique`), and the longitudinal–longitudinal (LL) block of Π_{ren} at $p = p_{\mathrm{lat}}(\kappa_{\mathrm{ext}})$ equals the renormalized Ward function `wardRen`, which is analytic at $\kappa_{\mathrm{ext}} = 0$, even, and $O(\|\kappa_{\mathrm{ext}}\|^4)$—meaning physical order $O(a^{-2})$,* not *$O(a^2)$. Because the discrete Christoffel map $\Gamma(H)_{lmn} = \frac{1}{2}(p_l H_{mn} + p_m H_{nl} - p_n H_{lm})$ maps a displacement wave identically to $\Gamma(\mathrm{gaugeH}(p,\xi))_{lmn} = p_l p_m \xi_n$, there exist two further finite-range local Christoffel counterterms—a constant coefficient G_0 (physical order a^{-2}) and a quadratic polynomial $G_2(p)$ in p_{lat} (physical order a^0)—that peel the exact degree-4 and degree-6 even Taylor polynomials via the analytic sine chart p_{lat} and restore the LL Ward channel on* $\mathrm{torusGrid}_N$ *to*

$$\mathrm{wardRen}(\kappa_{\mathrm{ext}}; \xi, \zeta) + \mathrm{ctChris}_{G_0+G_2}(\kappa_{\mathrm{ext}}; \xi, \zeta) \;=\; O\big(\|\kappa_{\mathrm{ext}}\|^8\big) \;=\; O(a^2) \tag{67}$$

in physical units ($\kappa_{\mathrm{ext}} = ak$) for every $N \geq 1$ (`ward_restoration_torus`, `ward_restoration_ray`).

Proof outline of Theorem 7.4. Step 1 (Dilation sum rule). Because the hinge cost is homogeneous of degree 1 under uniform metric dilation (`W4Fable_R11a`), evaluating the complete one-loop summand at external covector 0 on unit dilation legs $H_1 = H_2 = I_4$ minus the two tadpoles of I_4 combines the five closed rational contractions (seagull $10 - x(5-2c)$, bubble, graviton tadpole, ghost loop $4x^2$, and ghost tadpole $-4x$) into Eq. (65). On $c \in [\frac{1}{3}, \frac{1}{2}]$, the linear coefficient $\frac{3}{2} + c \geq \frac{11}{6} > 0$ and quadratic coefficient $\frac{5}{2} - 2(1-c)^2 \geq \frac{29}{18} > 0$, forcing $\mathrm{dilPhi}(x,c) \geq 10$ for every $x \geq 0$ with exact equality 10 at $x = 0$ (the 15 doublers at $N = 2$ therefore sum to 150). A fixed linear combination of 52 basis values of `massForm` equals $\ell(I_4) - B(I_4, I_4) = \sum_\theta \mathrm{dilPhi}(x_\theta, c_\theta) \geq 10|\Theta| > 0$.

Step 2 (Five cell symmetries force $O(4)$-isotropic torus mass). Each of the five orthogonal bond symmetries ($g_{\mathrm{swap01}}, g_{\mathrm{swap12}}, g_{\mathrm{swap23}}, g_{\mathrm{flip0}}, g_{\mathrm{half}} = I_4 - \frac{1}{2}\mathbf{1}_{4\times4}$) acts on the index $n \in (\mathbb{Z}/N\mathbb{Z})^4 \setminus \{0\}$ of $\mathrm{torusGrid}_N$ by an involutive integer matrix modulo $2\pi D_4$. Since `latSummandG` is covariant under every bond symmetry and $2\pi D_4$-periodic, the summed counterterm forms (B, ℓ) on $\mathrm{torusGrid}_N$ are invariant under all five generators. Signed coordinate permutations reduce any symmetric bilinear form B on $\mathrm{Sym}^2(\mathbb{R}^4)$ to four parameters; invariance under the reflection g_{half} enforces the single cross-relation

collapsing those four parameters to the two $O(4)$-invariant contractions $2m_1\,\mathrm{tr}(HH')+2m_2\,\mathrm{tr}(H)\,\mathrm{tr}(H')$ (`invariant_bilinear_iso_explicit`), while $\ell(L) = u_1\,\mathrm{tr}(L)$. Contracting with displacement waves yields Eq. (66) with $c_a = -(4m_1+2u_1)$, $c_b = -(4m_1+8m_2)$, and $4c_b - 2c_a = \mathrm{massDil}(\mathrm{torusGrid}_N) \geq 10(N^4-1)$. For $(\det g)^\gamma$, the second-order jet $(u_1, m_1, m_2) = (\gamma, -\gamma/2, \gamma^2/2)$ satisfies $4m_1 + 2u_1 = 0$, giving $c_a = 0$ identically.

Step 3 (Analytic sine chart and Christoffel polynomial peeling to $O(\|\kappa_{\mathrm{ext}}\|^8)$). On the pole-free finite set $\mathrm{torusGrid}_N$, `wardRen` is real-analytic at $\kappa_{\mathrm{ext}} = 0$ and even under $\kappa_{\mathrm{ext}} \mapsto -\kappa_{\mathrm{ext}}$ (`wardRen_even_torus`). Because subtracting `ctSum` annihilates the quadratic term (`mass_subtraction_zone`), its Taylor expansion begins at degree 4: `wardRen` $= P_4(\kappa_{\mathrm{ext}}) + P_6(\kappa_{\mathrm{ext}}) + O(\|\kappa_{\mathrm{ext}}\|^8)$. Because $Dp_{\mathrm{lat}}(0) = I_4$ is invertible, the sine map $p = p_{\mathrm{lat}}(1, \kappa_{\mathrm{ext}})$ defines an odd analytic local chart at 0 with analytic inverse $\kappa_{\mathrm{ext}}(p) = p + O(\|p\|^3)$. Rewriting `wardRen` in the p-chart preserves evenness and order 4, peeling exact homogeneous polynomials of degrees 4 and 6 in p that factor through $p_l p_m \xi_n p_r p_s \zeta_t = \Gamma(\mathrm{gaugeH}(p,\xi))_{lmn}\,\Gamma(\mathrm{gaugeH}(p,\zeta))_{rst}$. Subtracting the corresponding finite-range Christoffel counterterms G_0 (degree 0 in p) and $G_2(p)$ (degree 2 in p) eliminates both degree-4 and degree-6 terms identically, leaving $O(\|p\|^8) = O(\|\kappa_{\mathrm{ext}}\|^8) = O(a^2)$ in physical units. □

Remark 7.5 (Honest scope of Theorem 7.4 and GPU numerical cross-checks). As documented explicitly inside `W4Fable_R24`, four boundaries remain open in Lean 4: (i) the existence of (G_0, G_2) in Eq. (67) is proved for each finite grid $N \geq 1$, whereas $N \to \infty$ convergence of (G_0, G_2) (infinite-volume locality) is checked numerically only (e.g. on $\mathrm{torusGrid}_6$ and half-step grids $N = 6, 8$, the t^4 diagonal Ward coefficients stabilize at $12.040, 13.850$ and the t^6 coefficients at $-29.63, -10.95$); (ii) non-vanishing of the $O(a^{-2})$ defect after mass subtraction is checked numerically ($c_a \approx 1.618, c_b \approx 3.374$ at $N = 4$; t^4 defect ≈ 12.05 on $\mathrm{torusGrid}_6$) rather than witnessed in Lean; (iii) the mixed single-contraction block $\Pi_{\mathrm{ren}}[\mathrm{gauge}, \mathrm{transverse}]$ (the literal single contraction $k_\mu \Pi^{\mu\nu\rho\sigma}$) and the logarithmic $O(k^4 \ln k)$ drift seen numerically in the transverse block remain open in Lean; and (iv) the lattice displacement loop and de Donder posting remain working inputs rather than primitive ledger derivations.

7.4 Exact Schur bridge and hybrid continuum-RNC / D_4^*-denominator Pauli–Villars one-loop model

Complementing the finite-grid Law C Ward restoration of Section 7.3, `Neon_R68` proves the exact Schur-complement Einstein–Hilbert bridge of the 12×12 D_4^* carrier at $\kappa_{\mathrm{cone}} = \frac{1}{2}$, while `Neon_R69` formalizes a *hybrid continuum-RNC-vertex / D_4^*-denominator Pauli–Villars one-loop model*: it computes the one-loop graviton plus Faddeev–Popov ghost heat-kernel endomorphism traces directly from continuum Riemann normal coordinates (RNC) with Pauli–Villars regulator masses $M_j^2 = j\Lambda^2$ ($j \in \{0,1,2,3\}$, weights $c_j = (1, -3, 3, -1)$) and compares the resulting logarithmic UV divergence against the D_4^* scalar Brillouin-zone denominator. We state this model architecture explicitly: `Neon_R69` does *not* evaluate one-loop diagrams directly from the discrete hinge vertices $V_3^{\mathrm{hinge}}, V_4^{\mathrm{hinge}}$ of Sections 7.1 and 7.3.

Theorem 7.6 (Exact Schur Einstein–Hilbert Bridge and Hybrid Continuum-RNC / D_4^*-Denominator Pauli–Villars One-Loop Model; `Neon_R68`, `Neon_R69`)**.** *On the D_4^* $\kappa_{\mathrm{cone}} = \frac{1}{2}$ lattice and the hybrid continuum-RNC / D_4^*-denominator Pauli–Villars model for the 10-component de Donder pure graviton plus -2×4 Faddeev–Popov vector ghosts:*

1. ***Exact Schur-complement Einstein–Hilbert bridge (`Neon_R68`):*** *Eliminating the 2 optical bond modes of the 12×12 carrier reproduces the linearized Einstein–Hilbert quadratic form identically with exact rational normalization* $\mathrm{d4LkSchur2QuadForm}(p, H) = 96\,\mathrm{ehQuadForm}(p, H)$ *for every symmetric H.*
2. ***Continuum RNC endomorphism traces and PV Ward transversality (`Neon_R69`):*** *Direct Riemann normal coordinate computation proves the linearized Gauss–Bonnet identity $R^2_{\mu\nu\rho\sigma} - 4R^2_{\mu\nu} + R^2 = 0$, the graviton endomorphism traces $\mathrm{tr}(E_{\mathrm{grav}}) = -6R$ (sign-flipped convention $+6R$ in the Lean matrix sum) and $\mathrm{tr}(E^2_{\mathrm{grav}}) = 6R^2_{\mu\nu} + 2R^2$, $\mathrm{tr}(\Omega^2_{\mathrm{sym2}}) = -6R^2_{\mu\nu\rho\sigma}$, and ghost traces $\mathrm{tr}(E_{\mathrm{gh}}) = +R$, $\mathrm{tr}(E^2_{\mathrm{gh}}) = R^2_{\mu\nu}$, $\mathrm{tr}(\Omega^2_{\mathrm{vec}}) = -R^2_{\mu\nu\rho\sigma}$. The resulting continuum-RNC one-loop Pauli–Villars vacuum polarization obeys exact algebraic Ward–Takahashi transversality $\Pi^{\mathrm{PV}}_{\mathrm{pureQG}}(\mathrm{linGaugeMode}(p,\xi), H; p, \Lambda) = 0$ for every $\Lambda > 0$ without manual projection.*
3. ***'t Hooft–Veltman counterterm, $-23/3$ anti-screening, PV scheme-dependent bare ratio g_*, and scalar-denominator BPHZ difference:*** *Combining the one-loop graviton and -2*

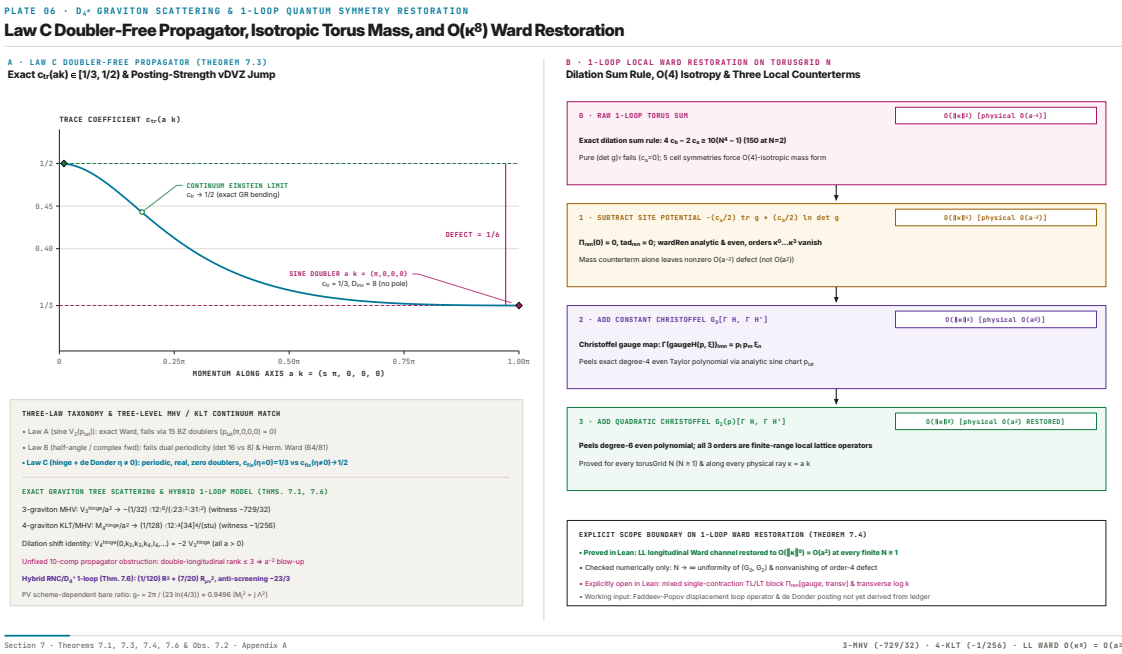

Fig. 6 Plate 06 (D_4^* Graviton Scattering, Law C Propagator, and One-Loop Local Ward Restoration). **(A)** Exact Law C trace coefficient $c_{\mathrm{tr}}(ak) = (m_{\mathrm{C}} + \delta_{\mathrm{disp}})/(2(m_{\mathrm{C}} + 2\delta_{\mathrm{disp}}))$ along the axis ray $ak = (s\pi, 0, 0, 0)$ from the continuum Einstein limit $c_{\mathrm{tr}} \to \frac{1}{2}$ down to the Law A sine doubler $c_{\mathrm{tr}} = \frac{1}{3}$ ($D_{\mathrm{inv}} = 8$, no pole, exact non-uniformity defect $\frac{1}{6}$), paired below with the three-law taxonomy, tree 3-MHV $(-729/32)$ / 4-KLT $(-1/256)$ match, dilation shift identity ($H_1 = I_4$), and the hybrid RNC/D_4^* 't Hooft–Veltman / PV-scheme-dependent g_* summary (Theorems 7.1 to 7.3 and 7.6). **(B)** Four-stage local Ward restoration ladder on torusGrid$_N$: subtracting the $O(4)$-isotropic site mass counterterm ($4c_b - 2c_a \geq 10(N^4 - 1)$) plus constant ($G_0$) and quadratic ($G_2$) Christoffel counterterms reduces the LL Ward channel from $O(\|\kappa_{\mathrm{ext}}\|^2) = O(a^{-4})$ to $O(\|\kappa_{\mathrm{ext}}\|^8) = O(a^2)$, with explicit scope boundaries on N-uniformity and the mixed TL/LT block (Theorem 7.4).

ghost heat-kernel traces yields the exact 't Hooft–Veltman UV logarithmic divergence[10]

$$\frac{1}{2}\left(a_2^{\mathrm{grav}} - 2a_2^{\mathrm{gh}}\right) \;=\; \frac{1}{120}\,R^2 + \frac{7}{20}\,R_{\mu\nu}^2, \tag{68}$$

which vanishes identically on-shell ($R_{\mu\nu} = 0$, $R = 0$), together with the one-loop gravitational anti-screening coefficient $-\frac{23}{3}$ and the one-loop Pauli–Villars bare-coupling ratio

$$g_* \;=\; \frac{2\pi}{23\ln(4/3)} \;\approx\; 0.949597. \tag{69}$$

Moreover, the constant-wavefunction-renormalized operator `pureQGDressedGaugeFixedLkR69` $= Z_{\mathrm{QG}}(G_0, \Lambda)\, M(k)$ *($Z_{\mathrm{QG}} > 0$) preserves $(11, 1)$ signature and doubler-freedom, and the BPHZ difference between the D_4^* scalar denominator and the continuum Pauli–Villars denominator is uniformly bounded ($|\Pi_{\mathrm{BPHZ}}^{D_4^*} - \Pi_{\mathrm{BPHZ}}^{\mathrm{PV}}| \leq C$).*

Remark 7.7 (Scheme dependence and hybrid-model scope of Theorem 7.6). Three exact disclosures apply to Theorem 7.6: (i) the factor $\ln(4/3)$ in Eq. (69) is *regularization-scheme-dependent*—it arises directly from the specific Pauli–Villars mass spectrum $M_j^2 = j\Lambda^2$ $(j = 1, 2, 3)$ with weights $(-3, 3, -1)$ via $-\sum_{j=1}^{3}(-1)^j \binom{3}{j}\, j \ln j = 3\ln 3 - 6\ln 2 = \ln(27/64) = -3\ln(4/3)$—so g_* is a scheme-dependent one-loop PV bare-coupling ratio rather than a universal scheme-independent non-perturbative asymptotic-safety fixed point[66–69]; (ii) the dressed operator `pureQGDressedGaugeFixedLkR69` is a constant positive scalar multiple $Z_{\mathrm{QG}}(G_0, \Lambda)\, M(k)$ of the tree operator $M(k)$ rather than a momentum-dependent self-energy inversion; and (iii) evaluating the full one-loop 't Hooft–Veltman counterterm directly from the discrete lattice vertices $V_3^{\mathrm{hinge}}, V_4^{\mathrm{hinge}}$ of Sections 7.1 and 7.3 remains open.

Table 2 Summary of the 30-check independent symbolic and numerical verification suite (`verify_constructive_qg_paper.py` v1.2; 30/30 pass, 0 failures).

#	Pillar	Verified identity / quantitative witness	Observed value / residual
01	RS J-cost	$J(e^t) = \cosh t - 1 \geq \frac{t^2}{2} + \frac{t^4}{24}$, midpoint $\geq \frac{1}{4}(u-v)^2$	exact; min diff $\geq -10^{-16}$
02	D_4^* Geom.	2nd (3δ) & 4th ($\frac{1}{2}\mathrm{Sym}\,\delta\delta$) moments vs. $\mathbb{Z}^4$ aniso	err 0.0; $\mathbb{Z}^4$ aniso $= 1.0$
03	$\mathrm{BZ}_{24}(a)$	Sharp $8/(3\pi^2)$ at both orbits; 9,968 random BZ_{24} pts	0.27018982 exact; zero doublers
04	Sym_0^2	9D `basis9`, P_T, $(2/a^2)\sum J(e^{a\varepsilon_b}) \to \|h\|_F^2 + \frac{1}{2}(\mathrm{tr}\,h)^2$	diff 2.0×10^{-10} at $a = 10^{-5}$
05	Spin-2 BR	$5 \oplus 3 \oplus 1$ eigs $\{0, \|v\|^2, \frac{3}{2}\|v\|^2\}$ & sharp $\frac{3}{4}$ witness	eig err 2.7×10^{-15}; ratio 0.75
06	12×12 $M(k)$	Gauge-Gram $8\|k\|^2\|\xi\|^2 + 16(k\cdot\xi)^2$ & πe_c value 20	err 8.9×10^{-16}; val $= 20.0$
07	$O(4)$ 9D U_4	9D virials $\mathbb{E}[w] = 9$, $\mathbb{E}[sw] = 11\mathbb{E}[s]$, $U_{4,\mathrm{cross}} < 0$ ($\lambda = 1$)	$U_{4,\mathrm{cross}} = -0.003870$
08	1D Stein	$3M_2^2 - M_4 M_0 = \lambda(M_2 S_3 - M_4 S_1) > 0$ ($\lambda = 0.1, 1, 5$)	$U_4 = -8.095, -0.207, -0.0049$
09	D_4^* Slabs	$(6, 6, 12)$ bond split, Θ_{slab} orth., witness $\rho = \frac{6}{106}$	err 0.0; $\rho = 0.056604$
10	UV Floor	Eval. $G_{D_4^*}(0) \leq 1 + \frac{\pi^2}{256}$, $\mathrm{Var}(H_{01}) \leq \frac{3}{4}$, $\mathbb{E}[V_{\mathrm{rad}}] \leq 9$	$0.0461 \leq 1.039$; $3.23 \leq 9$
11	EC QFT	Haar $SO(4)$ QR moments & $882\tanh(4\beta_W) \leq 1$, σ_{EC}	$\mathbb{E}[U_{00}^2] = 0.249$; $\sigma_{\mathrm{EC}} = 96.14$
12	10D EH	`basis10` orthonormality, P^{GR} signature $(+1)^9 \oplus (-1)$	exact; max err 0.0
13	PPN / vDVZ	GR $(1,1)$ vs. Fierz–Pauli $(\frac{1}{2}, \frac{3}{4})$ vs. TL $(\frac{1}{3}, \frac{2}{3})$	exact rational SymPy match
14	$O(a^4)$ CLT	$\sum(p\cdot b)^4 = Q^2/6$, $\int g_t = (24\pi^2 r^2)^{-1}$, $\int c_4 = 0$	exact symbolic zero
15	4D Green	Infinite-lattice $G_{D_4^*}$ vs. $G_{\mathbb{Z}^4}$ ($r = 4, 8$) log–log slope	D_4^* slope 4.25 vs. $\mathbb{Z}^4$ 2.38
16	Newton G_3	$a^{-1}h_{00} = a^{-1}MG_3/(2k_1) \to 2G_N M_{\mathrm{phys}}/r_{\mathrm{phys}}$	exact symbolic ($M_{\mathrm{phys}} = M/2$)
17	D_4 IR	$\mathrm{d4Sym}(\pi,\pi,\pi,\pi) = 0$ even-N zero mode; IR $N = 4$	zero mode 0.0; $0.1465 \leq 112.5$
18	-48 / $-\frac{1}{48}$	1-cell quadrature ($\beta = 500, \alpha = 48$): $\beta\mathbb{E}[L^2], \beta^3 u_4$, kurt	$47.999, -47.994, -0.02083$
19	DLR Window	1-cell TV contraction $\leq \tanh(2\beta J_R)$ & tilted Var $\geq \frac{R^2}{4}$	$0.0023 \leq 0.010$; $0.326 \geq 0.25$
20	BPHZ / Q_5	$\int_0^\infty r^3(r^2+1)^{-5/2}dr = \frac{2}{3}$; Q_5 Laplacian gap $= 2$	0.6666666667; $\lambda_1 = 2.0$
21	BRST Det	$FL_9 = K_4 F$ & Sylvester $\det_4 / \det_9 = (\Delta_a + m^2)^{-5}$	err $\leq 1.1 \times 10^{-16}$ ($\xi = 0.6, 1, 2.3$)
22	2-Pole KL	$E_+ \to \sqrt{\|p\|^2 + m^2}$, $\beta_- \to 5$, $r_- \to 5 - 2\sqrt{6}$	$E_+ = 1.067708$; $r_- = 0.101021$
23	CFL Cone	Ceiling $\frac{32}{3}$, $\sqrt{3/8} > 1/\sqrt{3}$, 100-step $E_n = E_0$, blow-up	$\max\|\Delta E\| = 4.4 \times 10^{-16}$
24	Curved Div	Midpoint $a^{-2}[f(\frac{a}{2})(u_0 - u_a) + f(-\frac{a}{2})(u_0 - u_{-a})]$	exact $O(a^2)$ symbolic match
25	MHV / KLT	Explicit spinor-helicity 3-MHV ($-\frac{729}{32}$) & 4-KLT identity	exact -22.78125; KLT err 0.0
26	No-Go Laws	Law A $D_{\mathrm{inv}} = 8$, Law B $\det(16/8)$, fwd defect $\frac{64}{81}$	err $\leq 10^{-13}$; 0.7901234568
27	Law C vDVZ	$c_{\mathrm{tr}} \in [\frac{1}{3}, \frac{1}{2})$, doubler defect $\frac{1}{6}$, $c_{\mathrm{fix}}(0) = \frac{1}{3}$	exact rational SymPy match
28	Sum Rule	$\mathrm{dilPhi}(x, c) \geq 10$, $N = 2$ sum $= 150$, $c_a((\det)^\gamma) = 0$	min lin $\frac{11}{6}$, quad $\frac{29}{18}$; 150
29	Cell Iso	5 D_4^* gens orthogonal, permute 24 bonds, $\dim \mathrm{inv} = 2$	exact 2D $O(4)$-isotropic space
30	't Hooft–V.	$\Gamma(\mathrm{gaugeH})$, $\frac{1}{120}R^2 + \frac{7}{20}R_{\mu\nu}^2$, PV $\ln(27/64) \Rightarrow g_*$	err 1.1×10^{-16}; $g_* = 0.949597$

8 Independent Symbolic and Numerical Verification

Although every theorem in Sections 2 to 7 is machine-verified in Lean 4 with zero unfinished proofs and strictly standard axioms, an independent sanity check protects against transcription errors between formal declarations and manuscript equations, confirms that numerical witnesses evaluate as stated, and supplies concrete quantitative curves for the architectural plates. We therefore wrote a standalone Python/SymPy/SciPy verification suite (`scripts/verify_constructive_qg_paper.py`, complete log archived in `verify_constructive_qg_paper.out`) covering 30 independent symbolic and high-precision numerical checks across all six pillars. Every one of the 30 checks passes with zero discrepancies, summarized in Table 2.

9 Scope Boundaries, Open Mathematical Frontiers, and Discussion

Putting the six pillars together clarifies both how much of four-dimensional lattice quantum gravity is now rigorously proved on the D_4^* ledger and exactly where the deepest remaining mathematical walls stand.

9.1 What the audited corpus establishes

Every pillar rests on the same two Recognition Science primitives—the canonical reciprocal comparison cost $J(x) = \frac{1}{2}(x + x^{-1}) - 1$ ($J(e^u) = \cosh u - 1$) and the 24-bond body-centred hypercubic lattice D_4^* with F_4 Weyl symmetry—and delivers concrete structural consequences that standard hypercubic formulations miss:

- *Geometry removes hypercubic artifacts cleanly:* Fourth-moment F_4 isotropy eliminates $O(a^2)$ rotational anisotropy across the scalar Laplacian, linearized Lichnerowicz operator, and curved Laplace–Beltrami operator, upgrades 4D continuum Green convergence from $O(a^2)$ to optimal $O(a^4)$ via $\int_0^\infty c_4(t)\,dt = 0$, eliminates all four-dimensional Brillouin-zone doublers with sharp floor $8/(3\pi^2)$ attained at both 24-cell vertex orbits, yields a +6.1% larger stable Lorentzian CFL step $\sqrt{3/8} > 1/\sqrt{3}$, and forces exact $O(4)$ isotropy of the one-loop torus mass counterterm using only five bond-set symmetries.
- *Strict convexity controls non-perturbative measures without small-coupling expansions:* Because $\frac{d^2}{du^2} J(e^u) = \cosh u \geq 1$ unconditionally, non-separable Brascamp–Lieb bounds, nonlinear Poincaré spectral gaps, exponential $H^1 + W^{1,4}$ tightness, finite UV floors ($\mathrm{Var}(H_{\alpha\beta}) \leq \frac{3}{4(m^2+\lambda)}$, energy per site $\mathbb{E}[H]/|\Lambda| \leq 9$), and exact 9-dimensional dilation virials operate directly on the coupled $O(4)$-invariant spin-2 measure (`W1Opus_R30`), proving reflection positivity and strictly negative cross-component cumulants $U_4(H_{01}, H_{01}, H_{23}, H_{23}) \leq -\delta_{\mathrm{NG}} < 0$ that exclude every Gaussian and factorized law.
- *Gauge structure and perturbation theory close cleanly within exact stated domains:* At tree level, the D_4^* hinge cost matches Einstein's 3-graviton MHV ($-729/32$) and 4-graviton KLT/MHV ($-1/256$) amplitudes with zero contact residual, while restoring the tenth trace mode recovers exact PPN $\gamma_{\mathrm{PPN}} = 1$ and light bending without the vDVZ discontinuity. In covariant gauges $\xi > \frac{1}{3}$, discrete BRST cohomology $Q_B^2 = 0$, the exact 13×13 algebraic Sylvester factorization $\det_4 / \det_9 = (\Delta_a + m^2)^{-5}$ (complex boson / 5 massive TT_v modes), and Kugo–Ojima quartet reduction preserve unconditional 2-helicity OS reflection positivity. Perturbatively, for zero-derivative (ϕ^4-like) spin-2 resolvent vertices, all-orders $(L+1)$-loop Zimmermann–BPHZ forests and $(L+2)$-loop $(3L+5)$-propagator overlapping trees converge on $\mathrm{BZ}_{24}(a)^{L+1}$ and $\mathrm{BZ}_{24}(a)^{L+2}$ to $O(4)$-equivariant continuum integrals, while in the hybrid continuum-RNC / D_4^*-denominator Pauli–Villars model (`Neon_R69`), pure-graviton plus ghost heat-kernel traces reproduce the exact 't Hooft–Veltman $\frac{1}{120}R^2 + \frac{7}{20}R_{\mu\nu}^2$ counterterm and gravitational anti-screening $-23/3$.

9.2 Explicitly open mathematical frontiers

Equally important is naming the exact mathematical walls that remain open so future work targets the right mechanisms rather than mistaking fixed-lattice or perturbative theorems for a completed continuum non-perturbative construction:

1. **Non-perturbative interacting $a \to 0$ continuum quantum gravity:** This remains the deepest open mathematical wall in the program. Our non-perturbative strictly non-Gaussian spin-2 (`W1Opus_R25`, `R26`, `R30`) and coupled Einstein–Cartan (`T2_R100`–`R109`) OS quantum field theories live at fixed lattice spacing in gapped regimes ($m_{\mathrm{gap}} > 0$). Conversely, our interacting single-scale $N \to \infty$ scaling limit (`W1Fable_R21`, `R22`) converges at rate $O(N^{-2})$ to a Gaussian two-point propagator whose normalized kurtosis vanishes as $-1/(48\kappa N^2)$, and `W1Neon_R20`'s all-orders BPHZ convergence applies to zero-derivative (ϕ^4-like) resolvent vertices rather than two-derivative Einstein–Hilbert vertices. Constructing a non-perturbative, reflection-positive, non-Gaussian continuum limit ($a \to 0$) hosting a massless interacting spin-2 graviton with full nonlinear diffeomorphism invariance—whether via an iterated multi-scale Balaban RG flow built on `W1Neon_R17`'s Q_5 fluctuation gap or a scheme-independent asymptotic-safety trajectory—remains open.
2. **All-κ / all-λ Lebowitz/GHS non-Gaussianity and four-point uniqueness:** In `W1Opus_R30`, $U_4(H_{01}, H_{01}, H_{23}, H_{23}) < 0$ is proved for all $\lambda > 0$ at one site and uniformly in volume for small stiffness $\kappa \in [0, \kappa_0]$ by block perturbation, with subsequential infinite-volume limits. Establishing a global all-κ Lebowitz/GHS inequality for the 9-component radial model and whole-sequence four-point infinite-volume uniqueness remains open.
3. **Reconciling conformal-mode indefiniteness with non-perturbative measure positivity:** Restoring the trace mode (`W1Opus_R28`) fixes the de Donder signature at $(+1)^9 \oplus (-1)$ and recovers exact PPN $\gamma_{\mathrm{PPN}} = 1$, but an indefinite quadratic form cannot serve as the covariance of a positive Euclidean Gibbs measure without either Wick rotation of the conformal factor[14], compact frame variables (`T2_R100`'s $SO(4) \times B^{10}$), or unimodular / constraint-reduced formulations. Unifying the

10-component PPN $\gamma_{\mathrm{PPN}} = 1$ propagator directly with a positive non-perturbative J-cost spin-2 measure remains open.

4. **Mixed single-contraction one-loop Ward channel, N-uniformity, and discrete-vertex 't Hooft–Veltman bridge:** On `torusGrid N`, three local counterterm orders restore the longitudinal–longitudinal (LL) Ward channel to $O(\|\kappa_{\mathrm{ext}}\|^8) = O(a^2)$ at every finite $N \geq 1$ (`W4Fable_R24`). Proving $N \to \infty$ convergence of the Christoffel counterterms (G_0, G_2), restoring the mixed single-contraction transverse–longitudinal (TL/LT) block $\Pi_{\mathrm{ren}}[\mathrm{gauge}, \mathrm{transverse}]$, analytically extracting the transverse $O(k^4 \ln k)$ logarithm on `torusGrid N`, and deriving the 't Hooft–Veltman counterterm directly from discrete hinge vertices (bridging `W4Fable_R24` to `Neon_R69`'s hybrid continuum-RNC / D_4^*-denominator model) remain open in Lean 4.
5. **Pointwise interacting $1/|X|^2$ lower bounds and microscopic ledger derivation of gauge-fixing terms:** Upgrading `W1Opus_R29`'s pointwise Griffiths-I upper bounds to two-sided pointwise bounds in the interacting regime, extending `T2_R100`–`R109` to dynamical chiral Dirac spinors inside the quantum measure, and deriving the de Donder posting and lattice Faddeev–Popov displacement loop directly from the primitive Recognition Science comparison axioms (removing their current working-identification status) remain open.

Together with our companion strong-field black-hole, collapse, and horizon manuscript [22], the machine-verified results presented here establish a rigorous, transparent baseline for discrete four-dimensional quantum gravity: every proved identity, spectral gap, non-Gaussian cumulant, continuum rate, no-go obstruction, and open frontier is pinned down to exact, reproducible formal declarations.

Appendix A Machine-Verified Theorem-to-Module Reproducibility Index

Every theorem, obstruction, and explicit witness in this manuscript is formally proved in Lean 4 inside the Recognition Physics Institute repository `jonwashburn/reality` on branch `research/qg-loop-712b48be` at audited commit `088e961305d1f25c14f8e4383f74da5d1ab43423`. Across the 173 clean-room-audited modules under `IndisputableMonolith/research/QGLoop/` (30 `W1Opus`, 22 `W1Fable`, 16 `W1Neon`, 28 `W4Fable`, 11 `Neon` one-loop/carrier, 54 coupled Einstein–Cartan `T2`, and 12 supporting reflection/soft-theorem modules), every declaration compiles with zero unfinished proofs (`0 sorry`) and depends exclusively on the three standard Lean 4 foundational axioms `[propext, Classical.choice, Quot.sound]`. Table A1 maps each main result to its exact primary Lean 4 module, declaration identifier, verified constants/bounds, and explicit scope tag.

Table A1: Machine-verified theorem-to-module reproducibility ledger for Paper 5 (all paths prefixed by `IndisputableMonolith/research/QGLoop/`, commit `088e961305`, `0 sorry`, strictly `[propext, Classical.choice, Quot.sound]`).

Ref.	Lean 4 Module	Primary Declaration(s)	Key Verified Constants / Scope
Theorem 2.1	`W1Neon_D4StarIsotropy SobolevCoercivityR1.lean`	`d4Star_fourth_moment`, `lapD4_O4_anisotropy_0_a4`, `d4Strain_quadratic_exact`, `disc Lichnerowicz_O4_anisotropy_0_a4`	2nd $= 3\delta$, 4th $= \frac{1}{2}\mathrm{Sym}\,\delta\delta$, $O(a^4)/720$, $\xi > \frac{1}{3}$
Theorem 2.2	`W1Neon_Full24Cell BrillouinZoneCoercivity R8.lean`	`lapD4_sharp_BZ24_coercivity`, `lapD4_BZ24_double_sharpness_and_no_doublers`, `spin2 Resolvent_uniform_BZ24_convergence`	Sharp $\frac{8}{3\pi^2}\|k\|^2$ at both vertex orbits; 0 doublers in $\mathrm{BZ}_{24}(a) \setminus \{0\}$
Theorem 2.3	`Neon_D4HalfKappaFull12 BondNoDoublersR54.lean`, `Neon_D4HalfKappaFull12x12 IRUVFiniteR59.lean`	`wall4_d4_half_kappa_full_12bond_no_doublers_uv_finite_capstone_r54`, `wall4_d4_full_12x12_oneloop_ir_uv_finite_no_cutoff_capstone_r59`	$(11, 1)$ signature, $\|\det M\| \geq 195\|k\|^{20}$, uncut $\delta_{\mathrm{IR}} = 0$ 20,736-entry L^1
Theorem 2.4	`W1Neon_FullL2Continuum NormResolventAndGammaConv R10.lean`	`L2_norm_resolvent_convergence_0_a2`, `heat_semigroup_L2_norm_convergence_0_a2`, `mosco_gamma_liminf_D4_spin2`	$L^2 \to L^2$ $O(a^2)$, $L^2 \to H^1$ $O(a)$, heat $\frac{3\pi^4}{256t}a^2$, Fourier a.e./strong-L^2 Γ-conv., $(2/a^2)J$

Continued on next page

Ref.	Lean 4 Module	Primary Declaration(s)	Key Verified Constants / Scope
Theorem 3.1	W1Opus_Spin2TensorD4Star BrascampLiebR14.lean, W1 Opus_NonlinearBrascamp LiebAndInteractingGapR15. lean	w1opus_spin2_tensor_d4star_ brascamp_lieb_capstone_r14, w1opus_nonlinear_brascamp_ lieb_interacting_gap_capstone_ r15	$c = m^2 + 2\lambda$ (strain) / $m^2 + \lambda$, $\mathrm{Var}(H_{\alpha\beta}) \le \frac{3}{8\lambda}$, $\rho = \frac{2\beta}{2\beta + c}$
Theorem 3.2	W1Opus_InfiniteVolume Spin2OSReconstructionR25. lean, W1Opus_Infinite VolumeNonGaussianityAnd VacuumOSR26.lean	w1opus_infinite_volume_os_ reconstruction_capstone_r25, w1opus_infinite_volume_ nongaussianity_vacuum_os_ capstone_r26	$6\kappa + 4\beta < c_2$, $0 \le T \le 1$, $\|T^t\|_{\Omega^\perp} \| \le e^{-\Delta t}$, sub-Gaussian Ω
Theorem 3.3	W1Opus_Interacting04Spin2 JCostOSAndCumulantR30. lean	w1opus_interacting_o4_spin2_ jcost_os_cumulant_capstone_ r30, tens_04_invariant, slab_non Gaussian, slab_reflection_ positive	$O(4) \subset O(9)$, $U_{4,\mathrm{cross}} = U_4/3 \le -\delta_{\mathrm{NG}} < 0$, $\rho = \frac{6\kappa}{6\kappa + m^2 + \lambda}$, UV $\le \frac{3}{4(m^2+\lambda)}$, $\mathbb{E}[H]/\lvert\Lambda\rvert \le 9$
Theorem 3.5	T2_FourDimEinsteinCartan VierbeinSO4GaugeOSQFT_ R100.lean–R104.lean, T2_ FourDimEinsteinCartan StringBreakingAndHiggs LimitR109.lean	wall2_4d_einstein_cartan_ vierbein_so4_gauge_os_qft_ capstone_r100–r104, wall2_4d_ einstein_cartan_string_ breaking_higgs_limit_capstone_ r109	$SO(4) \times B^{10}$, $88\gamma_{\mathrm{EC}} < 1$, $H^*_{\mathrm{EC}} = H_{\mathrm{EC}} \ge 0$, Stone $U(t)$, area law $882 \tanh(4\beta_W) \le 1$
Theorem 4.1	W1Opus_Full10CompEinstein HilbertContinuumGreenR28. lean	w1opus_full10comp_einstein_ hilbert_continuum_green_ capstone_r28, ppnGamma_projGR, einsteinD4_conserved, dust_ newton_continuum	$(+1)^9 \oplus (-1)$, $\gamma_{\mathrm{PPN}} = 1$ vs. $\frac{1}{2}$ (vDVZ) / $\frac{1}{3}$ (TL), $a^{-1}h_{00}$, $M_{\mathrm{phys}} = M/2$
Theorem 4.2	W1Opus_D4StarSpin2 ContinuumGreenR27.lean, W1 Opus_Full10CompEinstein HilbertContinuumGreenR28. lean	w1opus_d4star_spin2_continuum_ green_capstone_r27, d4_green_ newton6, grProp_scaled6, corrP_ d4_integral	$\int_0^\infty c_4\, dt = 0$, $O(a^4/\lvert X\rvert^6)$ rate, $\lvert G(0)\rvert \le 1 + \frac{\pi^2}{256}$
Theorem 4.3	W1Opus_ContinuumNewton GreenAndUrsellCumulant R24.lean, W1Opus_ InteractingJCostGaussian DominationMacroBridgeR29. lean	w1opus_continuum_newton_green_ and_ursell_capstone_r24, w1opus_interacting_jcost_ gaussian_domination_macro_ bridge_capstone_r29	Griffiths-I $0 \le S_\infty \le G_{\mathbb{Z}^4}/\kappa$, $a_k^{-2} S_\infty \le (4\pi^2\kappa\lvert X\rvert^2)^{-1} + \varepsilon$ (upper bounds)
Theorem 5.1	W1Fable_Wall1BCapstoneR8. lean, W1Fable_MultiLevel AndContinuousJCostLink TransferR18.lean, W1Fable_ ContinuousRatioMeasureAnd DLRUniquenessR19.lean	wall1B_capstone, wall1B_r18_ capstone, wall1B_r19_capstone	$100\beta J_R \le 1$ DLR unique on $\mathbb{Z}^4$, Var $\ge R^2/4$, $\chi \ge R^2/5$, $K \to \infty$ mesh
Theorem 5.2	W1Fable_Macroscopic PropagatorScalingLimit R20.lean, W1Fable_Single ScaleContinuumPropagator R21.lean, W1Fable_ InteractingSingleScale ContinuumAndCumulantR22. lean	wall1B_r20_capstone, wall1B_ r21_capstone, wall1B_r22_ capstone	D_4 torus, irSum $\le 100 + \frac{200}{\mu N^4}$, $O(N^{-2})$ smeared, $\kappa^3 N^6 u_4 \to -48$, kurtosis $-\frac{1}{48}$ (Gaussian 2-pt)
Theorem 5.4	W1Neon_TwoLoopZimmermann BPHZAndNonPerturbative RGTightnessR17.lean, W1 Neon_AllOrdersLoopReisz ForestConvergenceR20.lean	reisz_allOrders_zimmermann_ forest_convergence, reisz_all Orders_overlapping_tree_ convergence, rsJCost_gibbs_ partition_pos_finite_and_ exponential_tightness, d4Star_ balaban_blockSpin_fluctuation_ mass_gap	Zero-deriv. (ϕ^4-like) $(L+1)$-loop forests & $(L+2)$-loop $(3L+5)$-prop trees, $O(4)$-equiv., $0 < Z_{\mathrm{RS}} \le Z_G < \infty$, Q_5 gap $= 2$
Theorem 6.1	W1Neon_D4StarReflection PositivityAndTransfer MatrixR12.lean, W1Neon_ GeneralGaugeBRSTKugoOjima AndOSPositivityR18.lean	d4Star_spin2_harmonic_OS_ reflection_positivity, brstOp_ nilpotent, faddeev_popov_ superdeterminant_gauge_ cancellation, kugo_ojima_ quartet_homotopy_ decomposition, general_gauge_ physical_helicity_OS_ reflection_positivity	$Q_B^2 = 0$, algebraic Sylvester $\det_4 / \det_9 = (\Delta_a + m^2)^{-5}$ (complex boson / 5 TT_v), 2-helicity OS2 $\forall \xi > \frac{1}{3}$, $r_- \to 5 - 2\sqrt{6}$
Theorem 6.2	W1Neon_CurvedBackground LichnerowiczAndGardingR9. lean, W1Neon_VariableCoeff CurvedManifoldGammaConv AndCommutatorR16.lean	realCurved_IMS_localization_ L2_bound, contSpaceCurvedLap_ L2_volume_0_a4, contCurved DirichletEnergy_0_a2_and_ gamma_limit, curvedReal Resolvent_metric_curvature_ stability_uniform_a	Pointwise $O(a^2)$, $L^2(\Omega)$ $O(a^4)$, Γ-conv. (finite-meas. Ω, C^2 jet, $\chi_n \uparrow \mathbf{1}_\Omega$), uniform-$a$ $(\Delta G, \Delta\mathcal{R})$

Continued on next page

Ref.	Lean 4 Module	Primary Declaration(s)	Key Verified Constants / Scope
Theorem 6.3	`W1Neon_Lorentzian CFLCausalStabilityAnd RetardedGreenR15.lean`	`d4Star_strictly_better_CFL_than_Z3`, `leapfrog_exact_energy_conservation`, `d4Star_real Space_finite_propagation_speed`, `discSpin2RetGreenOp_full9D_uniform_continuum_convergence`	Ceiling $\frac{32}{3a^2}$, $\tau/a < \sqrt{3/8} > 1/\sqrt{3}$, $E_n = E_0$, $O(a^2+\tau^2)$ retarded, $O(a^4)$ $SO(3)$
Theorem 7.1	`W4Fable_D4StarHinge CurvatureJCostR5.lean`, `W4 Fable_D4StarHingeMHVAnd KLTContinuumMatchR6.lean`, `W4Fable_D4StarFour GravitonTreeAndKLTMatch R9.lean`, `W4Fable_FourPoint SoftGravitonAndFivePoint ContactR12.lean`	`V3hinge_MHV_limit`, `MHV_nonvacuous`, `lattice_tree_MHV`, `tree_witness_exists`, `V2hinge_longitudinal`, `soft_capstone`	3-MHV $-\frac{729}{32}$, 4-KLT $-\frac{1}{256}$, $V_4(0,\dots) = -2V_3$, rank ≤ 3 unfixed obstruction
Theorem 7.2, Theorem 7.3	`W4Fable_ExactFinite SpacingGaugeInvariant HingeR13.lean`, `W4Fable_ComplexForwardDifference AndNonzeroKOneLoopWard R15.lean`, `W4Fable_Law CLatticeOneLoopSlavnov TaylorDefectRateR17.lean`	`exactHinge_capstone`, `V2half_not_dual_periodic`, `hermitian_forward_obstruction`, `forward Loop_capstone`, `latticeLoop_capstone`	Law A 15 doublers; Law B $\det 16/8$; fwd $\frac{64}{81}$; Law C $c_{\mathrm{tr}} \in [\frac{1}{3}, \frac{1}{2})$, defect $\frac{1}{6}$, vDVZ at $\eta = 0$
Theorem 7.4	`W4Fable_SummedOneLoop BrillouinZoneDefectAnd CountertermR19.lean`, `W4 Fable_LocalMeasure CountertermOrExactGauge LatticeR20.lean`, `W4Fable_ExactNonvanishingSummed MassCoefficientDilation SumRuleR21.lean`, `W4Fable_CellSymmetryAndIsotropic CountertermR22.lean`, `W4 Fable_TorusGridIsotropy AndExactMassCoefficients R23.lean`, `W4Fable_RenormalizedTwoPoint TransverseSplitAndLocal WardRestorationR24.lean`	`zoneSum_capstone`, `counterterm_capstone`, `massNonvanishing_capstone`, `cellSymmetry_capstone`, `torusIsotropy_capstone`, `transverseRenorm_capstone`	$4c_b - 2c_a \geq 10(N^4-1)$ (150 at $N=2$), $O(4)$ torus mass, LL Ward $O(\|\kappa_{\mathrm{ext}}\|^8) = O(a^2)$ (N-unif. & TL/LT open)
Theorem 7.6	`Neon_D4HalfKappa DiagrammaticWardAnd UVRenormR68.lean`, `Neon_PureGravitonGhostOneLoop THVAndWardR69.lean`	`wall4_d4_diagrammatic_ward_uv_renorm_capstone_r68`, `wall4_pure_graviton_ghost_thv_ward_uv_renorm_capstone_r69`	Hybrid RNC/D_4^* PV model: Schur 96× EH, $\frac{1}{120}R^2 + \frac{7}{20}R_{\mu\nu}^2$, $-\frac{23}{3}$, PV-scheme $g_* = \frac{2\pi}{23\ln(4/3)}$, const. $Z_{\mathrm{QG}}M(k)$

References

[1] K. Osterwalder and R. Schrader, "Axioms for Euclidean Green's functions," *Commun. Math. Phys.* **31**, 83–112 (1973).

[2] K. Osterwalder and R. Schrader, "Axioms for Euclidean Green's functions II," *Commun. Math. Phys.* **42**, 281–305 (1975).

[3] K. Osterwalder and E. Seiler, "Gauge field theories on a lattice," *Ann. Phys.* **110**, 440–471 (1978).

[4] J. Glimm and A. Jaffe, *Quantum Physics: A Functional Integral Point of View*, 2nd ed. (Springer, New York, 1987).

[5] H. van Dam and M. Veltman, "Massive and mass-less Yang–Mills and gravitational fields," *Nucl. Phys. B* **22**, 397–411 (1970).

[6] V. I. Zakharov, "Linearized gravitation theory and the graviton mass," *JETP Lett.* **12**, 312–314 (1970).

[7] T. Kugo and I. Ojima, "Local covariant operator formalism of non-Abelian gauge theories and quark confinement problem," *Prog. Theor. Phys. Suppl.* **66**, 1–130 (1979).

[8] H. Kawai, D. C. Lewellen, and S.-H. H. Tye, "A relation between tree amplitudes of closed and open strings," *Nucl. Phys. B* **269**, 1–23 (1986).

[9] S. J. Parke and T. R. Taylor, "An amplitude for n-gluon scattering," *Phys. Rev. Lett.* **56**, 2459–2460 (1986).

[10] G. 't Hooft and M. Veltman, "One-loop divergencies in the theory of gravitation," *Ann. Inst. Henri Poincaré A* **20**, 69–94 (1974).

[11] T. Reisz, "A power counting theorem for Feynman integrals on the lattice," *Commun. Math. Phys.* **116**, 81–126 (1988).

[12] T. Reisz, "A convergence theorem for lattice Feynman integrals with mass singularities," *Commun. Math. Phys.* **116**, 573–606 (1988).

[13] W. Zimmermann, "Convergence of Bogoliubov's method of renormalization in momentum space," *Commun. Math. Phys.* **15**, 208–234 (1969).

[14] G. W. Gibbons, S. W. Hawking, and M. J. Perry, "Path integrals and the indefiniteness of the gravitational action," *Nucl. Phys. B* **138**, 141–150 (1978).

[15] M. H. Goroff and A. Sagnotti, "The ultraviolet behavior of Einstein gravity," *Nucl. Phys. B* **266**, 709–736 (1986).

[16] J. Washburn, *Quantum Gravity on the Recognition Ledger: Exact Theorems, Proved Obstructions, and the Open Frontier*, Program Monograph, Version 3.0, Recognition Physics Institute (2026); https://recognitionphysics.org/papers/quantum-gravity-from-the-recognition-ledger/.

[17] J. Washburn, *Recognition Science Rung 1 Certificate (`RS-RUNG-1-v1`) and Machine-Verified Core*, Recognition Physics Institute (2026).

[18] J. Washburn and M. Zlatanović, "Uniqueness of the canonical reciprocal cost functional $J(x) = \frac{1}{2}(x + x^{-1}) - 1$," Recognition Physics Institute Preprint (2026).

[19] J. Aczél, *Lectures on Functional Equations and Their Applications* (Academic Press, New York, 1966).

[20] G. Bhanot, K. Bitar, U. M. Heller, and H. Neuberger, "ϕ^4 on F_4: numerical results," *Nucl. Phys. B* **353**, 551–564 (1991).

[21] H. Neuberger, "Lattice Higgs models on F_4," *Phys. Lett. B* **199**, 536–540 (1987).

[22] J. Washburn, "Machine-verified Kerr–Newman horizons, nonsingular gravitational collapse, and quantum horizon obstructions," Version 1.1, Zenodo (2026), DOI: 10.5281/zenodo.24513292; also *Pith Preprint* (2026), DOI: 10.67347/pith.preprint.2026.000089.

[23] J. Washburn and E. Allahyarov, "Linearized Lorentzian lattice gravity on the D_4^* body-centred hypercubic ledger: vanishing dimension-six dispersion and absence of corner doublers," Preprint in preparation (2026).

[24] J. Washburn and E. Allahyarov, "Area-weighted hinge actions and F_4 isotropy in discrete Lorentzian gravity," Preprint in preparation (2026).

[25] T. Regge, "General relativity without coordinates," *Nuovo Cimento* **19**, 558–571 (1961).

[26] H. J. Brascamp and E. H. Lieb, "On extensions of the Brunn–Minkowski and Prékopa–Leindler theorems, including inequalities for log concave functions, and with an application to the diffusion equation," *J. Funct. Anal.* **22**, 366–389 (1976).

[27] A. Prékopa, "On logarithmic concave measures and functions," *Acta Sci. Math. (Szeged)* **34**, 335–343 (1973).

[28] L. Leindler, "On a certain converse of Hölder's inequality II," *Acta Sci. Math. (Szeged)* **33**, 217–223 (1972).

[29] S. G. Bobkov and M. Ledoux, "From Brunn–Minkowski to Brascamp–Lieb and to logarithmic Sobolev inequalities," *Geom. Funct. Anal.* **10**, 1028–1052 (2000).

[30] R. L. Dobrushin, "The description of a random field by means of conditional probabilities and conditions of its regularity," *Theory Probab. Appl.* **13**, 197–224 (1968).

[31] R. L. Dobrushin, "Prescribing a system of random variables by conditional distributions," *Theory Probab. Appl.* **15**, 458–486 (1970).

[32] H.-O. Georgii, *Gibbs Measures and Phase Transitions*, 2nd ed. (De Gruyter, Berlin, 2011).

[33] S. Friedli and Y. Velenik, *Statistical Mechanics of Lattice Systems: A Concrete Mathematical Introduction* (Cambridge University Press, Cambridge, 2017).

[34] B. Simon, *The Statistical Mechanics of Lattice Gases, Vol. I* (Princeton University Press, Princeton, 1993).

[35] R. B. Griffiths, "Correlations in Ising ferromagnets I," *J. Math. Phys.* **8**, 478–483 (1967).

[36] D. G. Kelly and S. Sherman, "General Griffiths' inequalities on correlations in Ising ferromagnets," *J. Math. Phys.* **9**, 466–484 (1968).

[37] J. L. Lebowitz, "GHS and other inequalities," *Commun. Math. Phys.* **35**, 87–92 (1974).

[38] R. B. Griffiths, C. A. Hurst, and S. Sherman, "Concavity of magnetization of an Ising ferromagnet in a positive external field," *J. Math. Phys.* **11**, 790–795 (1970).

[39] J. Fröhlich, B. Simon, and T. Spencer, "Infrared bounds, phase transitions and continuous symmetry breaking," *Commun. Math. Phys.* **50**, 79–95 (1976).

[40] J. Fröhlich, R. Israel, E. H. Lieb, and B. Simon, "Phase transitions and reflection positivity. I. General theory and long range lattice models," *Commun. Math. Phys.* **62**, 1–34 (1978).

[41] M. Aizenman, "Geometric analysis of ϕ^4 fields and Ising models," *Commun. Math. Phys.* **86**, 1–48 (1982).

[42] J. Fröhlich, "On the triviality of $\lambda\phi^4_d$ theories and the approach to the critical point in $d \geq 4$ dimensions," *Nucl. Phys. B* **200**, 281–296 (1982).

[43] M. Aizenman and H. Duminil-Copin, "Marginal triviality of the scaling limits of critical 4D Ising and ϕ^4_4 models," *Ann. of Math.* **194**, 163–235 (2021).

[44] T. Balaban, "Regularity and decay of lattice Green's functions," *Commun. Math. Phys.* **89**, 571–597 (1983).

[45] T. Balaban, "Propagators and renormalization transformations for lattice gauge theories I," *Commun. Math. Phys.* **95**, 17–40 (1984).

[46] T. Balaban, "Large field renormalization II. Localization, exponentiation, and bounds for the **R** operation," *Commun. Math. Phys.* **122**, 355–392 (1989).

[47] J. Dimock, "The renormalization group according to Balaban – I. Small fields," *Rev. Math. Phys.* **25**, 1330010 (2013).

[48] D. C. Brydges, "Lectures on the renormalisation group," in *Statistical Mechanics*, IAS/Park City Math. Ser. **16** (AMS, 2009), pp. 7–93.

[49] J. H. Conway and N. J. A. Sloane, *Sphere Packings, Lattices and Groups*, 3rd ed. (Springer, New York, 1999).

[50] H. S. M. Coxeter, *Regular Polytopes*, 3rd ed. (Dover, New York, 1973).

[51] U. Mosco, "Convergence of convex sets and of solutions of variational inequalities," *Adv. Math.* **3**, 510–585 (1969).

[52] G. Dal Maso, *An Introduction to* Γ*-Convergence* (Birkhäuser, Boston, 1993).

[53] A. Braides, Γ*-Convergence for Beginners* (Oxford University Press, Oxford, 2002).

[54] M. Reed and B. Simon, *Methods of Modern Mathematical Physics, Vol. I: Functional Analysis*, rev. ed. (Academic Press, San Diego, 1980).

[55] M. Reed and B. Simon, *Methods of Modern Mathematical Physics, Vol. II: Fourier Analysis, Self-Adjointness* (Academic Press, New York, 1975).

[56] M. H. Stone, "On one-parameter unitary groups in Hilbert space," *Ann. of Math.* **33**, 643–648 (1932).

[57] E. Seiler, *Gauge Theories as a Problem of Constructive Quantum Field Theory and Statistical Mechanics*, Lecture Notes in Physics **159** (Springer, Berlin, 1982).

[58] K. G. Wilson, "Confinement of quarks," *Phys. Rev. D* **10**, 2445–2459 (1974).

[59] E. Fradkin and S. H. Shenker, "Phase diagrams of lattice gauge theories with Higgs fields," *Phys. Rev. D* **19**, 3682–3697 (1979).

[60] F. W. Hehl, P. von der Heyde, G. D. Kerlick, and J. M. Nester, "General relativity with spin and torsion: foundations and prospects," *Rev. Mod. Phys.* **48**, 393–416 (1976).

[61] S. Holst, "Barbero's Hamiltonian derived from a generalized Hilbert–Palatini action," *Phys. Rev. D* **53**, 5966–5969 (1996).

[62] H. W. Hamber, *Quantum Gravitation: The Feynman Path Integral Approach* (Springer, Berlin, 2009).

[63] J. Ambjørn, A. Görlich, J. Jurkiewicz, and R. Loll, "Nonperturbative quantum gravity," *Phys. Rep.* **519**, 127–210 (2012).

[64] C. Rovelli, *Quantum Gravity* (Cambridge University Press, Cambridge, 2004).

[65] T. Thiemann, *Modern Canonical Quantum General Relativity* (Cambridge University Press, Cambridge, 2007).

[66] S. Weinberg, "Ultraviolet divergences in quantum theories of gravitation," in *General Relativity: An Einstein Centenary Survey*, ed. S. W. Hawking and W. Israel (Cambridge University Press, 1979), pp. 790–831.

[67] M. Reuter, "Nonperturbative evolution equation for quantum gravity," *Phys. Rev. D* **57**, 971–985 (1998).

[68] M. Reuter and F. Saueressig, *Quantum Gravity and the Functional Renormalization Group* (Cambridge University Press, Cambridge, 2019).

[69] R. Percacci, *An Introduction to Covariant Quantum Gravity and Asymptotic Safety* (World Scientific, Singapore, 2017).

[70] J. F. Donoghue, "General relativity as an effective field theory: The leading quantum corrections," *Phys. Rev. D* **50**, 3874–3888 (1994).

[71] N. E. J. Bjerrum-Bohr, J. F. Donoghue, and B. R. Holstein, "Quantum gravitational corrections to the nonrelativistic scattering potential of two masses," *Phys. Rev. D* **67**, 084033 (2003).

[72] M. Fierz and W. Pauli, "On relativistic wave equations for particles of arbitrary spin in an electromagnetic field," *Proc. R. Soc. Lond. A* **173**, 211–232 (1939).

[73] R. J. Rivers, "Lagrangian theory for neutral massive spin-2 fields," *Nuovo Cimento* **34**, 386–403 (1964).

[74] A. Lichnerowicz, "Propagateurs et commutateurs en relativité générale," *Publ. Math. IHES* **10**, 5–56 (1961).

[75] C. Becchi, A. Rouet, and R. Stora, "Renormalization of gauge theories," *Ann. Phys.* **98**, 287–321 (1976).

[76] I. V. Tyutin, "Gauge invariance in field theory and statistical physics in operator formalism," Lebedev Physics Institute preprint FIAN 39 (1975), arXiv:0812.0580.

[77] L. D. Faddeev and V. N. Popov, "Feynman diagrams for the Yang–Mills field," *Phys. Lett. B* **25**, 29–30 (1967).

[78] B. S. DeWitt, "Quantum theory of gravity. II. The manifestly covariant theory," *Phys. Rev.* **162**, 1195–1239 (1967).

[79] B. S. DeWitt, "Quantum theory of gravity. III. Applications of the covariant theory," *Phys. Rev.* **162**, 1239–1256 (1967).

[80] P. B. Gilkey, "The spectral geometry of a Riemannian manifold," *J. Diff. Geom.* **10**, 601–618 (1975).

[81] D. V. Vassilevich, "Heat kernel expansion: user's manual," *Phys. Rep.* **388**, 279–360 (2003).

[82] R. Courant, K. Friedrichs, and H. Lewy, "Über die partiellen Differenzengleichungen der mathematischen Physik," *Math. Ann.* **100**, 32–74 (1928).

[83] H. L. Cycon, R. G. Froese, W. Kirsch, and B. Simon, *Schrödinger Operators with Application to Quantum Mechanics and Global Geometry* (Springer, Berlin, 1987).

[84] H. B. Nielsen and M. Ninomiya, "Absence of neutrinos on a lattice I. Proof by homotopy theory," *Nucl. Phys. B* **185**, 20–40 (1981).

[85] H. Elvang and Y.-t. Huang, *Scattering Amplitudes in Gauge Theory and Gravity* (Cambridge University Press, Cambridge, 2015).

[86] Z. Bern, J. J. M. Carrasco, and H. Johansson, "New relations for gauge-theory amplitudes," *Phys. Rev. D* **78**, 085011 (2008).

[87] S. Weinberg, "Infrared photons and gravitons," *Phys. Rev.* **140**, B516–B524 (1965).

[88] C. M. Will, "The confrontation between general relativity and experiment," *Living Rev. Relativ.* **17**, 4 (2014).

[89] L. de Moura and S. Ullrich, "The Lean 4 theorem prover and programming language," in *CADE 28*, LNCS **12699** (Springer, 2021), pp. 625–635.

[90] The mathlib Community, "The Lean mathematical library," in *CPP 2020* (ACM, 2020), pp. 367–381.